

Bulldog, the Reusable Rocket Space Launch System

1. Introduction

This report assesses the *Bulldog* Reusable Rocket Space Launch System, which includes the two-stage launch vehicles: The *Bulldog* and the *Bulldog Puppy*. This report's purpose is to define a justified design properties for the *Bulldog* vehicles when using the available liquid propellant rocket engines, like RD-171M¹ and NK-33/31/39², for boosting the 1st stage. Selection of the second stage's engine comes into scope together with the design properties' optimization.

In this report we review four primary versions of the launch vehicles with various combinations of the available engines, that provide the Low Earth Orbit (LEO) payload delivering capacity at 200 km altitude, 0° inclination:

- About 1 metric tonne
- 8-9 tonnes
- 14-16 tonnes
- 30-35 tonnes

In addition to that, we are proposing for a consideration a midget-sized suborbital demonstrator driven by mono-propellant engines (Hydrogen Peroxide) developed by Lin Industrial to concept test the Launch Vehicle's design in flight.

¹ Produced by Energomash company, forming a part of Roscosmos State Corporation for Space Activities (Russian: Роскосмос).

² Units of this engine type are owned by ODK-Kuznetsov company, which belongs to the state-owned JSC United Engine Corporation (Russian: Объединённая двигателестроительная корпорация).

2. The Goal and the Idea of the Project

We set as our goal a development of the reusable, scalable Earth-to-Space transportation system, that would be able to deliver payloads to the Earth orbit with the minimum expenses. The basic design concept of the *Bulldog* rocket system is a trifacial pyramidal truss frame structure, which picks up and distributes the static and dynamic loads, including the engine thrust load. Such a structural system can be built at a launch site from prefabricated parts. The manufacturing and assembling technology is similar to those applied in building construction, and the parts are put together with threaded joints.

2.1 The Space Launch Market

Introduction of a reusable space launch system is called up by the emerging shape of the space launch market. When analyzing the number of the committed space launches by year, we can see a pretty much linear growth of those. (Fig. 1.)

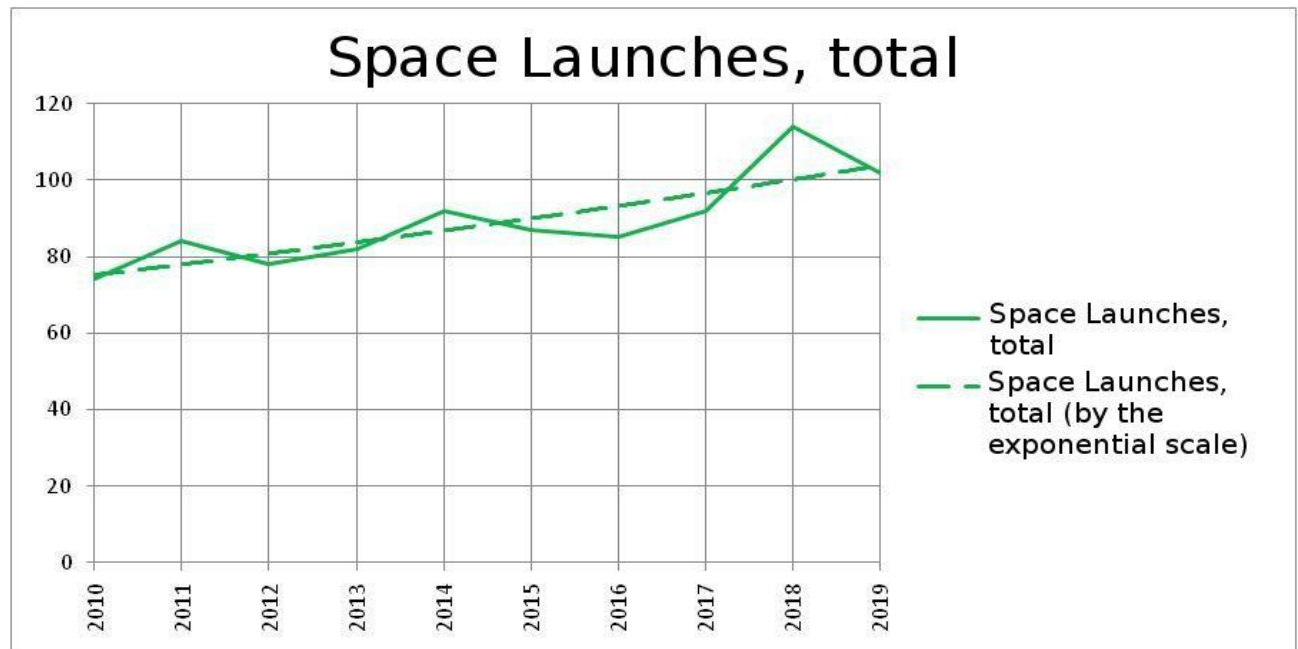


Fig. 1. The Trends in the Space Launch Market, worldwide.

The number of the satellites sent to Earth's orbit is growing almost exponentially (see Fig. 2.) Given that at the present time the volume of the launch market can be estimated as \$6-8 billion at the rate of 100-110 launches yearly, by the year 2030 these numbers may almost double: some forecasts have it like 240 launches per year, and the net earnings from the launch services will reach about \$12 billion.

Such a growth of the launch activity after many years of stagnation is primarily driven by the formation of the low orbital satellite constellations that provide communication services, such as Star Link and One Web. These constellations comprising many thousands of satellites in total, require tens, or, possibly, hundreds of orbital launches each year, just for the initial buildup. These factors boost the economical effectiveness of reusable launch systems.

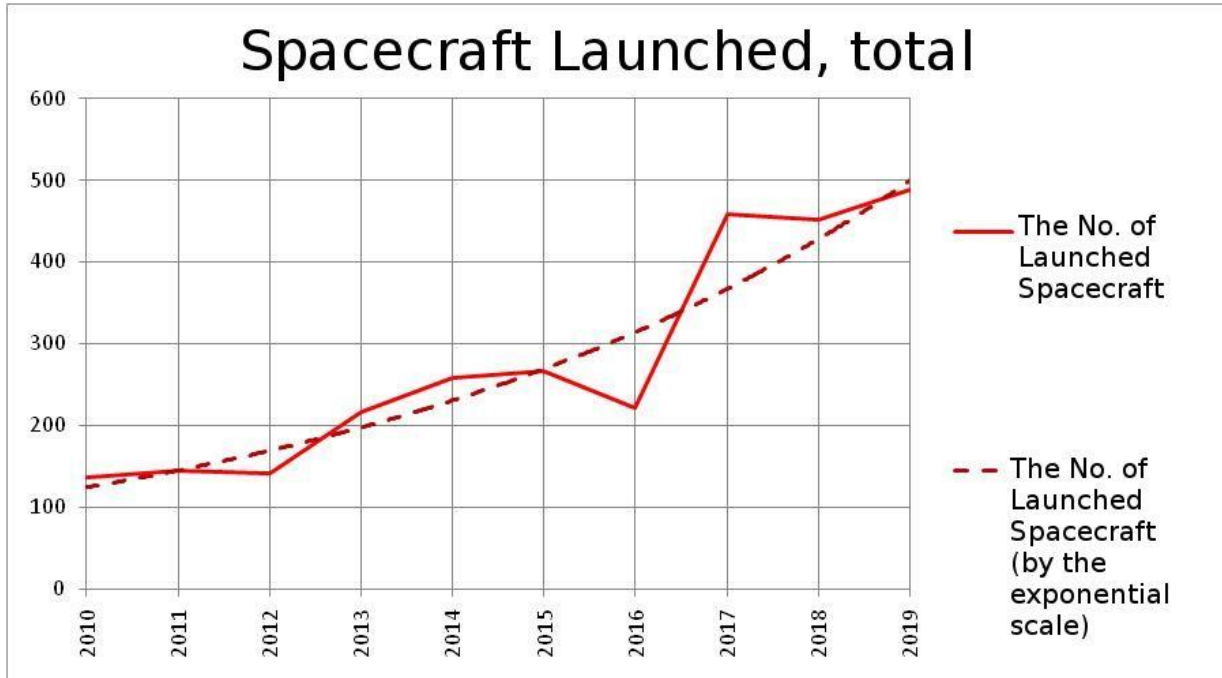


Fig. 2. The Trend of the Number of Spacecraft launched

2.2 The Strengths and Expected Benefits of the Project

The primary strengths of the proposed project are:

- Usage of the engineering materials freely available on the market;
- Application of the general construction building technology for the framework assembly;
- A possibility to build the rocket with a minimum site preparation (the example to consider is the assembling of Starship/Superheavy system at Boca Chica) not far away from the launch site;
- A possibility to launch from water without engaging with a complex ground-based infrastructure.

The expected benefits are: economy on the development cost, manufacturing cost, and, as the consequence, a decreased launch cost.

The launch system will also provide few additional possibilities:

- The second stage is potentially usable as a pressure-tight structural element of a large space station.

- A decreased launch cost allows to employ the system for clustered launching of small satellites to form or replenish low Earth's orbit satellite constellations, and also for delivering of propellant components to orbital refueling stations.

3. The Preliminary Ballistic Analysis of the System

The preliminary ballistic analysis has a dual purpose:

- 1) To determine the optimal vehicle mass at launch, and the optimal thrust for the second stage, that yields the largest possible payload mass delivered to the LEO at 200 km altitude and 0° inclination (we assume a launch from the ocean surface at the equator).
- 2) To define the initial values for configuring the vehicle and for the aerodynamic performance computation in the basic mode with a selected launching weight.
- 3) To choose the second stage's engine out the range of the existing offerings, that would be a best match for the optimal performance model. We can consider the following commercially available liquid propellant rocket engines applicable: RD-171M, NK-31, NK-39. By 2022-23, RD-120MS [1] engine might become available.

The following versions of *the Bulldog* LV have been considered:

- *Bulldog Big* – has three RD-171M engines on the 1st stage (each one is located at a corner of the pyramid's base.) The 2nd stage engine is selected based on the computation's outcome;
- *Bulldog Medium* – has six NK-33 on the 1st stage (places in pairs at the pyramid's base's corners.) The 2nd stage's engine can be either RD-120MS or NK-31/39;
- *Bulldog Little* – has three NK-33 (each one is located at a corner of the pyramid's base.) The 2nd stage engine is selected based on the computation's outcome;
- *Bulldog Puppy* – has three NK-39K (that's a variant of NK-39 with a shortened nozzle) at the pyramid's base corners. The 2nd stage's engine is 11D58M (also known as RD-58M.) This RD-58M is not yet market available, but there is no other engine in Russia, with the required thrust level, fed by liquid oxygen and kerosene.

3.1 The Initial Values and Assumptions.

We undertook the ballistic design analysis with the use of the graph from US 9,475,591 B1 patent (Fig. 1.) For the best computational convenience, we have approximated the graph with a 4th degree polynomial (see Fig. 2, which also displays the polynomial's expression.) The drag coefficient Cd for Mach numbers M>5 was assumed equal to 0.76.

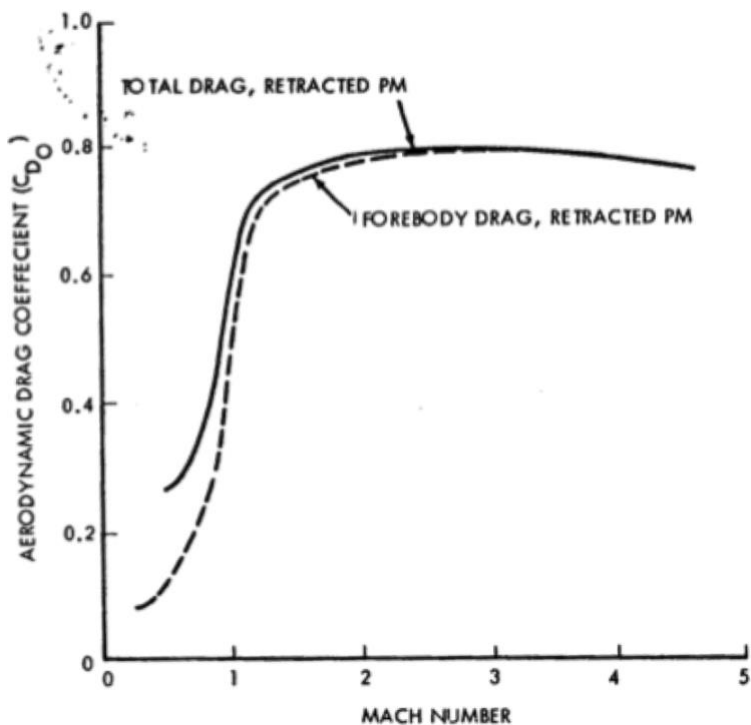


Fig. 1. Dependence of the Drag Coefficient of a Trifacial Pyramid upon the Mach Number, taken from US 9,475,591 B1 patent.

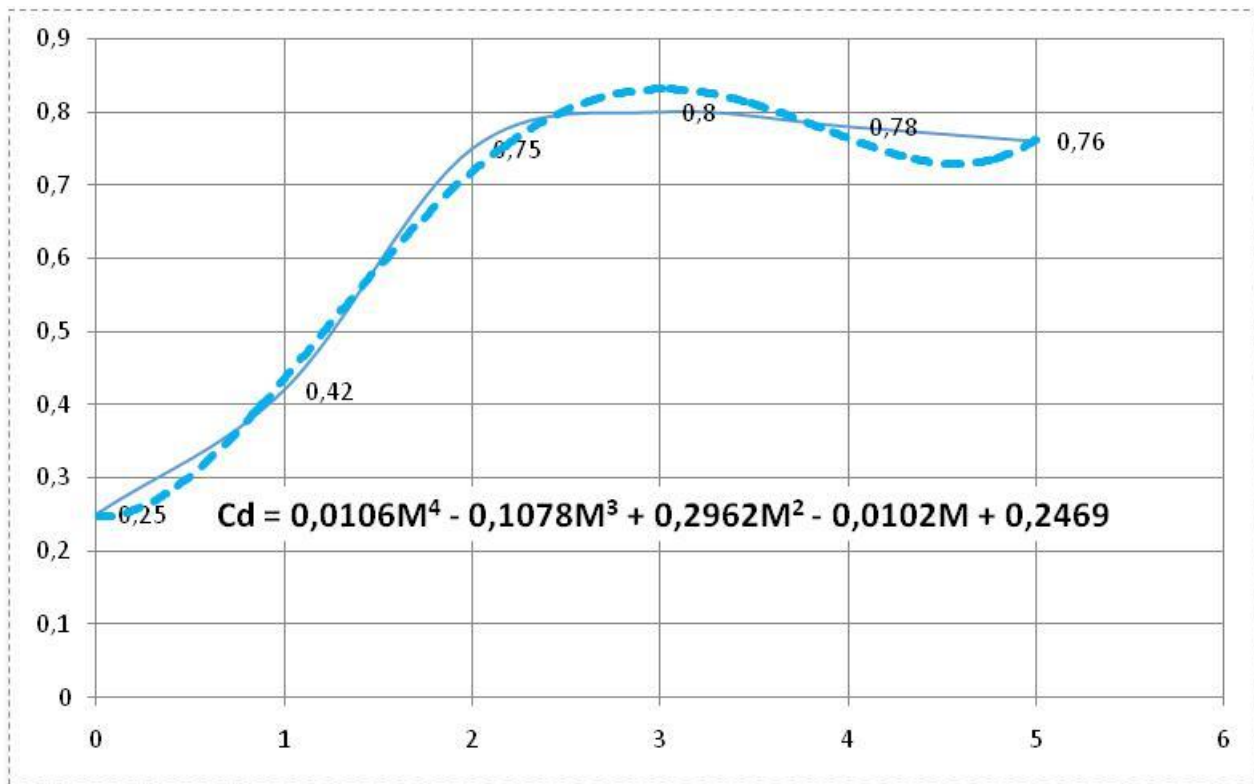


Fig. 2. Approximation of the $Cd(M)$ Dependence with a 4th Degree Polynomail.

For the purpose of the parametric study, *the Bulldog Big's* frontal area was assumed 363 m^2 (as such of the equilateral triangle with ≈ 29 meters side.)

We took the following values as characteristic for the figure of merit of the structure (Table 1) during the preliminary analysis.

Table 1. The Characteristics of the Figure of Merit of the Bulldog Big LV's Structure

Characteristic	Description	Value
Relative Mass of the Propellant Compartment	The ratio of the burnout mass (including the residual fuels and fluids) of the propellant compartment to the mass the burnt propellants	0.05
The Propulsion System's Specific Mass	The ratio of the entire propulsion system's mass (including the rocket engines, propellant feeding pipelines, the emergency protection system, valves, etc.) to the engines' thrust at the corresponding rocket stage's startup.	0.017 – for RD-171M 0.01 – for NK-33
The Other Compartments' Specific Mass	The ratio of the total mass of the rest of the compartments and systems (the framework, the outer shell, the guidance system, the stage separation system, the interstages, etc.) to the mass of the completely fueled stage.	0.05

We calculated the trajectory and performed optimization of the primary design parameters with help of Launch Model [1] program, based on MS EXCEL. We considered a planar (two-dimensional) movement of the rocket. The assumed condition was: moving through a central gravitational force field, over a spherical Earth with 6371 km radius. The pitch attitude program of the second stage is described by the equation:

$$\operatorname{tg} \varphi(t) = \operatorname{tg} \varphi_0 + (\operatorname{tg} \varphi_k - \operatorname{tg} \varphi_0) * t / t_k,$$

where t_k is the duration of the 2nd stage's burn,

φ_0 is the initial pitch angle,

φ_k is the final pitch angle.

The vacuum specific impulse for the 2nd stage was taken at 331 seconds, as NK-33 engine has.

3.2. Choosing the Launch Mass of the Bulldog Big Launch Vehicle

At the rocket *Bulldog Big* we apply three RD-171M engines on the 1st stage. The thrust of the 2nd stage is assumed to be a design value under optimization. The calculation shows that the launch mass range providing the largest payload-in-orbit mass value is between 1900 and 1950 metric tonnes (Fig. 3.). For the chosen launch mass value the

optimal thrust is 190 tonnes of force (Fig. 4). Within the selected range of the launch mass variation, the optimal 2nd thrust variance is between 180 and 190 tonnes of force.

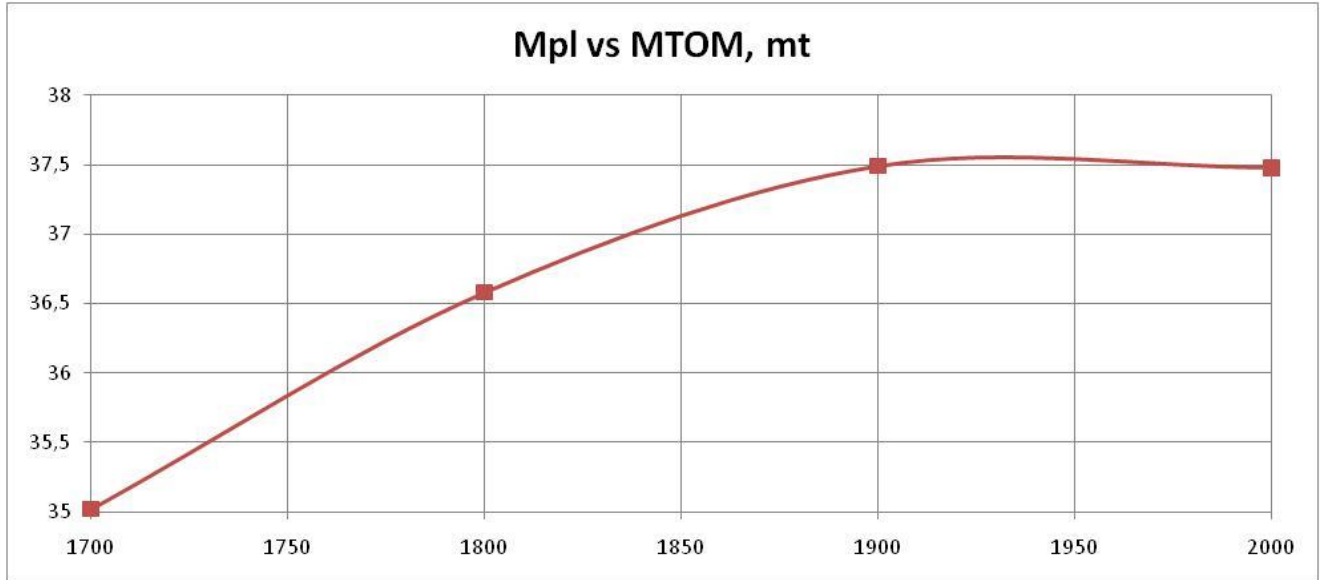


Fig. 3. Dependence of the Payload-in-Orbit Mass upon the Launch Mass for the *Bulldog Big LV*

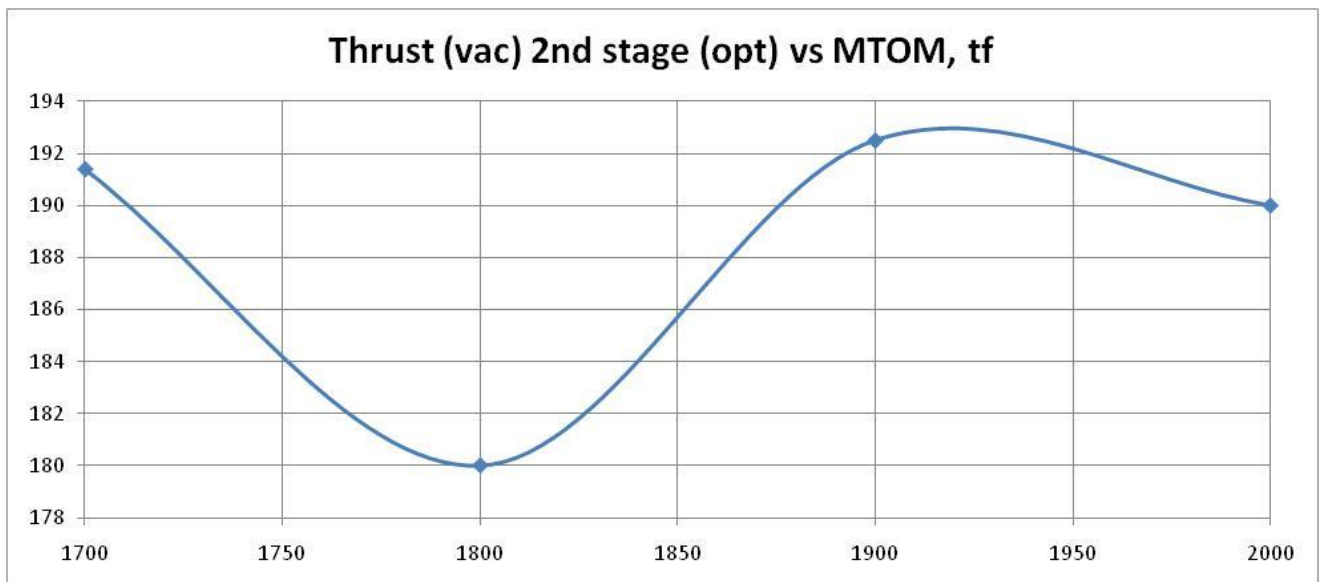


Fig. 4. Dependence of the 2nd Stage's Optimal Thrust upon the Launch Mass for the *Bulldog Big LV*

The kind of the dependence of the 2nd stage's optimal thrust upon the launch mass is shaped by two factors: not such a great precision of MS EXCEL based computation; a weak impact of the 2nd stage's thrust on the final payload-in-orbit mass value. Considering the relatively low fidelity of the estimating calculations, and to reserve some spare thrust we propose to set the launch mass at 1,850 metric tonnes, which plays out to 1.2 thrust to weight ratio.

Generally speaking, the near-optimal 2nd stage's thrust can be delivered by any single of the few now existing rocket engines, namely RD-191, 181, 193, and also NK-33, or NK-43. Out of these, the commercially available units are RD-181 (it's utilized in the *Antares* LV in the USA), and NK-33 (a number of these are kept in stock of JSC United Engine Corp.) Several AJ26-62 units (a refurbished version of NK-33 engine, which has been fit into the 1st stage of the *Antares* LV) are at possession of Aerojet Rocketdyne company. It's not yet clear how available RD-181 and NK-43 can be, while NK-33 are put up for sale by the United Engine Corp. This is why we optimized the design values for this specific liquid propellant engine (the vacuum thrust is 171.4 tonnes of force).

Since the second stage has only one engine, to be able to control the vehicle's flight in the pitch and yaw channels, we have to gimbal mount the engine (Fig. 5 and 6.)

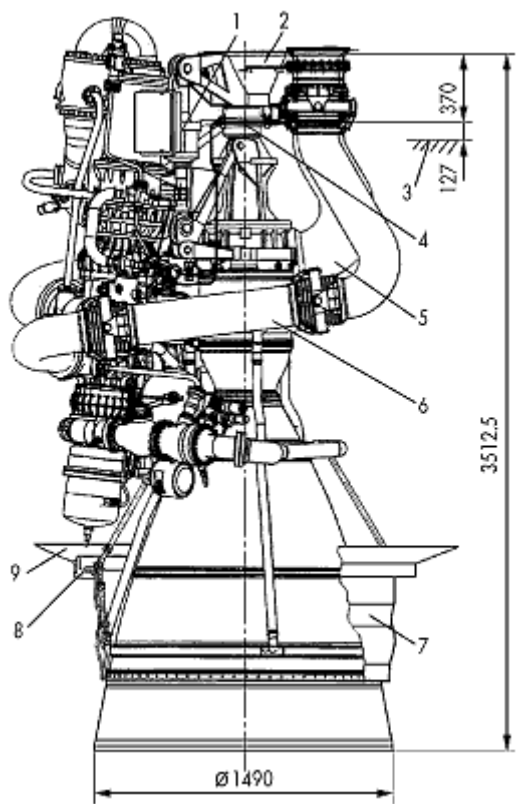


Fig. 5. A Gimbal Mounted Version of NK-33 Engine (NK-33-1)

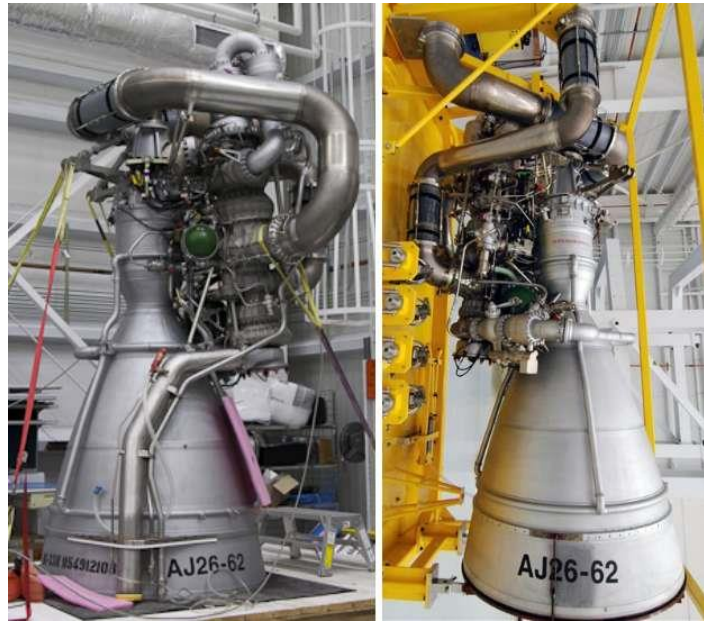


Fig. 6. AJ26-62 Engine.

3.3. Choosing the Launch Mass of the Bulldog Little Launch Vehicle

The *Bulldog Little* outfitted with triple NK-33 engines can be regarded as a counterpart to the *Soyuz-2*, the *Antares* or the *Atlas-V 401* launch vehicles. For the purpose of the preliminary parametric study of the *Bulldog Little* we assume the following values as characteristic for the figure of merit (Table 2.) The frontal area was assumed 97 m² (the square of an equilateral triangle with 15 meters side.)

Table 2. The Characteristics of the Figure of Merit of the *Bulldog Little* LV's Structure

Characteristic	Description	Value
Relative Mass of the Propellant Compartment	The ratio of the burnout mass (including the residual fuels and fluids) of the propellant compartment to the mass the burnt propellants	0.045 – for stage 1 0.06 – for stage 2
The Propulsion System's Specific Mass	The ratio of the entire propulsion system's mass (including the rocket engines, propellant feeding pipelines, the emergency protection system, valves, etc.) to the engines' thrust at the corresponding rocket stage's startup.	0.01 – for NK-33 (stage 1) 0.02 (stage 2)
The Other Compartments' Specific Mass	The ratio of the total mass of the rest of the compartments and systems (the framework, the outer shell, the guidance system, the stage separation system, the	0.05

	interstages, etc.) to the mass of the completely fueled stage.	
--	--	--

We took the specific impulse for the 2nd stage equal to 350 seconds (in vacuum), which is the value identical to what RD-120 provides for the *Zenit* LV.

The dependence of the in-orbit payload mass on the launching weight is shown at Fig. 7, and the dependence of the optimal thrust on the launching weight is at Fig. 8.

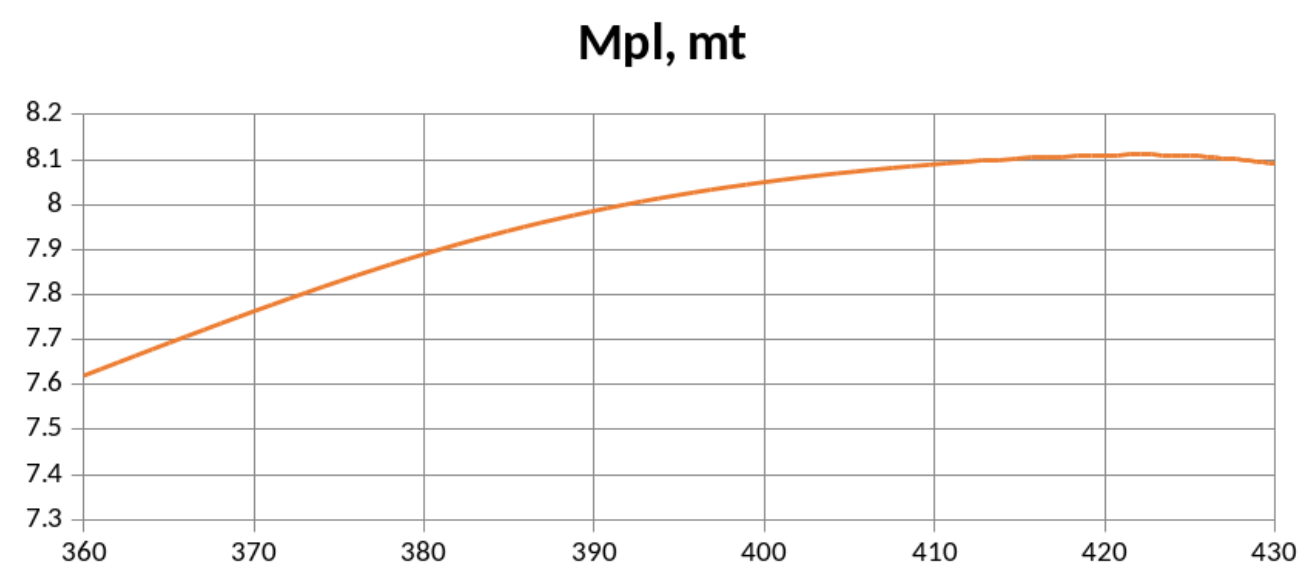


Fig. 7. Dependence of the Payload Mass Delivered to Orbit on the Mass of the *Bulldog Little* LV at Launch

The graph (at Fig. 7) shows that within the launching weight range 380..420 metric tonnes, the payload mass will change by just 220 kg (or about 2.7% of the maximum possible payload mass.)

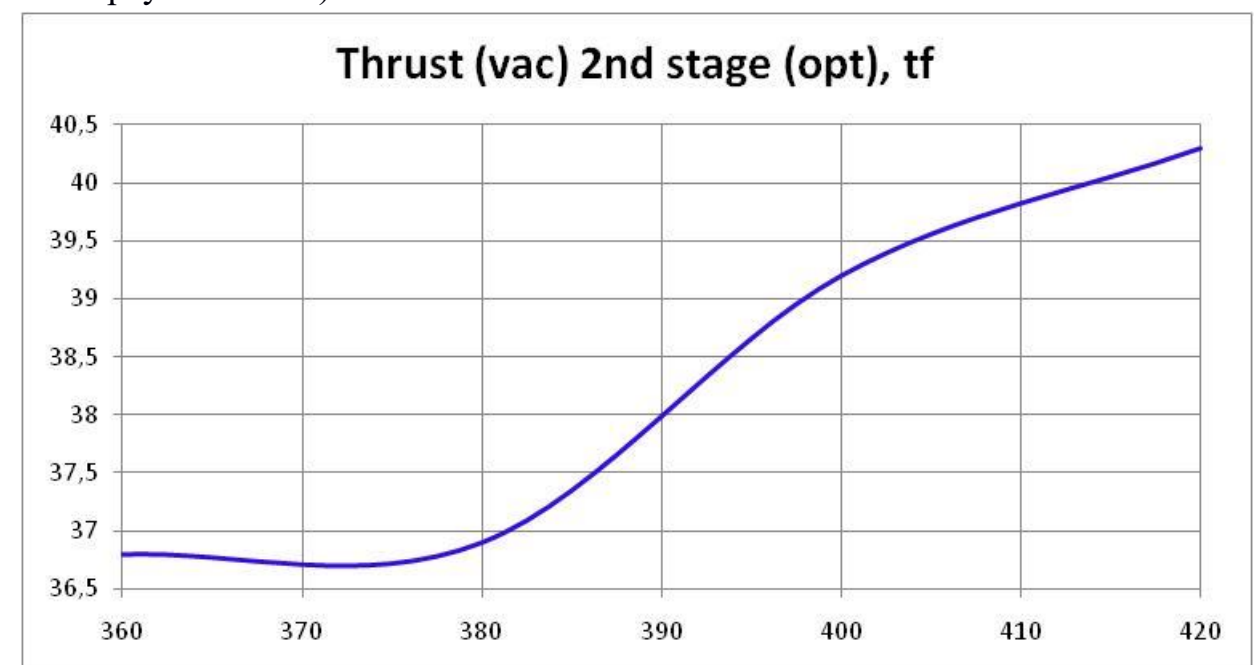


Fig. 8. Dependence of the Optimal 2nd Stage's Thrust on the Mass of the *Bulldog Little* LV at Launch

Therefore, considering the calculation precision, we can select any launching weight value within the indicated range. Let's assume the launching weight being equal to 390 metric tonnes, which results in 1.185 thrust to weight ratio at launch.

The optimal thrust for the *Bulldog Little* varies in the range 36..40.5 tonnes of force. A close to this value performance is attainable with Russian liquid propellant engines RD-0110 (vacuum thrust is 30 tf, applied at the Block I (Russian: Блок И) of the *Soyuz-2.1a* LV), RD-0124 (vacuum thrust is 30 tf, used in the *Soyuz-2.1b* and the *Soyuz-2.1v* LVs.) These two engines, however, don't appear to be commercially available. At the same time, the JSC United Engine Corp. Kuznetsov possesses some deal of NK-31/39 engines (certain sources indicate them keeping 10 units of NK-31 type and 10 units of NK-39 type), that have 41.5 tonnes of force thrust and 353 seconds specific impulse. Because of this, we propose to employ a single NK-31, which has a gimbal mount, enabling a two-axis control, as the 2nd stage engine for the *Bulldog Little* LV.

3.3. Choosing the Launch Mass of the Bulldog Medium and the Bulldog Puppy Launch Vehicles

The preliminary estimation has shown that the *Bulldog Medium* LV, outfitted with six NK-33 engines, will roughly match the *Zenit-2* launcher rocket by the payload capacity. Considering that the justified thrust to weight ratio at launch is about 1.2, we have chosen 770 metric tonnes as the launching weight value for the *Bulldog Medium*. The frontal projection area is 210 m² (the square of an equilateral triangle with 22 meters side.)

There is a certain vagueness about choosing the type and number of engines for the 2nd stage. Since the launching weight of the *Bulldog Medium* is almost double the launching weight of the *Bulldog Little*, we can presume the 2nd stage's thrust will grow by the same factor. Therefore, we have to mount two NK-31/39 engines on the stage two. However, with the selected structural layout of the stages, such a solution leads to an unreasonable widening of the whole rocket. That's why we considered the following versions: with a single NK-31; with two NK-31; with three NK-31/39; and with a single RD-120MS [3]. The derived parameters are put in the following Table 3:

Table 3.

Number and Type of Engines	6×NK-33	1×NK-31	6×NK-33	2×NK-31	6×NK-33	3×NK-31/39	6×NK-33	1×RD-120MS
Payload Mass, kg	13,621		15,875		15,365		15,650	
Maximum Lateral G-Load		≈7		≈5		≈4.5		≈5

The version with the double NK-31 has the best figures, however, as we said above, using those will widen the frontal area of the rocket and increase the drag. This, in turn, may degrade the payload capacity. RD-120MS engine might become available from 2022, but those plans are subject to a considerable economical risk. Meanwhile, NK-31/39 engines are present in stock and pack up well with the 1st stage's shape and structure without widening the cross-section. It is also important that the lateral G-load is not that substantial, which makes it unnecessary to throttle the 2nd stage's overall thrust. Besides, having three engines make it possible to control the rocket's flight using their thrust imbalance. This is why we decided to use NK-39 on the 2nd stage, since each such engine is by 138 kg lighter than an NK-31.

For the *Bulldog Puppy* LV we have chosen the 77 tonnes launching weight out of the need to provide for at least 1 tonne payload-in-orbit capacity. The frontal area is 27 m² (the square of an equilateral triangle with 8 meters side.) For the 1st stage we propose to employ three NK-39K engines (with shortened nozzles), totaling about 89 tonnes of force thrust at sea level. The previous calculation has shown that an optimal 2nd stage's thrust is less than the 1st stage's thrust by factor of 10-12. Respectively, the thrust for the 2nd stage of the *Bulldog Puppy* should be 7.5-9 tf. The only altitude engine of that kind offered in Russia is RD-58M (the thrust is 8.2 tf, the specific impulse is 356 seconds.) This engine is regarded as relatively expensive, it's produced in single quantities for the *Block DM* upper stages. Its commercial availability is highly unlikely. This is why we see it necessary to consider other types of engines further in the later design stages. For example, this might be: a triplet or quadruplet of Rutherford Vac (by RocketLab) or Hadley (by Ursa Major Technologies.)

4. The Primary Design Parameters and Projected Flight Performance for the *Bulldog Family* Launch Vehicles

4.1. The Primary Design Parameters of the *Bulldog Big LV*

The primary design parameters for the *Bulldog Big* were determined by the payload mass optimization given the planned set of engines for the rocket stages: triple RD-171M on the 1st stage and a single NK-33 on the 2nd stage. The selected parameters are shown in the Table 4.

Table 4. Primary Design Parameters of the *Bulldog Big LV*

Parameter	Value	
The Launcher Rocket		
Launching Weight, kg	1,850,000.00	
Payload Mass, kg (at 200×200 km LEO, $i=0^\circ$)	34,0748.7	
The Stages		
	I	II
Launching Weight, kg	1,636,210.7	179,040.6
Jettison Weight, kg	176,480.0	22,985.9
Specific Impulse (at sea level), s	309.4	297.4
Specific Impulse (in vacuum), s	337	331
The Engine Type	RD-171M	NK-33
Sea Level Thrust, tonnes of force	$3 \times 740 = 2,220$	154.4
Vacuum Thrust, tonnes of force	2,418.0	171.40
Propellants Consumption, kg/s	7,175.07	517.82
Burn Time	205.0	303.0
Maximum Lateral G-Load Exerted	Not exceeding 6.5	Not exceeding 3.0

The primary flight performance characteristics of the *Bulldog Big* are shown at the following diagrams (Fig. 9-14)

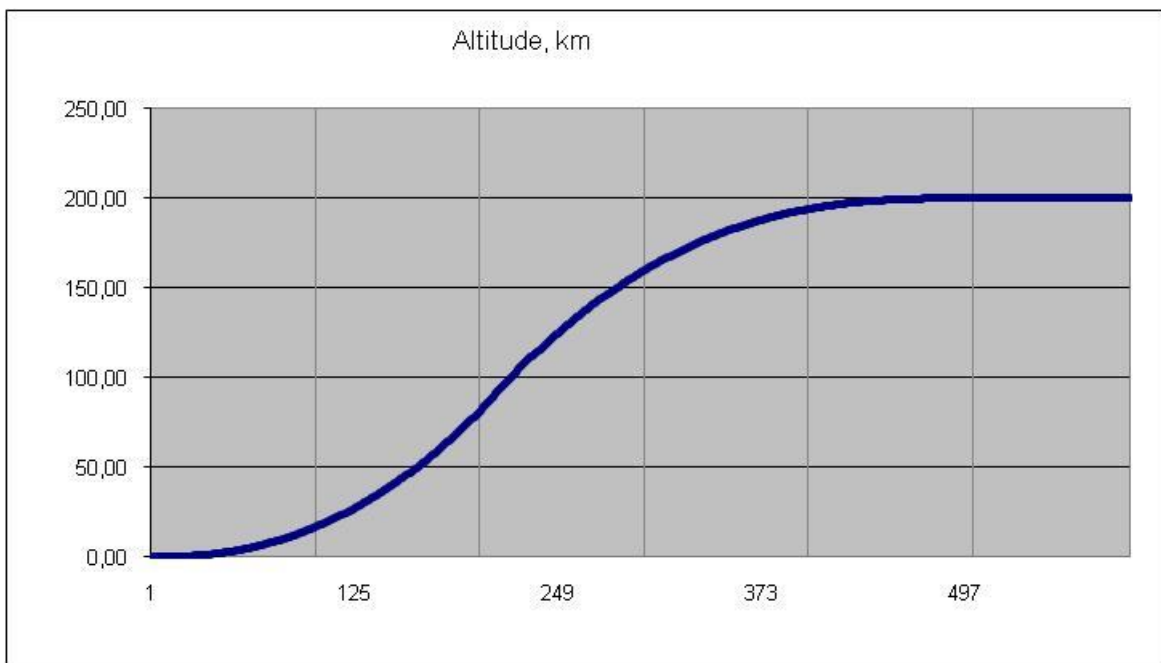


Fig. 9. Flight Altitude Change

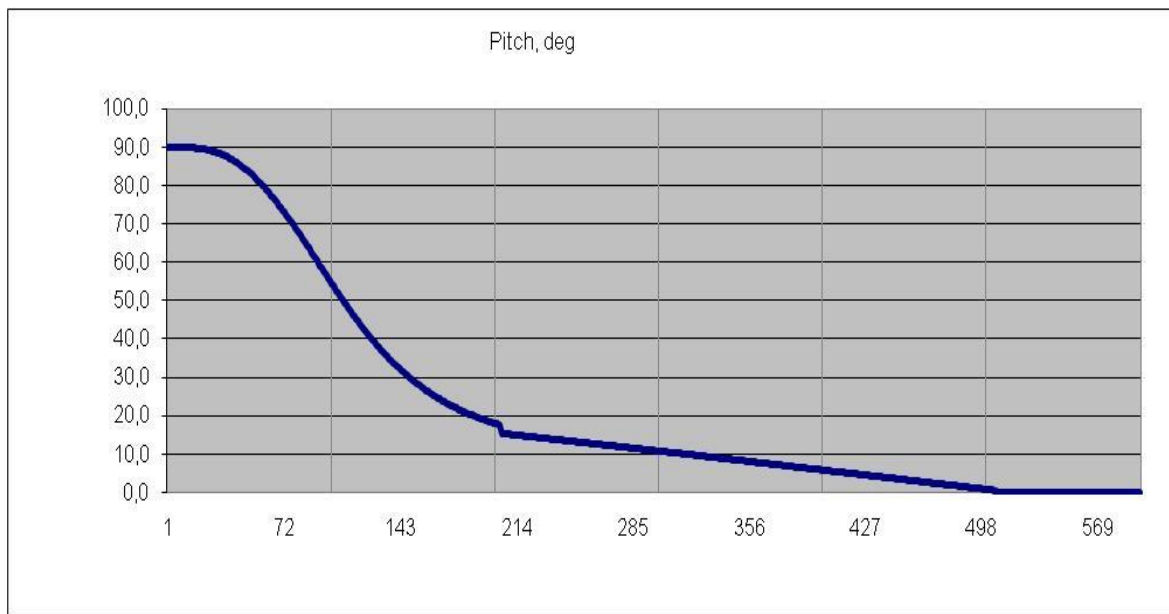


Fig. 10. Pitch Angle Change

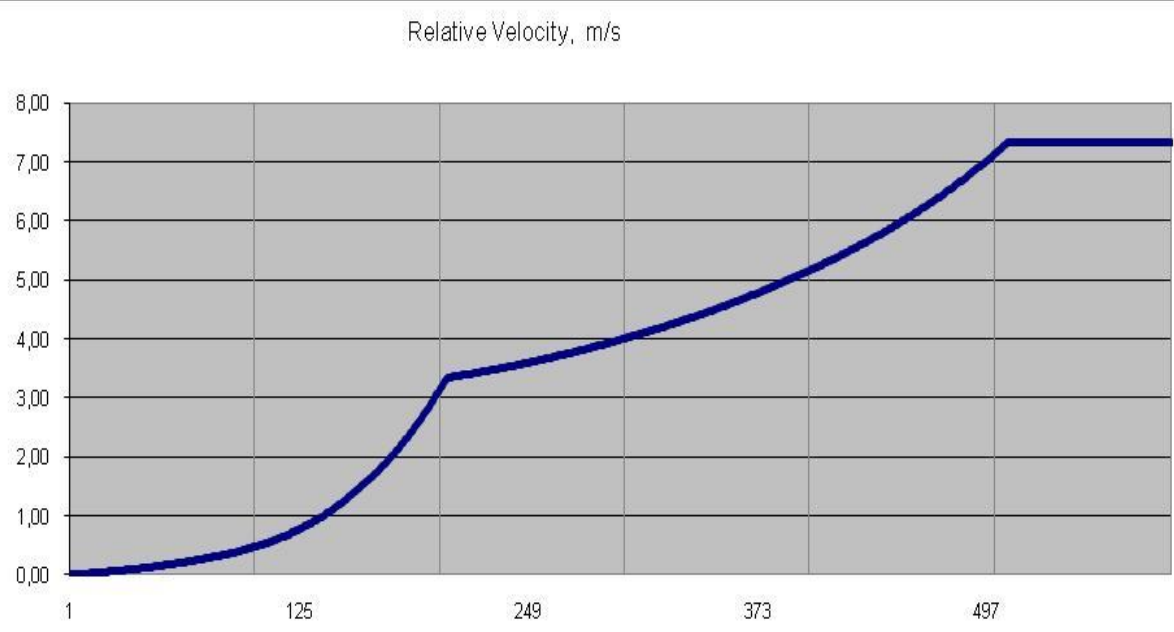


Fig. 11. Relative Velocity Change

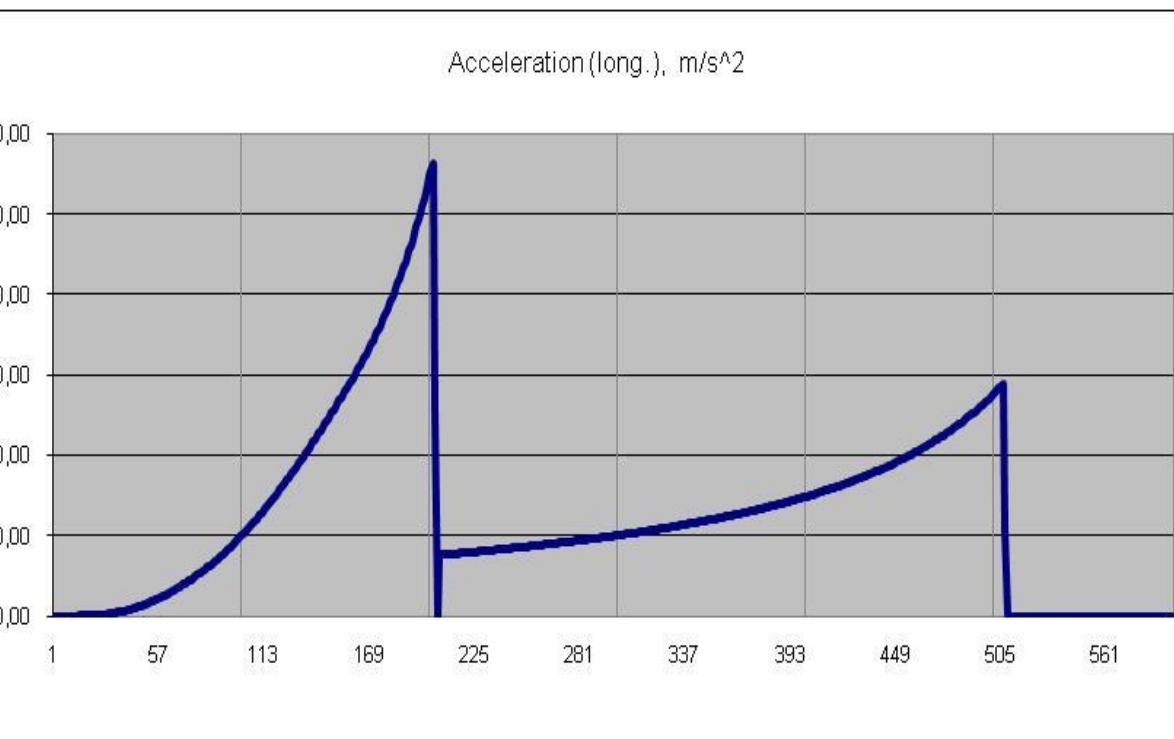


Fig. 12. Lateral Acceleration Change

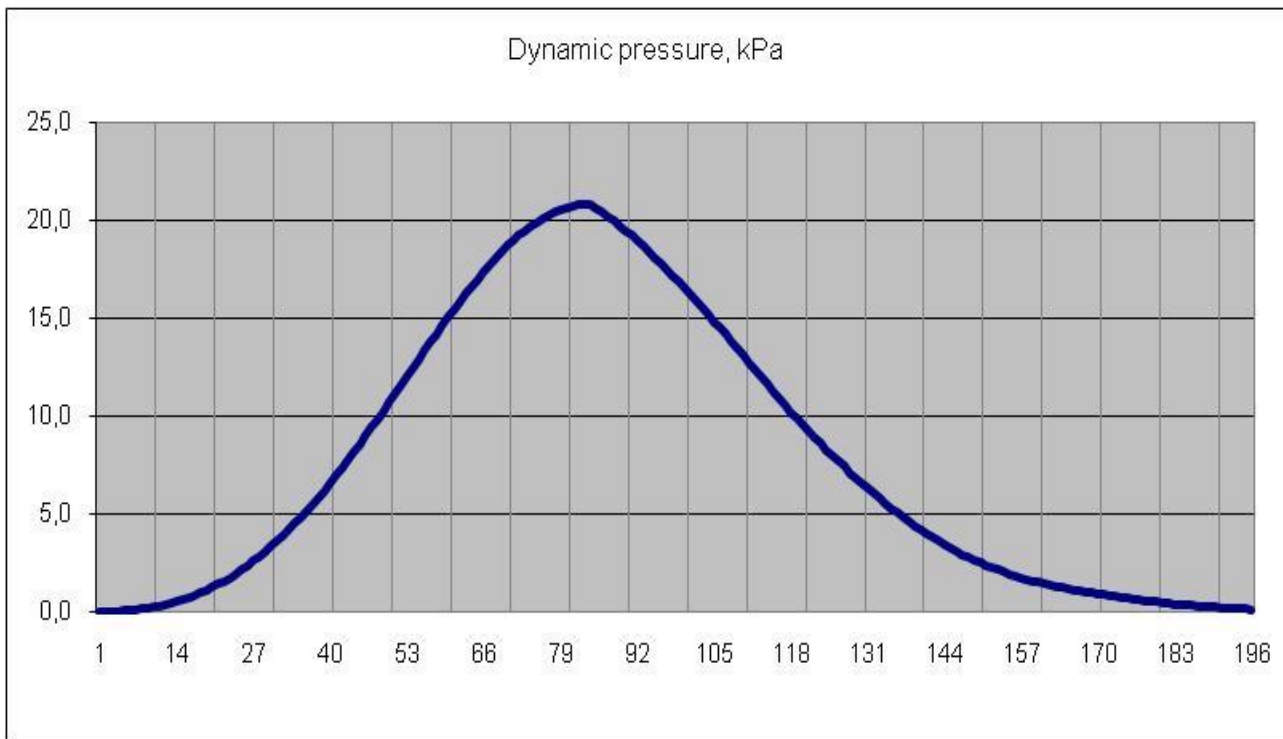


Fig. 13. Dynamic Pressure Change

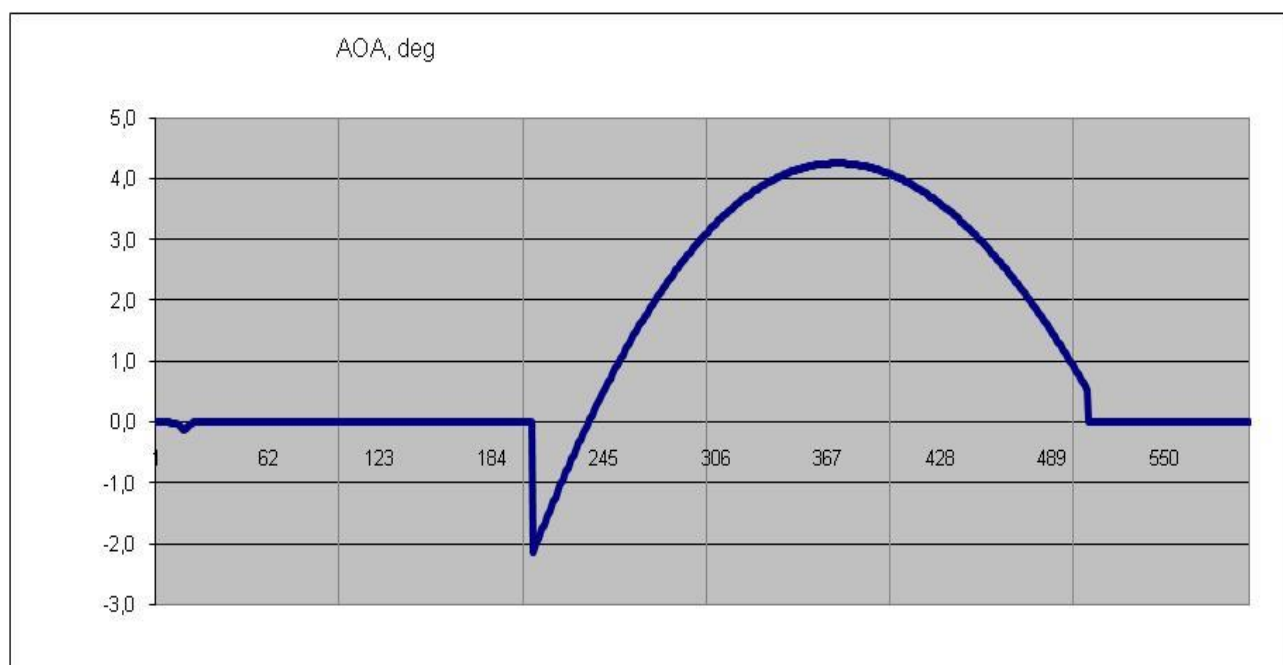


Fig. 14. Angle of Attack Change Program

4.2. The Primary Design Parameters of the Bulldog Medium LV

The primary design parameters for the *Bulldog Medium* were determined by the payload mass optimization given the planned set of engines for the rocket stages: six NK-33 on the 1st stage and three NK-39 on the 2nd stage. The selected parameters are shown in the Table 5.

Table 5. Primary Design Parameters of the *Bulldog Medium* LV

Parameter	Value	
The Launcher Rocket		
Launching Weight, kg	770,000.00	
Payload Mass, kg (at 200×200 km LEO, $i=0^\circ$)	15,365.01	
The Stages		
	I	II
Launching Weight, kg	635,836.0	118,799.0
Jettison Weight, kg	74,498.4	13,023.0
Specific Impulse (at sea level), s	297.4	-
Specific Impulse (in vacuum), s	331	353
The Engine Type	6×NK-33	3×NK-39
Sea Level Thrust, tonnes of force	462.00	-
Vacuum Thrust, tonnes of force	514.206	124.50
Propellants Consumption, kg/s	3,106.98	352.69
Burn Time	182	301
Maximum Lateral G-Load Exerted	Not exceeding 4.5	
	4.5	

The flight performance characteristics of the *Bulldog Medium* are shown at the following diagrams (Fig. 15-20)

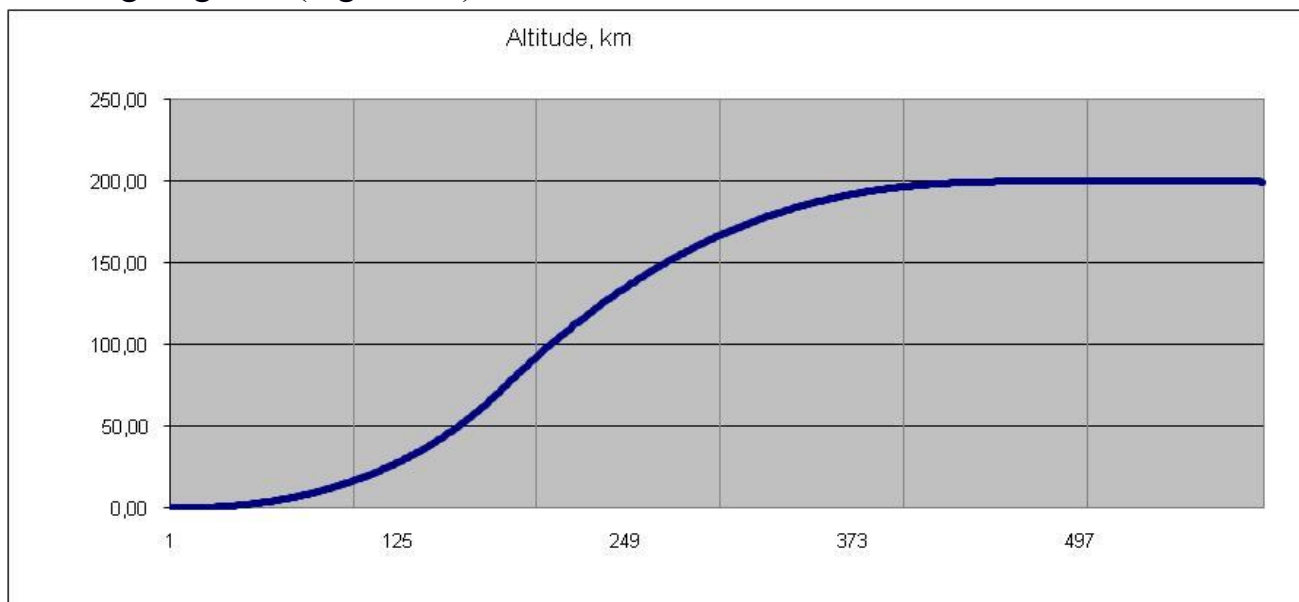


Fig. 15. Flight Altitude Change

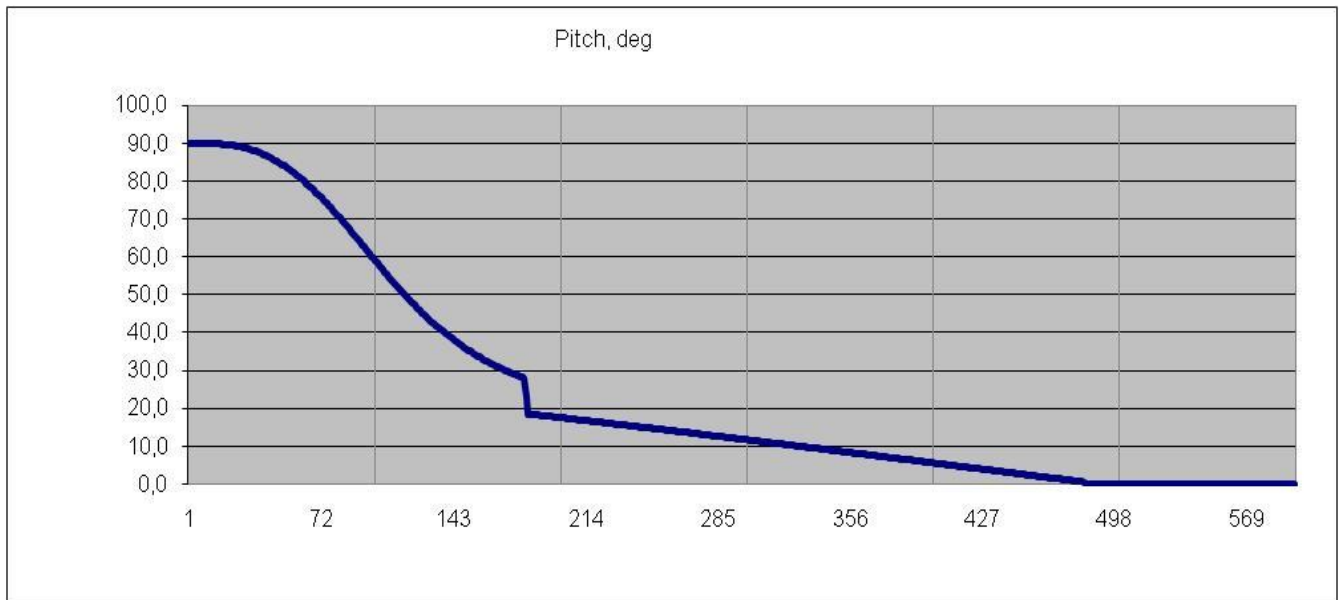


Fig. 16. Pitch Angle Change

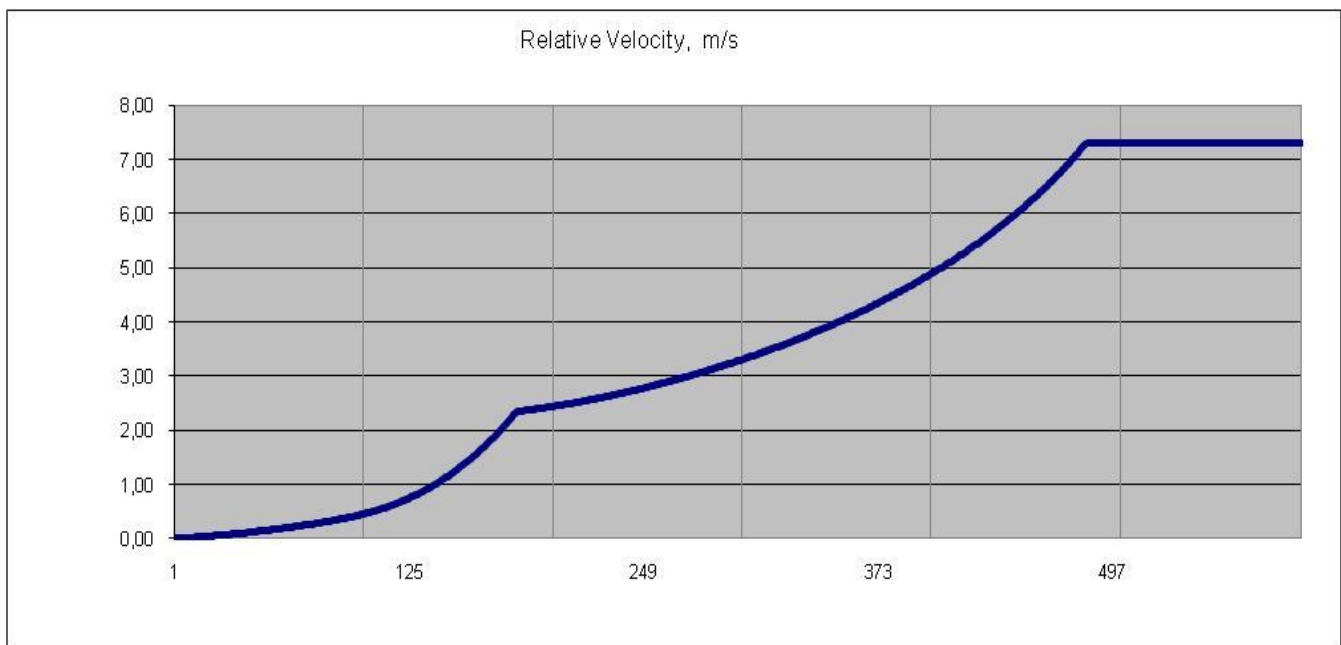


Fig. 17. Relative Velocity Change

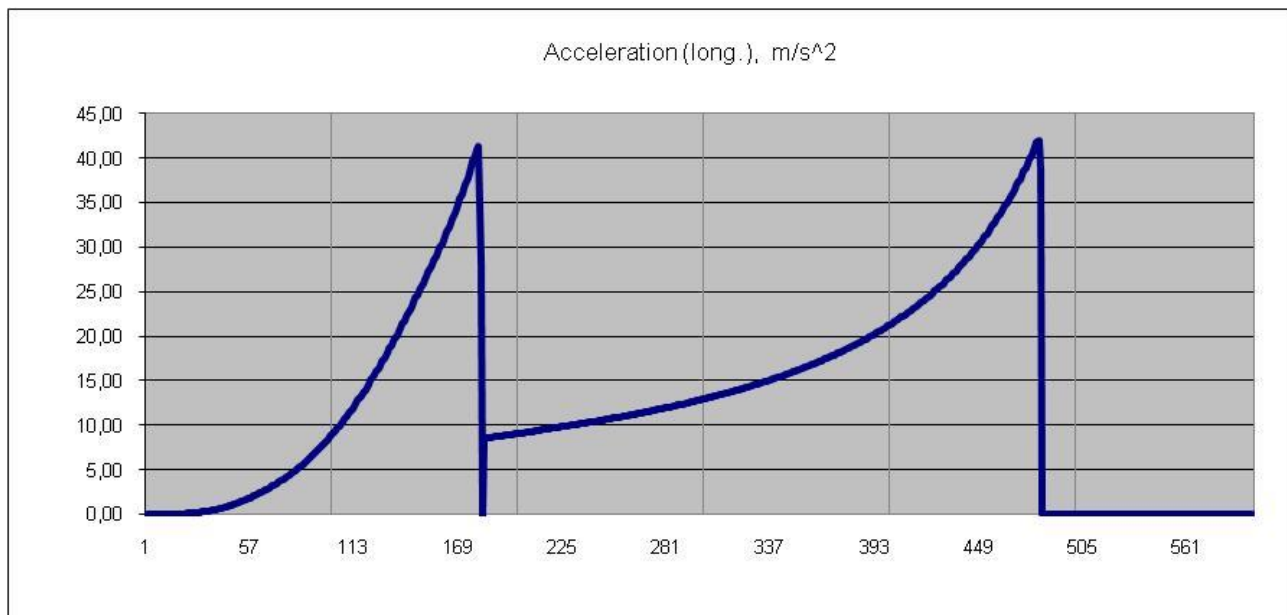


Fig. 18. Lateral Acceleration Change

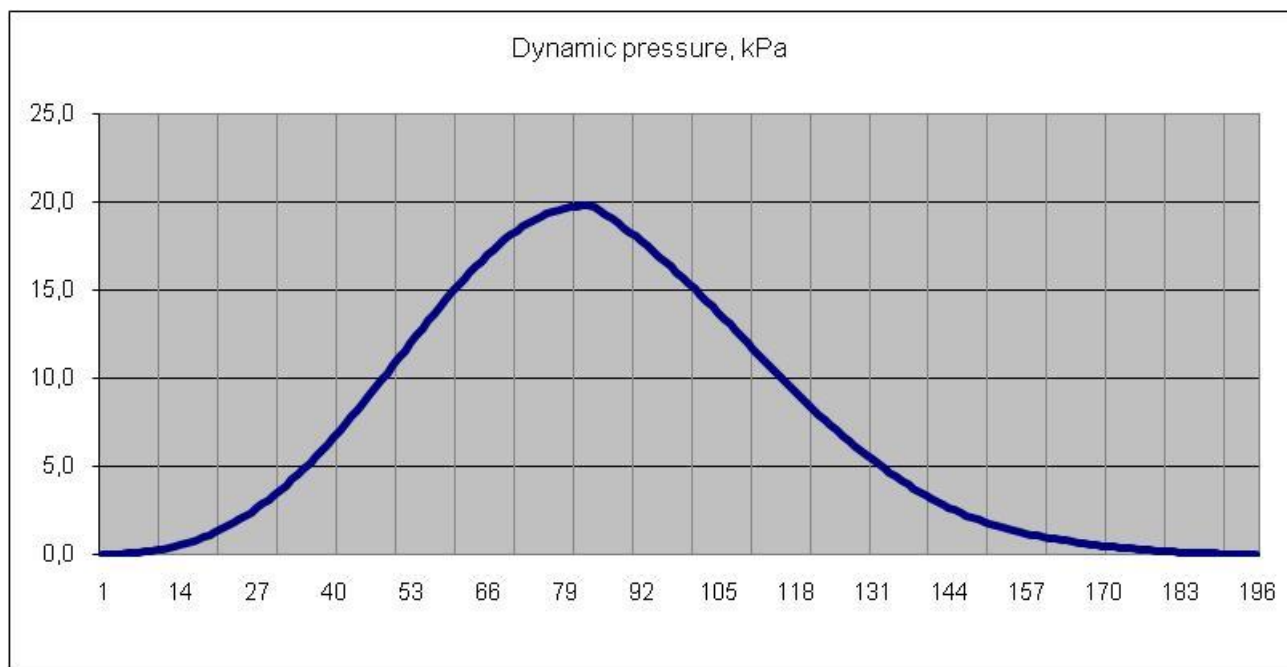


Fig. 19. Dynamic Pressure Change

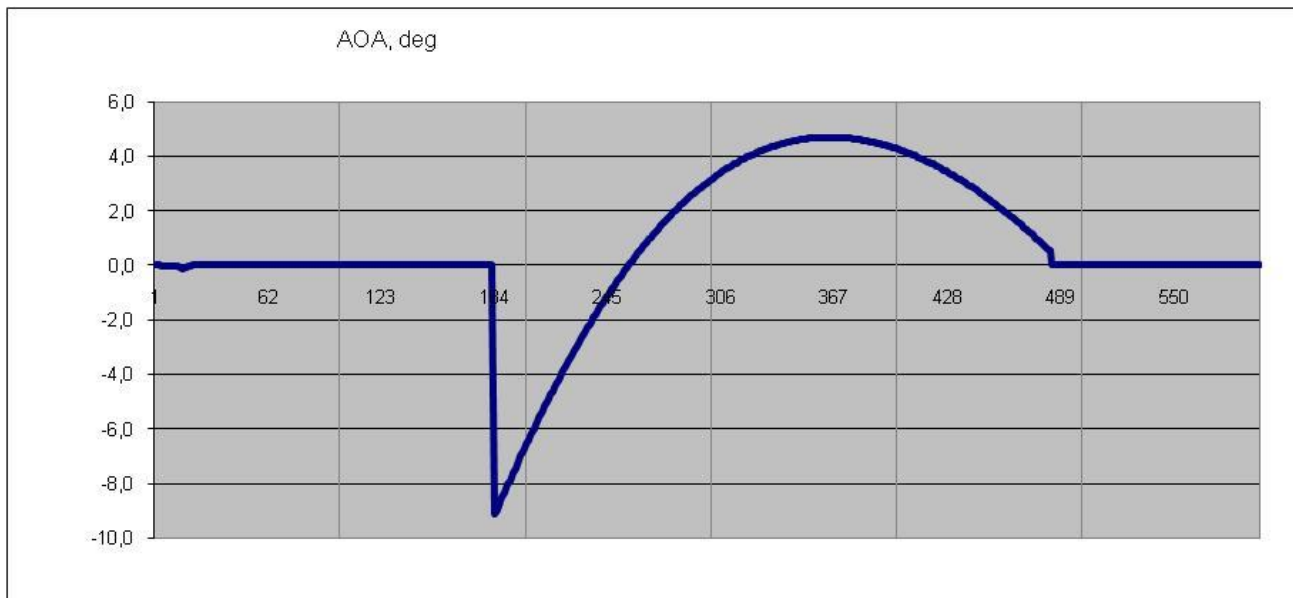


Fig. 20. Angle of Attack Change Program

4.3. The Primary Design Parameters of the Bulldog Little LV

The primary design parameters for the *Bulldog Little* were determined by the payload mass optimization given the planned set of engines for the rocket stages: triple NK-33 on the 1st stage and a single NK-31 on the 2nd stage. The selected parameters are shown in the Table 6.

Table 6. Primary Design Parameters of the *Bulldog Little* LV

Parameter	Value	
The Launcher Rocket		
Launching Weight, kg	390,000.00	
Payload Mass, kg (at 200×200 km LEO, $i=0^\circ$)	8,140.00	
The Stages		
	I	II
Launching Weight, kg	340,032.3	40,827.4
Jettison Weight, kg	34,424.0	5,019.8
Specific Impulse (at sea level), s	297.4	-
Specific Impulse (in vacuum), s	331	353
The Engine Type	$3 \times$ NK-33	NK-31
Sea Level Thrust, tonnes of force	462.00	-
Vacuum Thrust, tonnes of force	514.206	41.5
Propellants Consumption, kg/s	1,553.49	117.56

Burn Time	198	306
Maximum Lateral G-Load Exerted	Not exceeding 6.0	≈ 3.0

The primary flight performance characteristics of the *Bulldog Little* are shown at the following diagrams (Fig. 21-26)

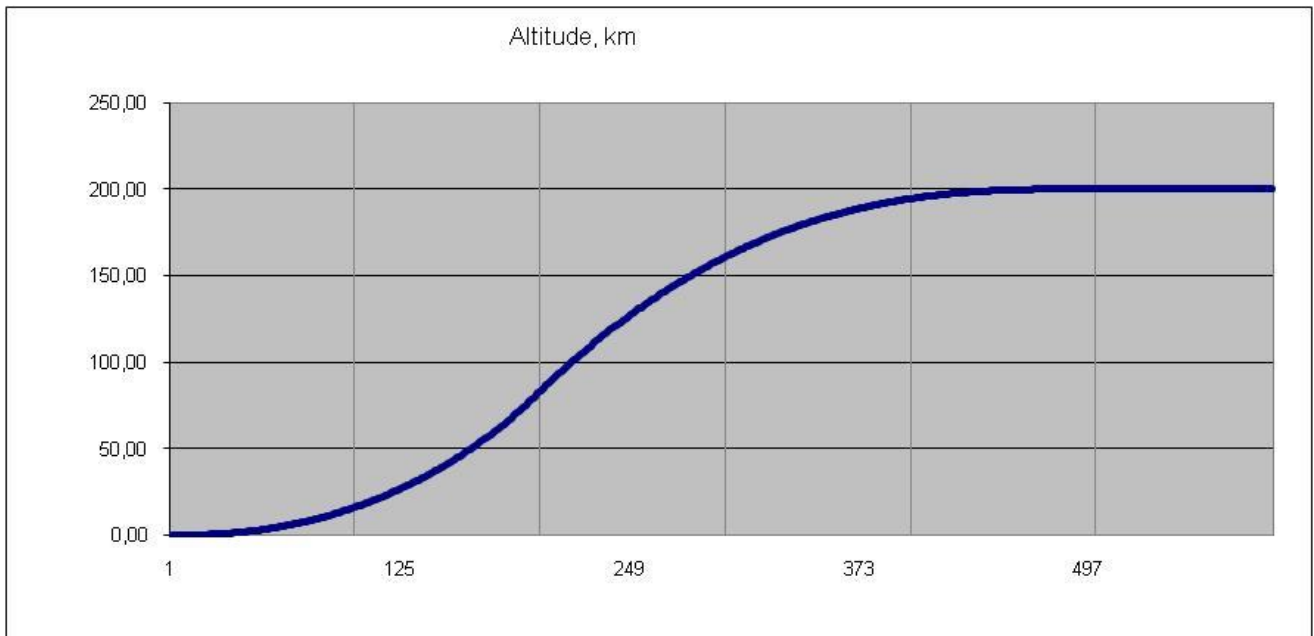


Fig. 21. Flight Altitude Change

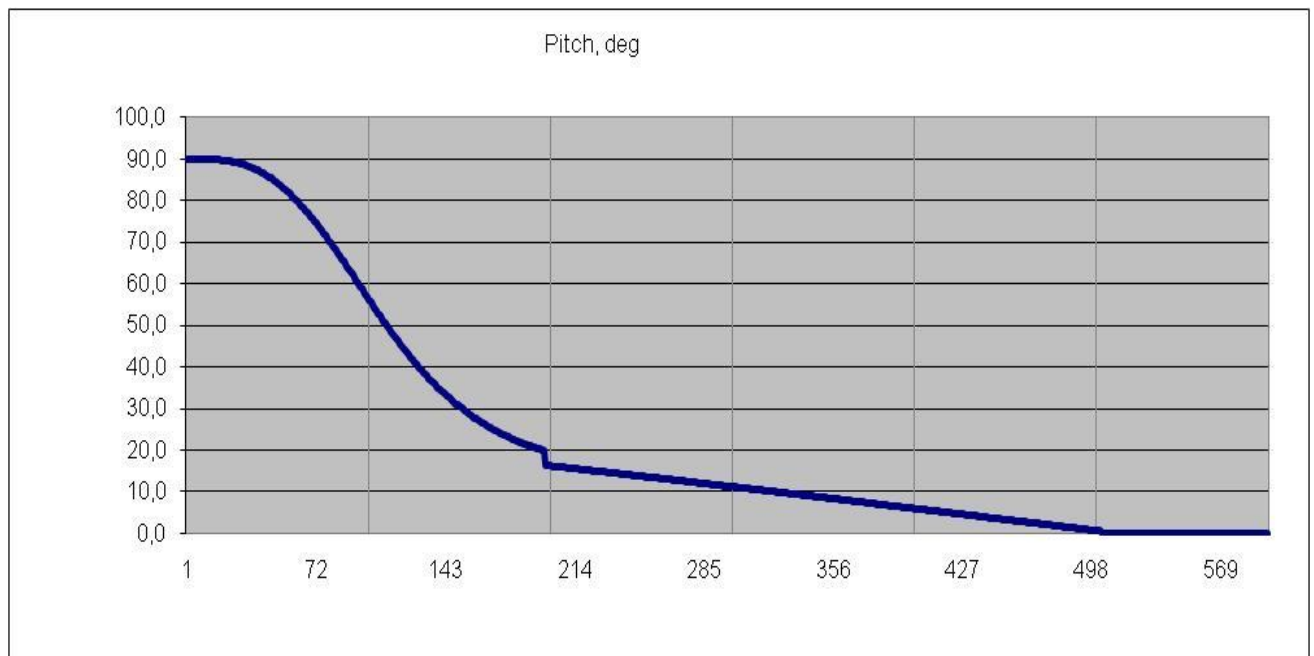


Fig. 22 Pitch Angle Change

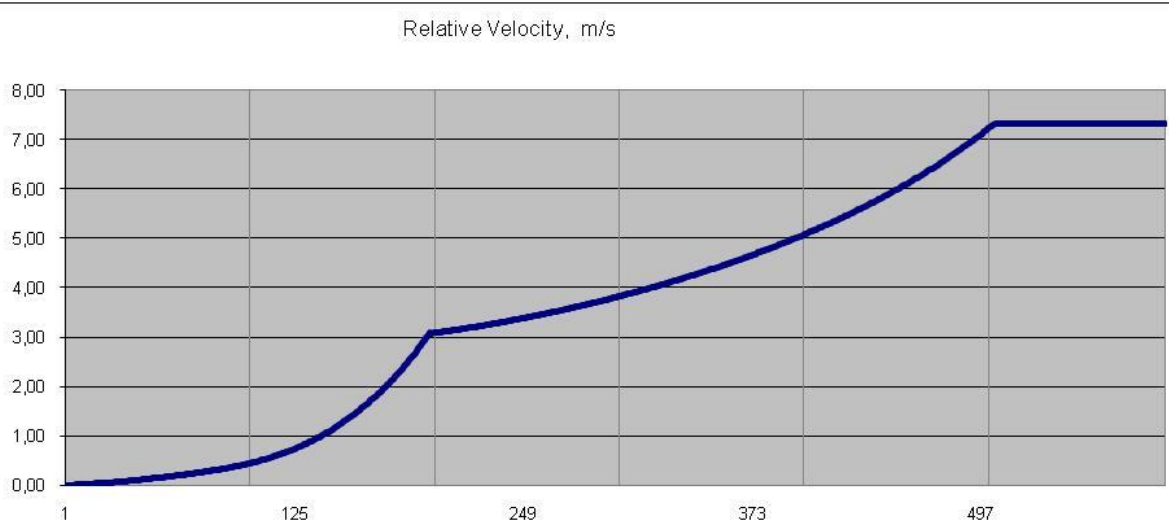


Fig. 23. Relative Velocity Change

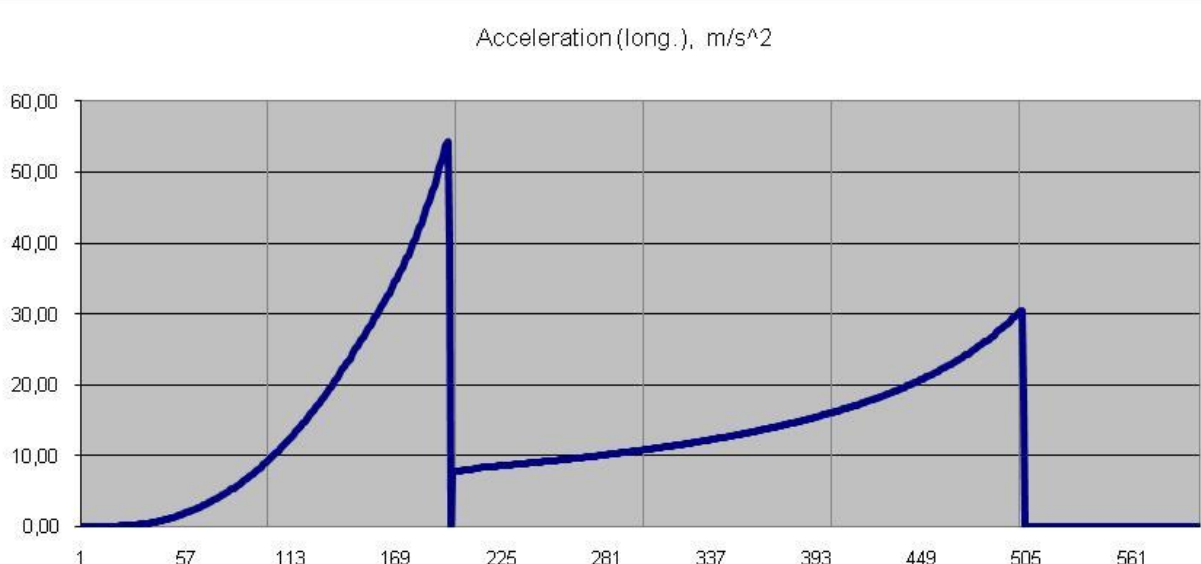


Fig. 24. Lateral Acceleration Change

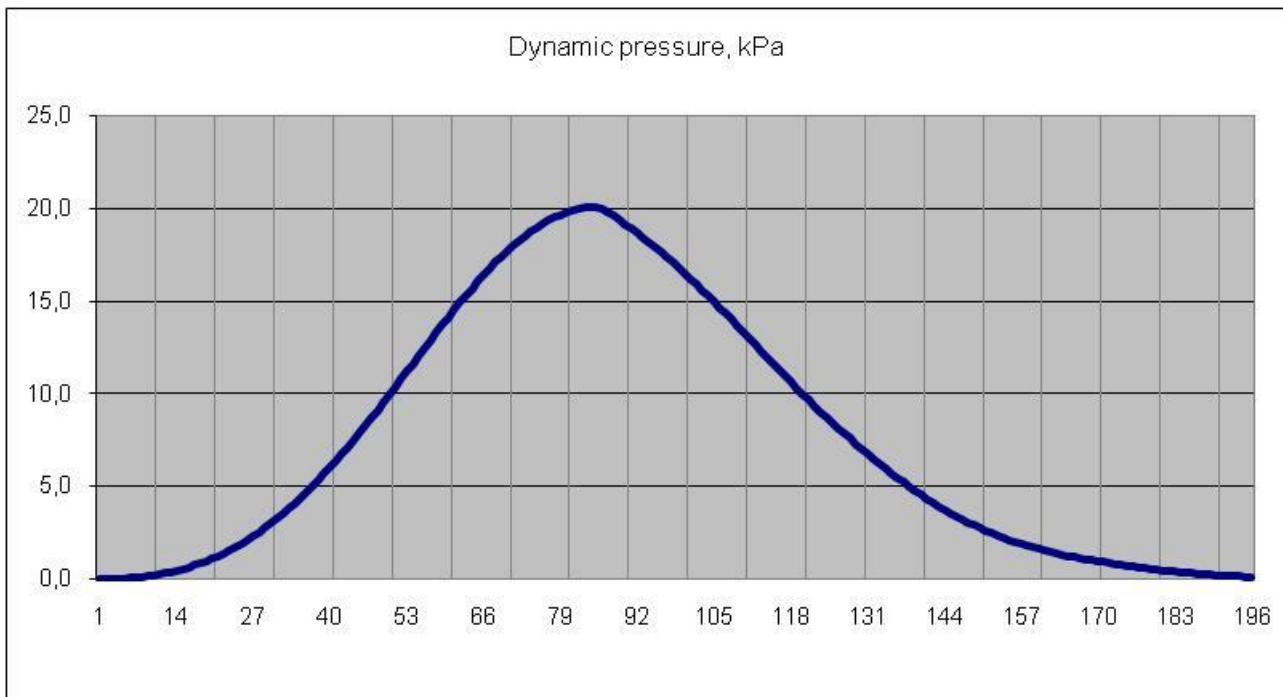


Fig. 25. Dynamic Pressure Change

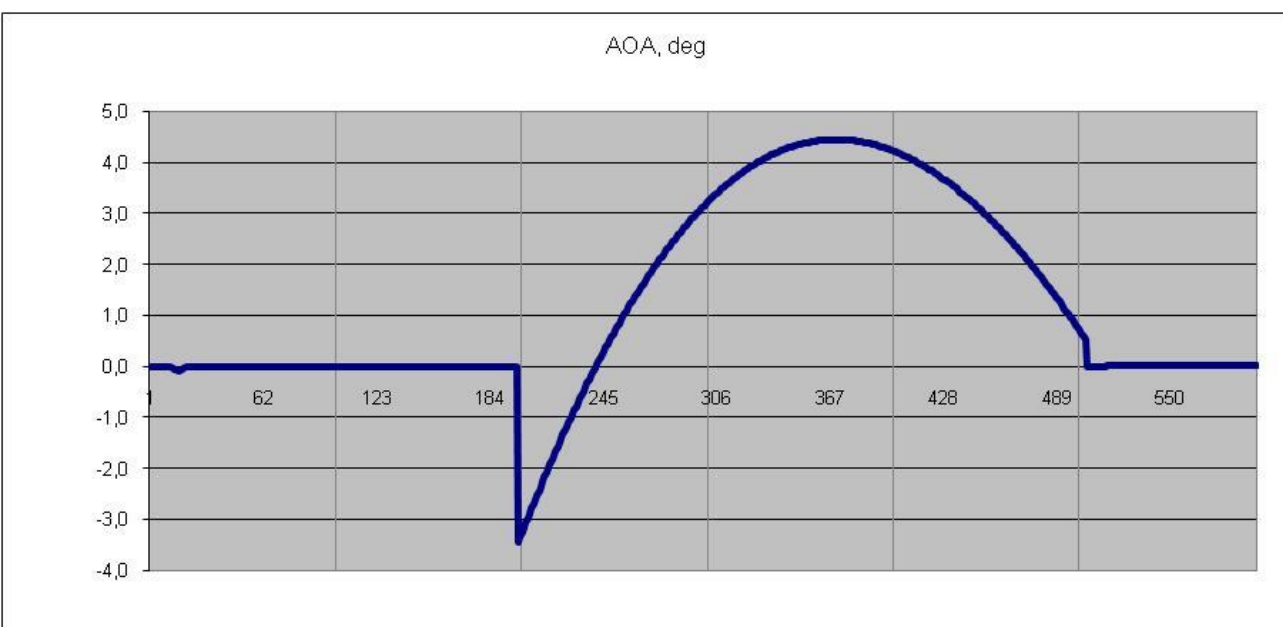


Fig. 26. Angle of Attack Change Program

4.4. The Primary Design Parameters of the Bulldog Puppy LV

The primary design parameters for the *Bulldog Puppy* were determined by the payload mass optimization given the planned set of engines for the rocket stages: triple NK-39 on the 1st stage and a single RD-58M on the 2nd stage. The selected parameters are shown in the Table 7.

Table 7. Primary Design Parameters of the *Bulldog Puppy* LV

Parameter	Value	
The Launcher Rocket		
Launching Weight, kg	77,000.00	
Payload Mass, kg (at 200×200 km LEO, $i=0^\circ$)	1,156.00	
The Stages		
	I	II
Launching Weight, kg	67,008.1	8,836.3
Jettison Weight, kg	8,871.6	935.1
Specific Impulse (at sea level), s	256.3	-
Specific Impulse (in vacuum), s	323.0	356
The Engine Type	3×NK-39	RD-58M
Sea Level Thrust, tonnes of force	89.4	-
Vacuum Thrust, tonnes of force	112.6	8.50
Propellants Consumption, kg/s	348.74	23.88
Burn Time	168	332
Maximum Lateral G-Load Exerted	Not exceeding 5.0	Not exceeding 4.0

The primary flight performance characteristics of the *Bulldog Puppy* are shown at the following diagrams (Fig. 27-32)

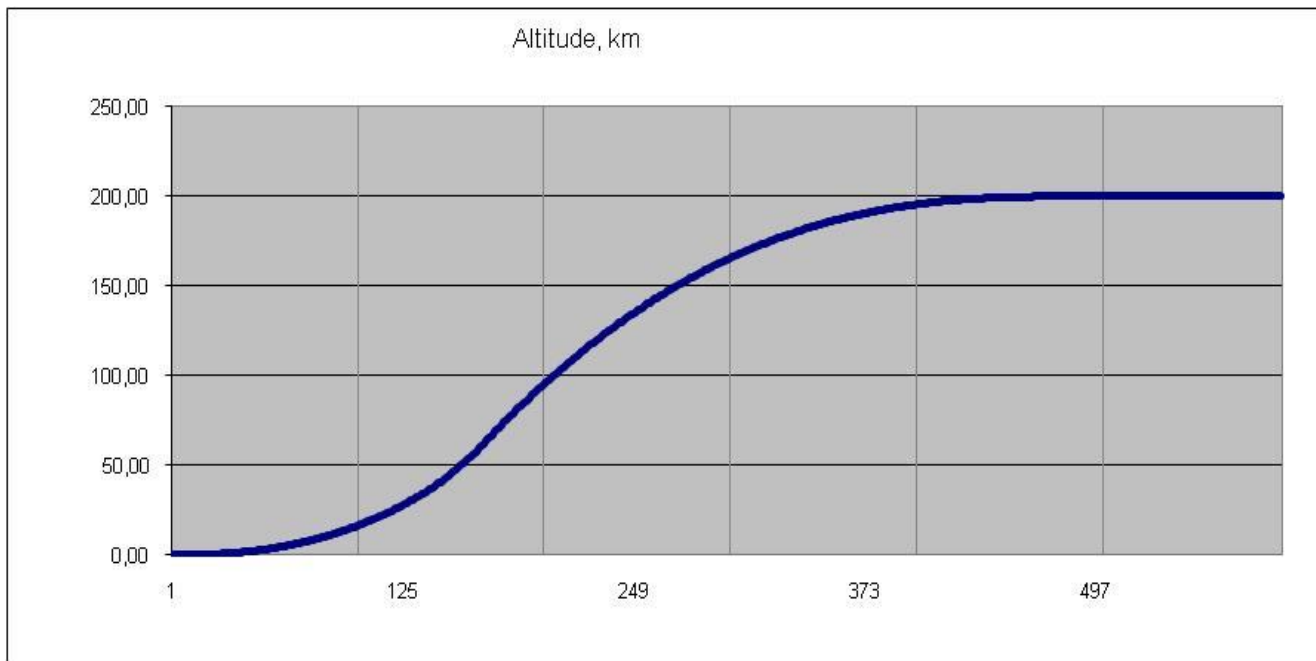


Fig. 27. Flight Altitude Change

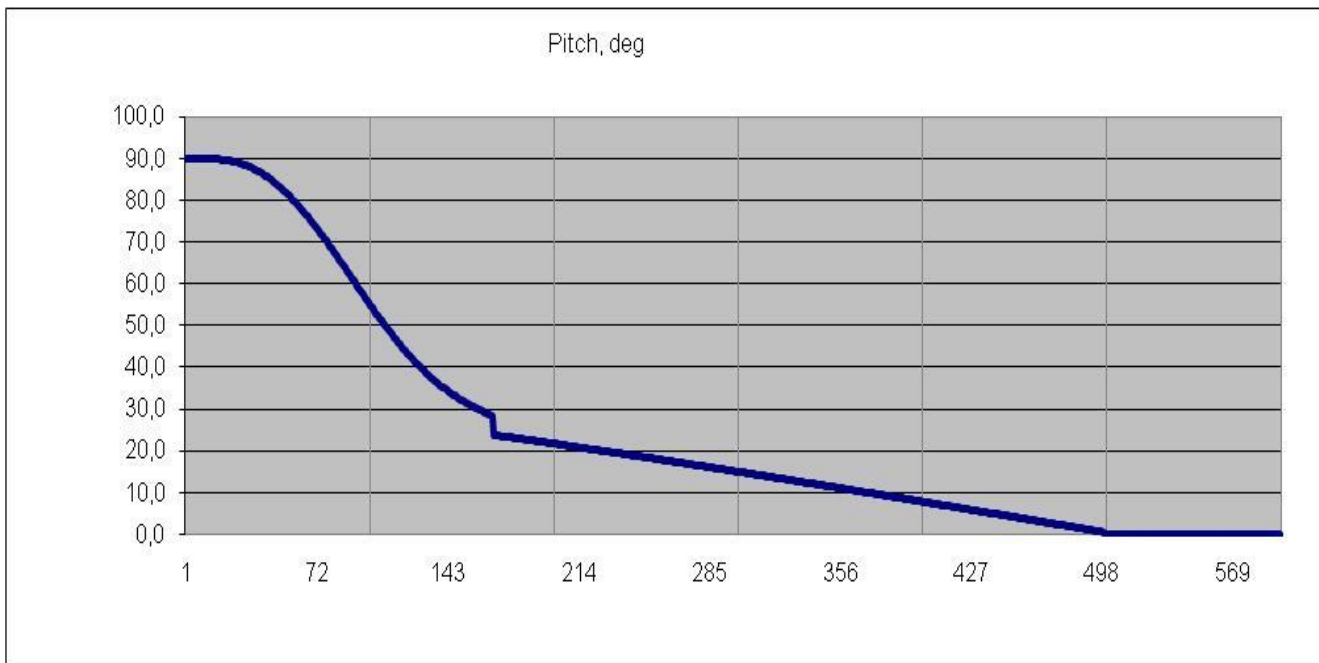


Fig. 28. Pitch Angle Change

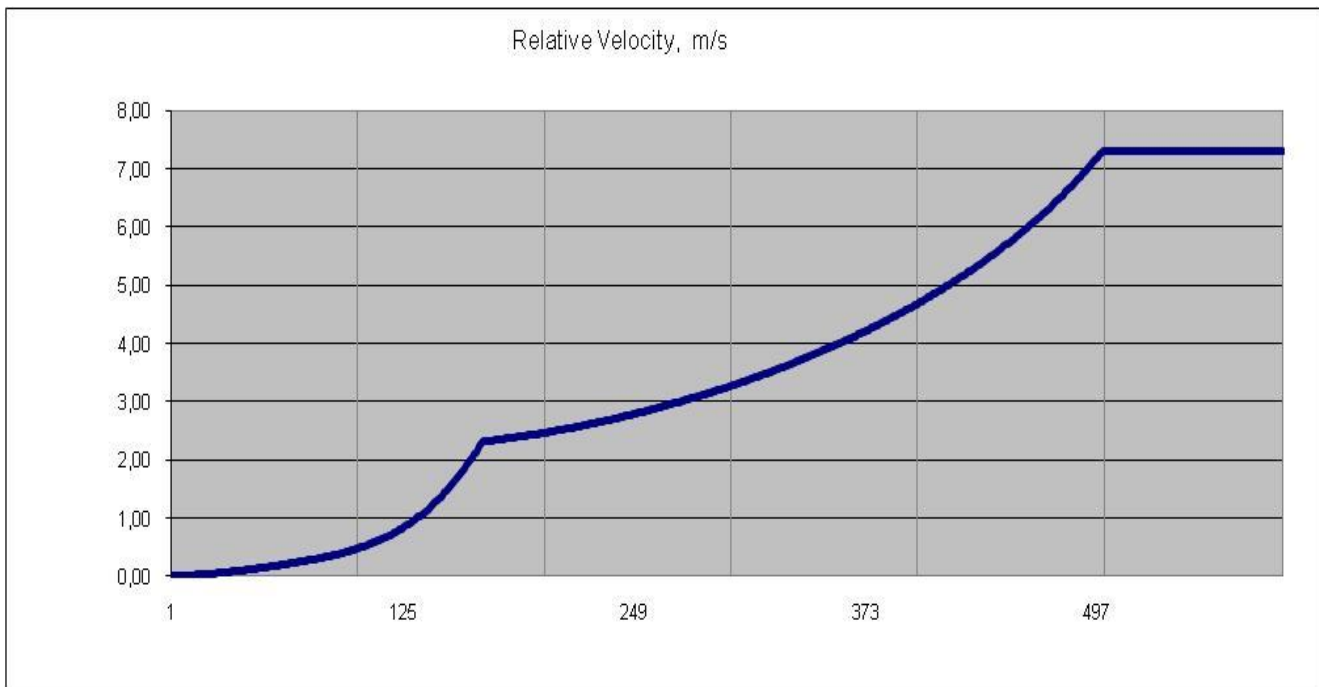


Fig. 29. Relative Velocity Change

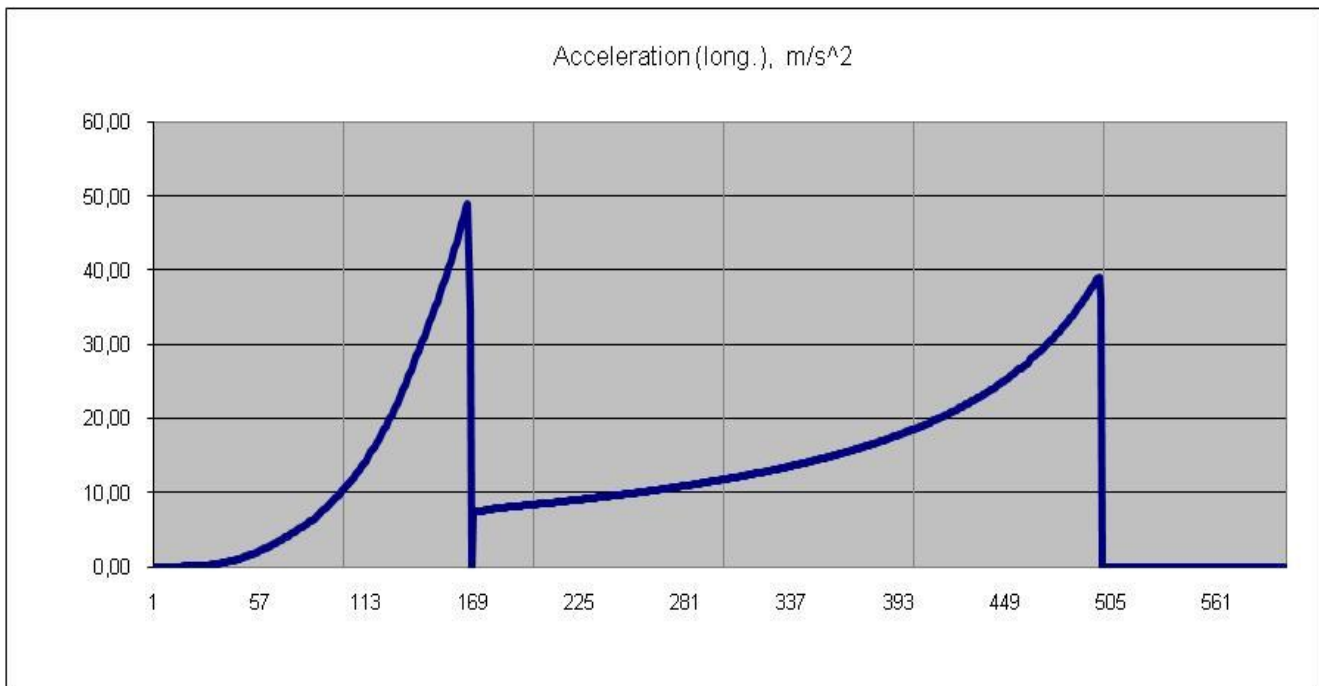


Fig. 30. Lateral Acceleration Change

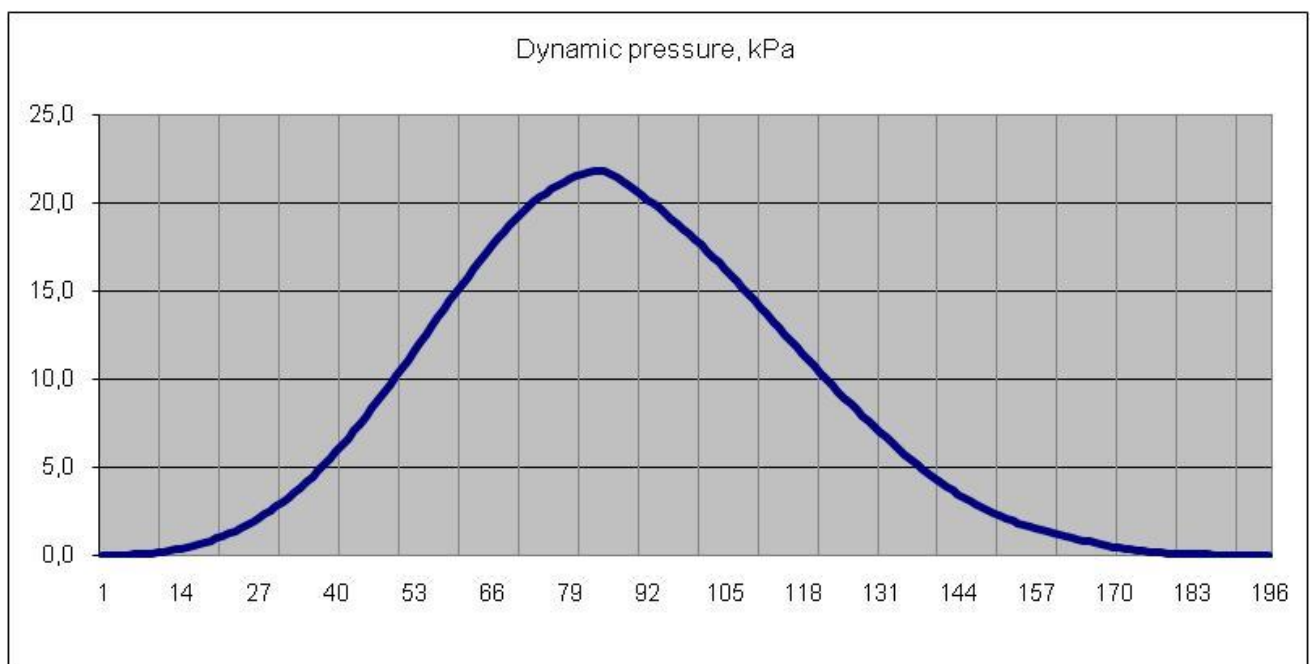


Fig. 31. Dynamic Pressure Change

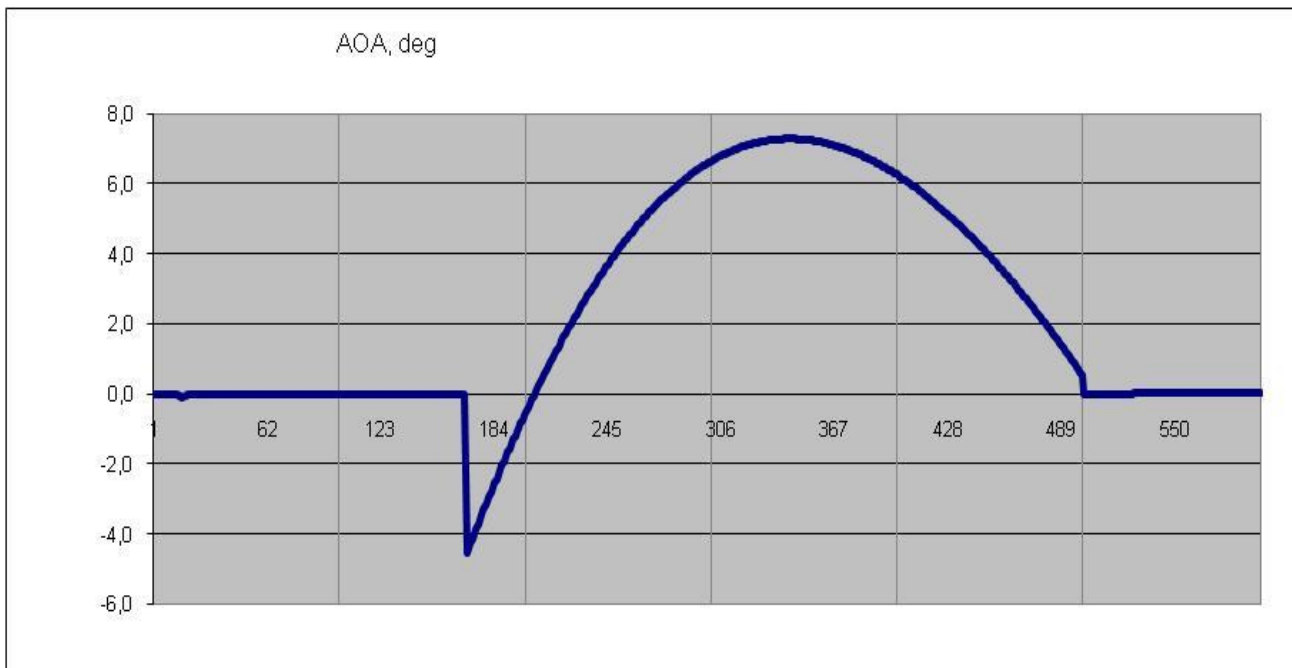


Fig. 32. Angle of Attack Change Program

Parameters of all the versions of the *Bulldog* family vehicles are gathered in the Table 8.

Table 8. Design Parameters of the *Bulldog* Family Vehicles Consolidated

Parameter	Bulldog Big	Bulldog Medium	Bulldog Little	Bulldog Puppy				
Appearance								
Launching Weight, kg	1,850,000.00	770,000.00	390,000.00	77,000.00				
Payload Mass, kg (at 200×200 km LEO, $i=0^\circ$)	34,748.7	15,365.01	8,140.00	1,156.00				
Stages								
	I	II	I	II	I	II	I	II
Launching Weight, kg	1,636,210.70	179,040.6	635,836.00	118,799	340,032.30	40,827.4	67,008.10	8,836.3
Jettison Weight, kg	176,480.00	22,985.9	74,498.40	13,023	34,424.00	5,019.8	8,871.60	935.1
Specific Impulse (at sea level), s	309.4	297.4	297.4	-	297.4	-	256.3	-
Specific Impulse (in vacuum), s	337	331	331	353	331	353	323	356
The Engine Type	3×RD-171M	NK-33	6×NK-33	3×NK-39	3×NK-33	NK-31	3×NK-39	RD-58M
Sea Level Thrust, tonnes of force	3×740 = 2,220	154.4	462	-	462	-	89.4	-
Vacuum Thrust, tonnes of force	2,418	171.4	514.206	124.5	514.206	41.5	112.6	8.5
Propellants Consumption, kg/s	7,17.07	517.82	3,106.98	352.69	1,553.49	117.56	348.74	23.88
Burn Time	205	303	182	301	198	306	168	332
Maximum Lateral G-Load Exerted	Not exceeding 6.5	Not exceeding 3.0	Not exceeding 4.5	4.5	Not exceeding 6.0	≈3.0	Not exceeding 5.0	Not exceeding 4.0

4.5. Some Considerations on the Possibilities of Recovering the First Stages on the Bulldog LVs

We consider recovering of the first stages of the *Bulldog* family launch vehicles. To maintain the aerodynamic envelope of the rocket while it moves through the dense atmosphere, we propose to apply a nose fairing which stays attached to the 1st stage and consists of three leaves. Before detaching the 2nd stage the fairing opens, and then closes back after the staging happens (see Fig. 33.) A possibility of splashing the returned 1st stage on water is worthy of consideration.

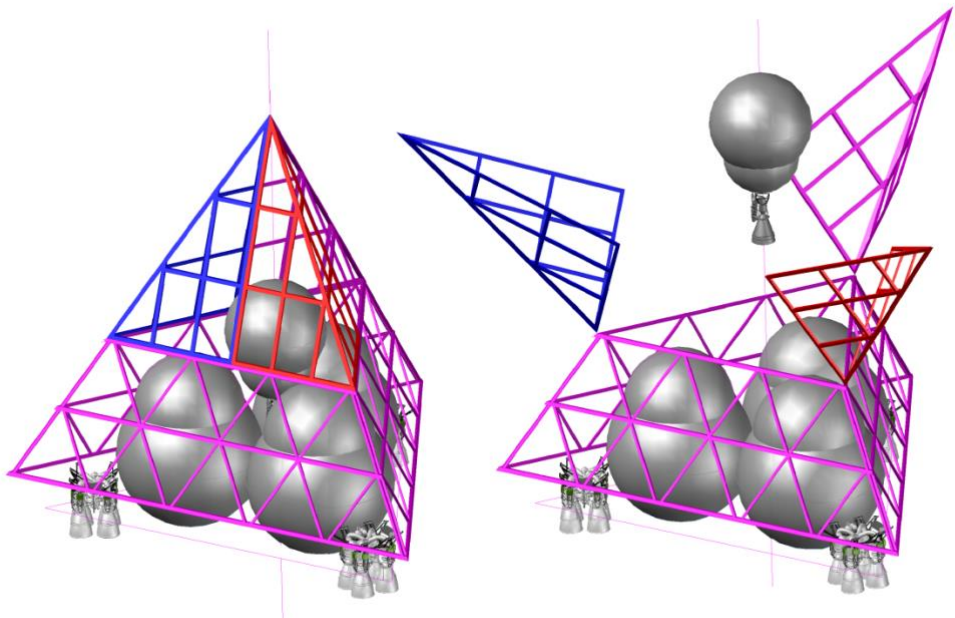


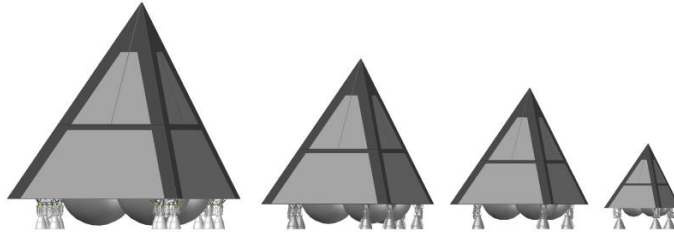
Fig. 33. Hinged Nose Fairing (one possible version shown)

It's self evident that to ensure splashing down in the “engines on top” position to rule out damaging the engines on impact, it's necessary to stabilize the returning stage in flight such way that it would be flying with the fairing aligned lengthwise to the velocity vector. The considerations of the attitude control and flight stability during the boosting and return phases alike, are beyond the scope of the current report, because they require a more complex modeling.

Let's instead estimate the water impact speed for every version of the *Bulldog* family rocket. To do so, we'll employ the Reentry Model, implemented as an MS EXCEL spreadsheet [4.] Let us assume the flight is ballistic (which means, no lift force is exerted³.) The initial data and the calculation results are shown in Table 9.

3 It's self evident, that such a condition requires maintaining zero angles of attack.

Table 9. Stage Return Trajectory Parameters

Parameter	The Bulldog LV Type			
	Big	Medium	Little	Puppy
Appearance				
Weight upon Return, kg	176,480.0	74,498.4	34,424.0	8,871.6
Frontal Area, m ²	363	210	97	27
Drag Coefficient Cd	1.0	1.0	1.0	1.0
Velocity at the Beginning of the Return Sequence, m/s	3,347	2,352.0	3,077.3	2,322.6
Altitude at the Beginning of the Return Sequence, m	87,000	74,500	81,400	63,200
Flightpath Vector Angle at the Beginning of the Return Sequence, degrees	17.6	28.1	19.9	28.5
Water Impact Velocity, m/s	92	77	77	74
Maximum Surface Equilibrium Temperature, Estimated, °C*	2,200	1,600	1,800	1,500

* - we assume the blunting radius at the critical point to be 0.1 m

The modeling results suggest that it's necessary to utilize a thermal protection in the top heating spots to prevent the stage's breaking up. The water impact velocity has to be regarded as excessive. To reduce it, we deem necessary to consider any air braking devices at the later stages of design (like parachutes, inflatable balloons, or braking rockets.)

An ordinary parachute system can deploy only at subsonic speeds, after the peak heating point is passed. This means that a parachute cannot serve to reduce the heating factor. The parachute's mass can take up to 5-10% of the recoverable stage's total mass. For example, the parachute to land the 1st stage of the *Bulldog Big* LV can be as heavy as 8.5-17 metric tonnes.

The braking rockets are also expected to have a considerable weight. Moreover, their usage requires careful guidance and attitude alignment of the stage prior to the splashdown.

We regard a usage of an inflatable parachute (a “space parachute”) a universal solution (Fig. 34.) Successful tests of inflatable air braking systems were undertaken in the USA, Russia, and China. Such parachutes can be deployed at supersonic speeds. They also help to reduce the structure's air friction heating in addition to reducing the splashdown velocity.

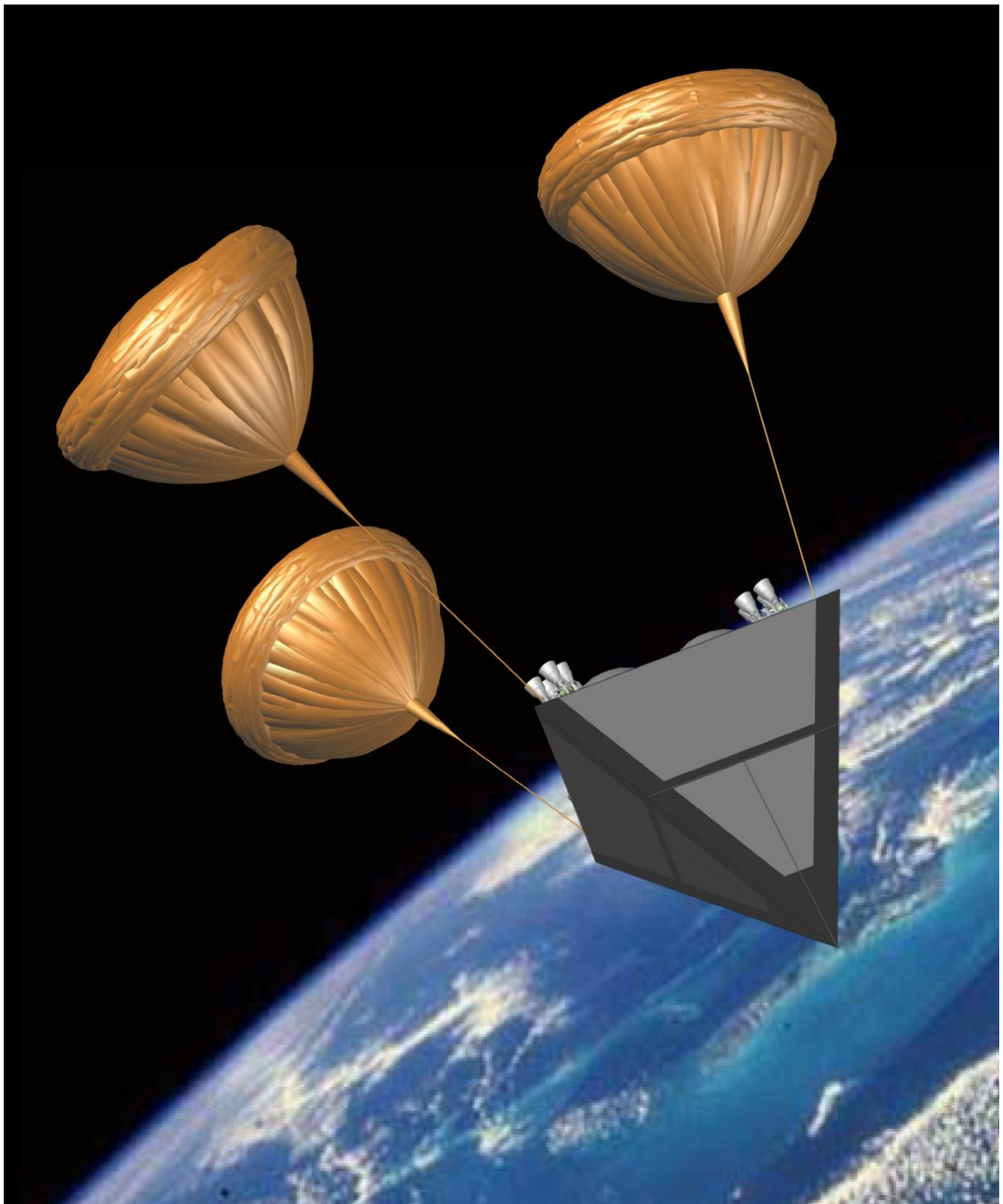


Fig 34. An Inflatable “Space Parachute”

5. Configuration, Structure, and Technology

The appearance of the *Bulldog* family rockets is that of a trifacial pyramid with an equilateral triangle shaped base. Each pyramid's face's outer shell consists of the structural framework and the skin. The framework and the skin are fabricated from stainless steels of AISI 301/304 type. The framework is a planar truss assembled with threaded joints from rectangular-sectioned thin wall pipes. The assembling diagram and the representative connection joints are shown in the Appendix 2.

The propellant tanks are welded from AISI 301/304 sheet steel. For the second stage of the *Bulldog Puppy* we recommend to fabricate the tanks from aluminum-scandium or aluminum-lithium alloys to save on the structure's weight. The selected tanks shape is a mutual intersection of two spheres (Fig. 34, 35.) Such a shape provides a denser configuration while maintaining a minimum weight. The 1st stages of the rockets hold three tank units, the 2nd stage has one such unit inside. For the *Bulldog Puppy* rocket alternative architectural layouts are considered.

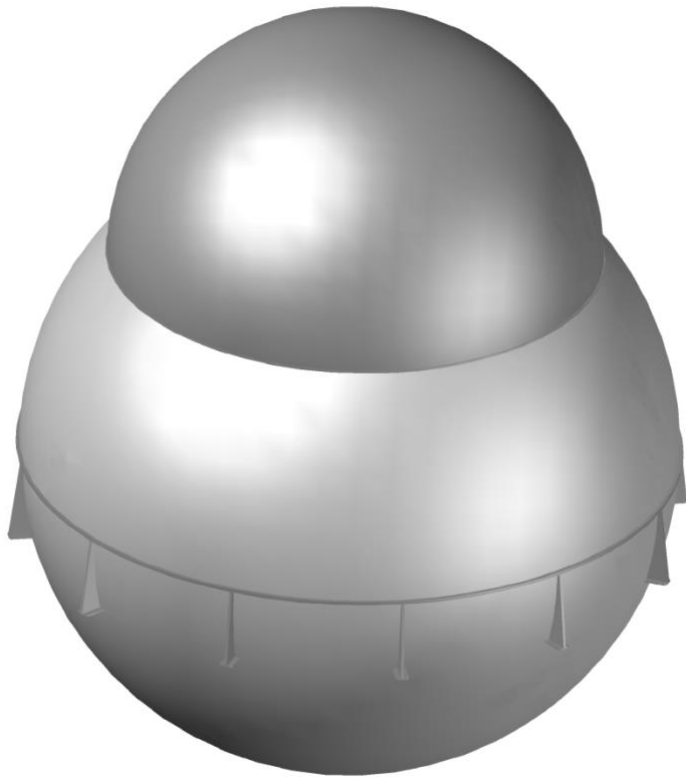


Fig. 34. Configuration of the Tank Unit of the First Stage

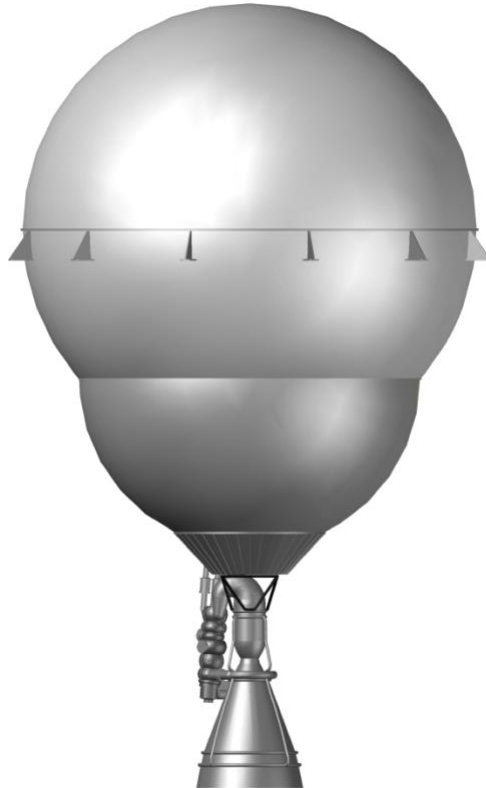


Fig. 35. The Tank Unit of the Second Stage

The tank unit volumes are shown in the Table 10.

Table 10. Tank Unit Volumes

Parameter	Bulldog Big		Bulldog Medium		Bulldog little		Bulldog Puppy	
	Stage I	Stage II	Stage I	Stage II	Stage I	Stage II	Stage I	Stage II
Number of the Tank Units	3	1	3	1	3	1	1	1
Number and Type of the Engines	3×RD-171M	1×NK-33	6×NK-33	3×NK-31	3×NK-33	1×NK-31	3×NK-39K	1×RM-58M
One Unit's Oxidizer Tank Volume, m ³	324.4	105.2	123.8	70.5	67.4	23.9	38.6	6.7
One Unit's Fuel Tank Volume, m ³	174.5	56.6	69.3	38.4	37.7	13.0	21.0	2.7

The structural design layouts of the *Bulldog* family vehicles are represented at the diagrams below (Fig. 36-39.) The design layout of the *Bulldog Puppy* rocket is studied in several variations. The primary design with integrated tanks is analogous to all the other *Bulldog* vehicles (Fig. 39a.) The alternative versions include a one-piece modular architecture (one module per the stage,) as well as a version with separate (Fig. 39b) fuel and oxidizer tanks. The second version provides for a simpler manufacturing and

assembling technology, and presumably lesser total weight of the structure. The offset of the center of gravity which emerges in this layout is easily made up for by shifting the engines by 0.2 m towards the oxidizer tanks.

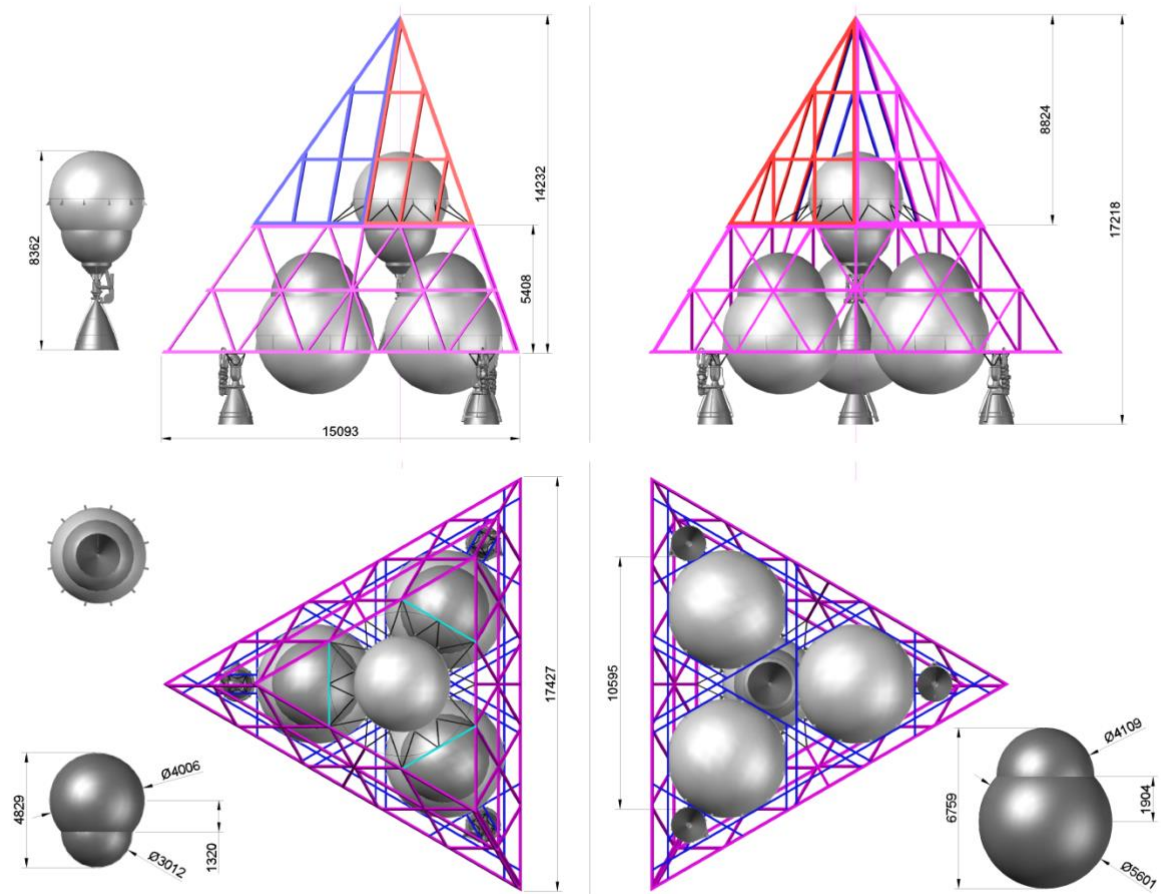


Fig. 36. Structural Layout of the *Bulldog Little* rocket

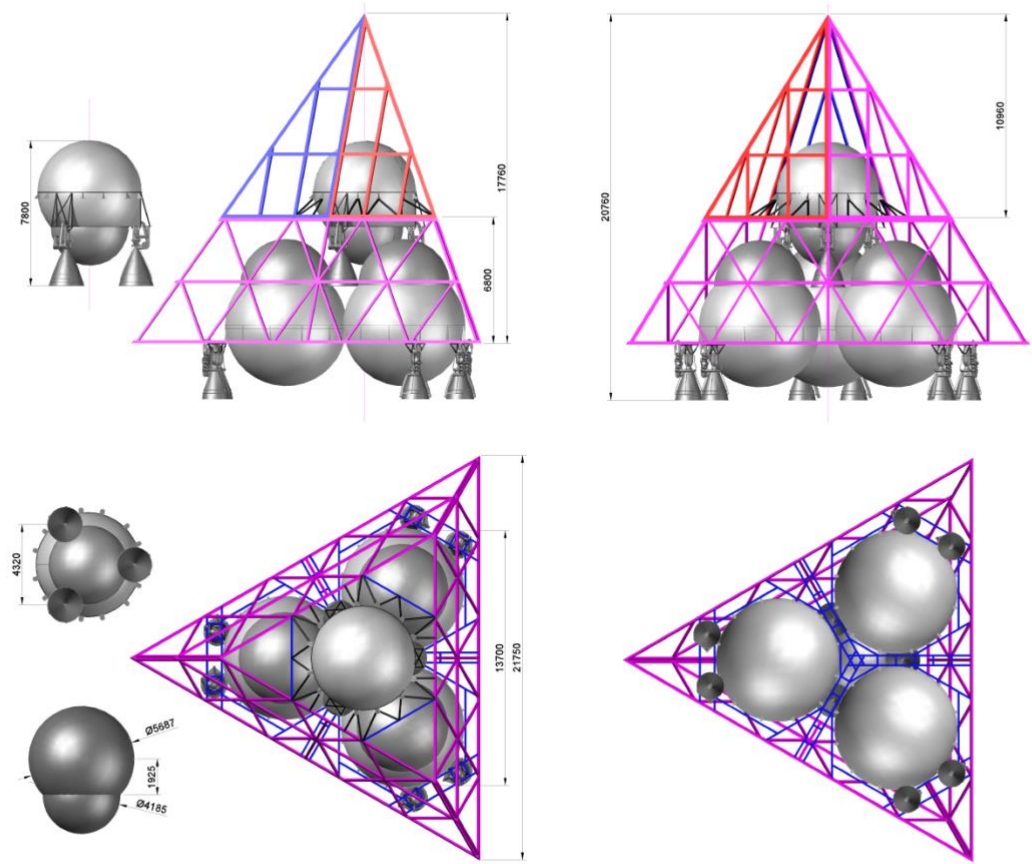


Fig. 37. Structural Layout of the *Bulldog Medium* rocket

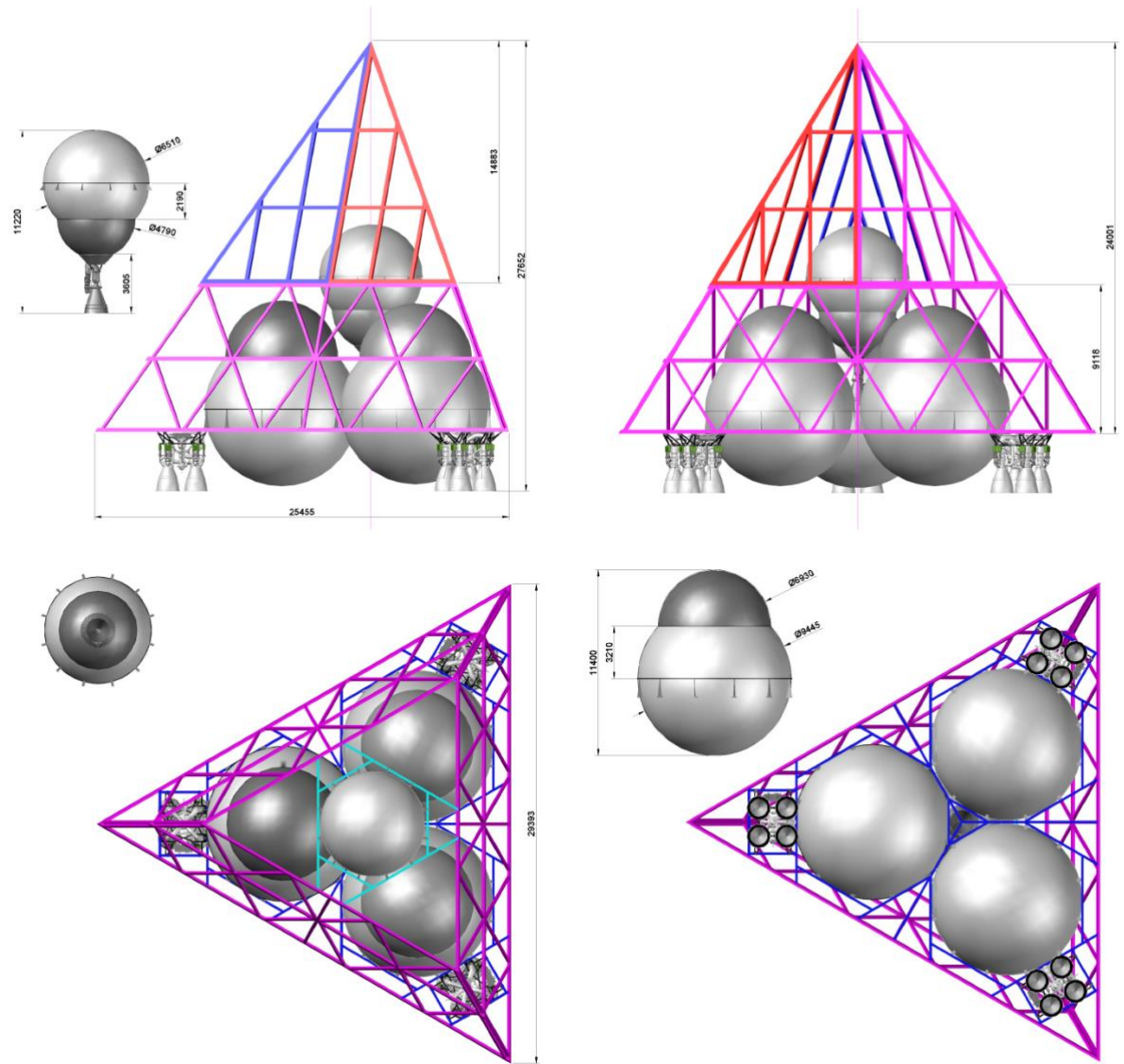


Fig. 38. Structural Layout of the *Bulldog Big* rocket

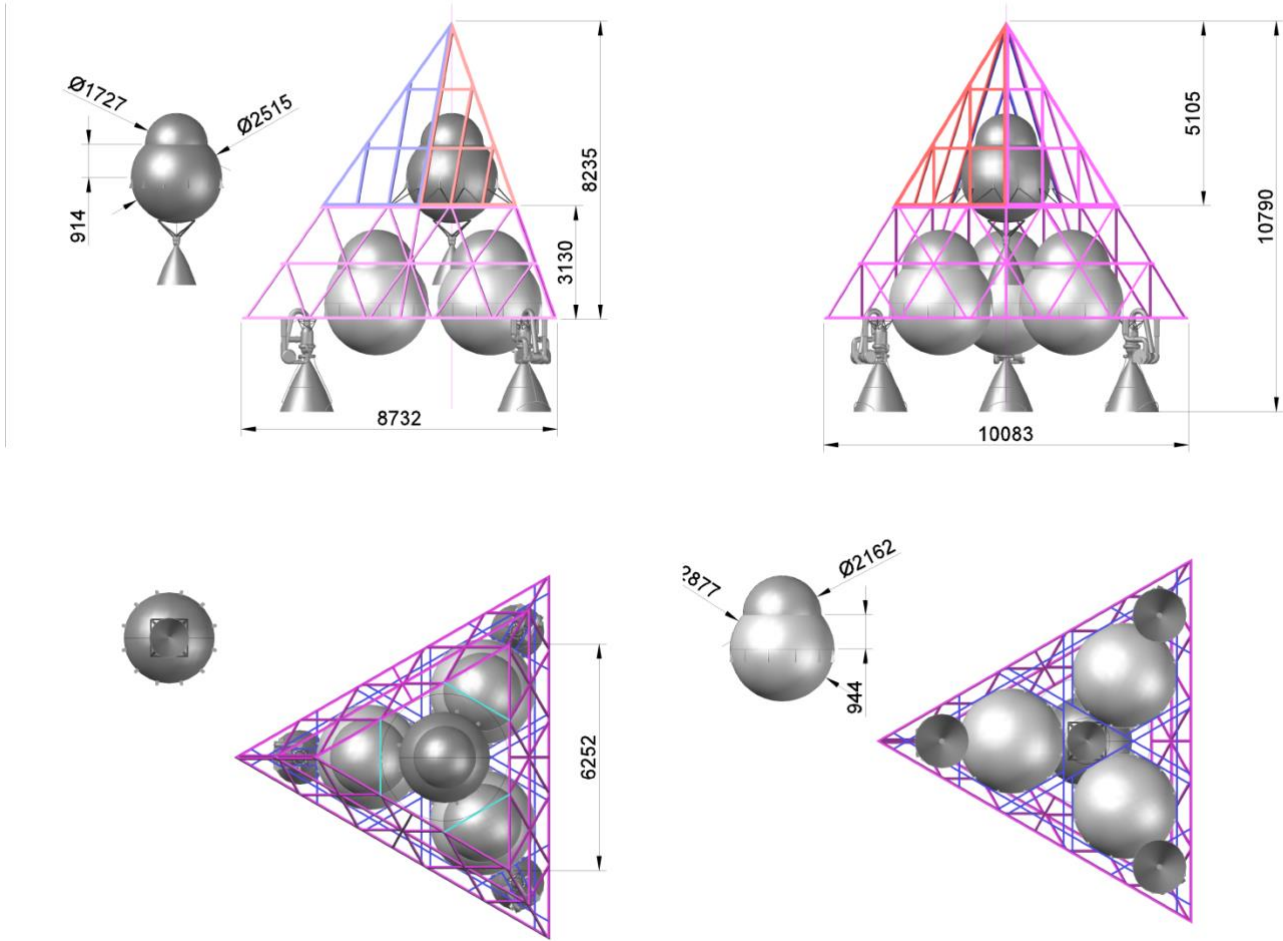


Fig. 39a. Structural Layout of the *Bulldog Puppy* rocket

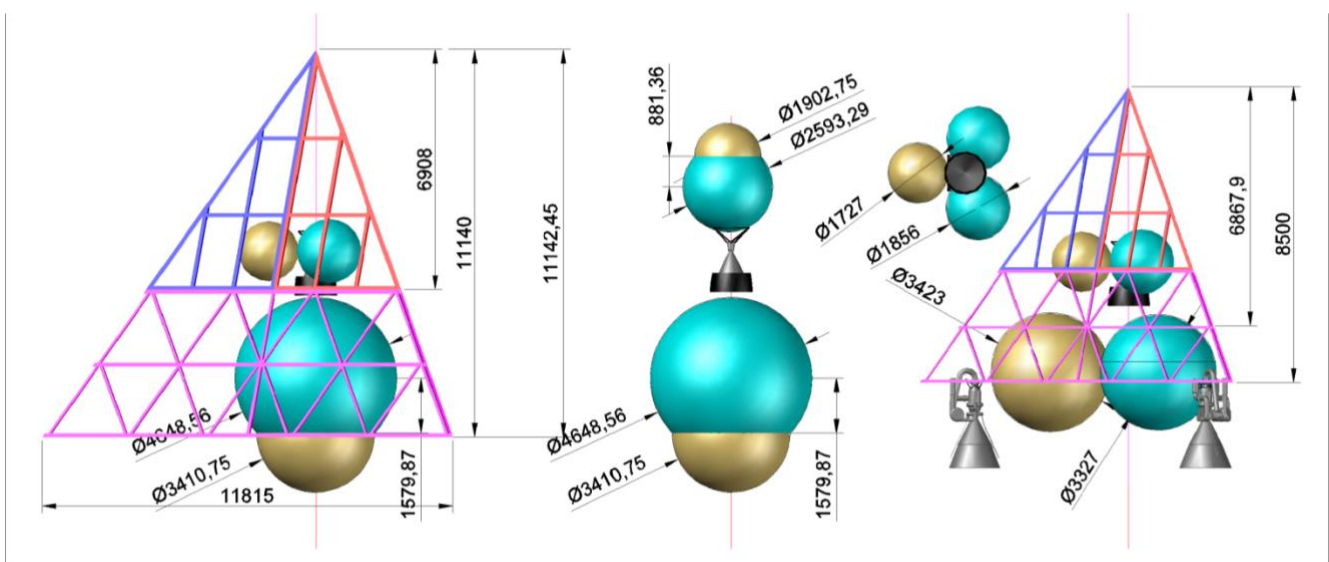


Fig. 39b. The Alternative Structural Layouts of the *Bulldog Puppy* rocket

6. Refinement of the Aerodynamic Characteristics and the Structure's Heating During the Boosting Phase

On request of Lin Industrial company an evaluation of the drag coefficient C_d^4 was performed (Appendix 2.) Because of a limited amount of resources at the performer's disposal, the evaluation was carried out for two Mach numbers, $M=0.5$ and $M=1.21$ (for the maximum dynamic pressure point.) The calculated drag coefficient values are equal to 0.57 and 0.96, correspondingly. This is much larger than it was presented in the Patent US 9,475,591 B1 (Fig. 1 and 2.) Specifically, the patent had it like 0.3 and 0.5 for the corresponding points.

The undertaken computations also indicate a vigorous aerodynamic heating: the maximum equilibrium temperature is sustained at 800°C at the pyramid's tip and up to 650°C at the pyramid's edge. Such high temperatures may cause the structure's disintegration, which calls for a heat protection measures even at the boosting phase of the flight (we had noted above that during the return phase the temperature might increase to $1500\text{--}1800^{\circ}\text{C}$.)

7. Estimating of Alternative Versions

The variations of the *Bulldog* vehicles described above are based on available Russian-made engines that operate on liquid oxygen and kerosene. While staying within the selected concept of a pyramidal shape, the alternatives boil down to selecting of other engines or different propellant components as well as engines.

7.1 Alternative Engines

Potentially, Merlin 1D+ and their altitude variation Merlin Vac can become commercially available. It makes sense to employ these on the 1st stage of the rocket (in sets of three at each corner of the pyramid.) The Merlin engines are distinctive for their low mass (the thrust to weight ratio in vacuum for the empty engine is about 200:1,) and an acceptable specific impulse. The design parameters for this alternative are shown in Table 11. It's clear, that improving the rocket's figure of merit will improve the payload capacity of the given type of a rocket.

Table 11. Design Parameters of the Bulldog Medium Vehicle with Merlin Engines

Parameter	Value	
The Launcher Rocket		
Launching Weight, kg	650,000.00	
Payload Mass, kg (at 200×200 km LEO, i=0°)	13,467.06	
The Stages		
	I	II
Launching Weight, kg	545,485.0	91,048.0
Jettison Weight, kg	59,994.2	7,662.4
Specific Impulse (at sea level), s	288.0	-
Specific Impulse (in vacuum), s	312	348
The Engine Type	9×Merlin 1D	1×Merlin Vac
Sea Level Thrust, tonnes of force	774.0	-
		95.21
Vacuum Thrust, tonnes of force	838.5	
Propellants Consumption, kg/s	2,687.50	273.59
Burn Time	182	306
Maximum Lateral G-Load Exerted	Not exceeding 5.0	Not exceeding 4.0

It's possible that the engines produced by Ursa Major Technologies [5] are also commercially available: The Hadley with about 2.2 tonnes of force thrust and Ripley with about 15.8 tonnes of force thrust. For example, we can hypothesize a *Bulldog Puppy*'s version with the Ripley engines on the 1st stage and the triple Hadley engines on the

second stage. Unfortunately, exact parameters of those engines are not disclosed, and therefore we could not do the design parameters estimation. However we can expect that the *Bulldog Puppy* might deliver up to 1000 kg of payload to the orbit on Ripley engines.

Out of the alternative propellants, the most promising are the Liquid Oxygen + Liquid Methane (a liquified natural gas), and Hydrogen Peroxide + Kerosene. Many regard Liquid Methane a promising fuel for rocket systems, and, in the first place, the reusable rockets, because of the following reasons:

- It does not produce hard deposits in the engine's lines;
- It has a great cooling ability;
- It freely evaporates from the engine's chambers, and no special post-flight purging is required;
- Its liquid state temperature is close to LOX temperature, which provides for a simple tank unit design with a common wall;
- Methane's molecular mass is little, and it can be used to pressurize methane tanks instead of Nitrogen or Helium;
- It's relatively cheap;
- It provides a greater specific impulse (by 3-5%) as opposed to Kerosene.

A considerable drawback of Methane is a lesser density, which results in a greater volume and weight of the Methane holding tank than we could have with Kerosene. However, a careful designing and accounting for all the positive qualities of Methane might even cut down the total weight of the propellant compartment by few percent as opposed to the same unit of a LOX+Kerosene rocket. Considering a greater specific impulse, usage of Methane provides for a 10-15% decrease of the launching weight of the rocket while maintaining the same payload capacity.

In the nearest future, BE-4 by Blue Origin company might become a commercially available Methane engine (Fig. 40.)



Fig. 40. BE-4 Engine

At the present moment, only the estimated thrust value for this engine is known: about 250 tonnes of force at sea level. We can then safely reckon, that this liquid

propellant engine can serve as a power plant only for the medium and heavy versions of the *Bulldog*.

Lin Industrial company stays ready to perform a study with the mentioned American-produced engines, in case the engine mass and specific impulse information becomes available.

Speaking about Hydrogen Peroxide, its advantages as an oxidizer are known for a long time:

- It's available on the market;
- It has a high density (by about 1/3 more, than LOX has;)
- It's can be stored for a long time;
- The Peroxide splits over a catalyst with heat emission, which simplifies the fuel ignition;
- In the normal conditions it stays in a liquid state, which provides for a simple tank unit design with a common wall with a Kerosene tank.

The disadvantages of Hydrogen Peroxide are a low specific impulse (about 10..15% less than LOX+Kerosene propellant pair has,) and a problematic storage at high concentrations. This calls for considering a use of Hydrogen Peroxide on the *Bulldog Puppy* rocket. Unfortunately, no Peroxide engines with a fitting thrust exist on the market, and designing them will be a brand new effort. Based on the accumulated experience of Lin Industrial with Peroxide engines, we can estimate the design parameters of the *Bulldog Puppy Peroxide* (Table 12):

Table 12. The Design Parameters of the *Bulldog Puppy Peroxide* rocket

Parameter	Value	
The Launcher Rocket		
Launching Weight, kg	71,981.50	
Payload Mass, kg (at 200×200 km LEO, i=0°)	1,100.00	
The Stages		
	I	II
Launching Weight, kg	62,426.18	8,455.28
Jettison Weight, kg	6,981.79	709.85
Specific Impulse (at sea level), s	263.6	-
Specific Impulse (in vacuum), s	290	312
The Engine Type	A New Item	A New Item
Sea Level Thrust, tonnes of force	108.0	-
Vacuum Thrust, tonnes of force	118.8	7.32
Propellants Consumption, kg/s	409.6	23.5
Burn Time	137	332
Maximum Lateral G-Load Exerted	Not exceeding 7.0	Not exceeding 4.0

8. Ground Infrastructure

The *Bulldog* rockets are expected to launch from a water-floating position, and therefore no ground-based infrastructure like a launch pad or towers are required. The rockets should be built at the seaside, which requires a construction area several hectares large. This must include:

- Warehouses to accumulate and hold structural steel and other construction materials;
- An assembling pad with the necessary equipment to manufacture the rocket;
- Welding workshops to weld the tanks;
- Propellant component storage;
- A launching slipway to put the ready rocket afloat.

It's possible that the rocket would be best built on a submersible pontoon. In this case, the rocket is towed to a launch spot with its engines protected from the salty water contact. After reaching the launch position, the pontoon is flooded, submerges and removed from under the rocket. But a proposal of Ripple Aerospace company (Norway) in the *Sea Serpent* rocket project (Fig. 41) [6] looks much more appealing: they are going to assemble the rocket in a floating drydock. In contrast to Ripple Aerospace's concept, the *Bulldog* rockets should be assembled in the upright position.

One or several towing ships will be required to tow the rocket to the launch spot, depending on how great the empty mass of the rocket is (the exact details need an additional elaboration on.)

To fuel the rocket, two service ships are necessary, one to bring and pump in the oxidizer, and another for the fuel. We can assume that these fueling ships can be built out of relatively small tankers, or they could be custom built. To control the launch, a command ship is necessary. One possibility is to merge the roles of the fuel delivering tanker and the command ship.

An important question is how bad an impact on the ecology of the launch would be, namely, the acoustic and the emission pollution factors. Even considering that pollutant emission is a negligible part of the total emission amount, starting up the engines in water can inflict a damage upon the oceanic life.

Generally speaking, launching the large rockets right from the ocean surface is poorly researched, because no practical experience in this field was yet accumulated by anyone. To research the problems posing a value for the project in the experimental way, we propose to build a technological flight demonstrator.

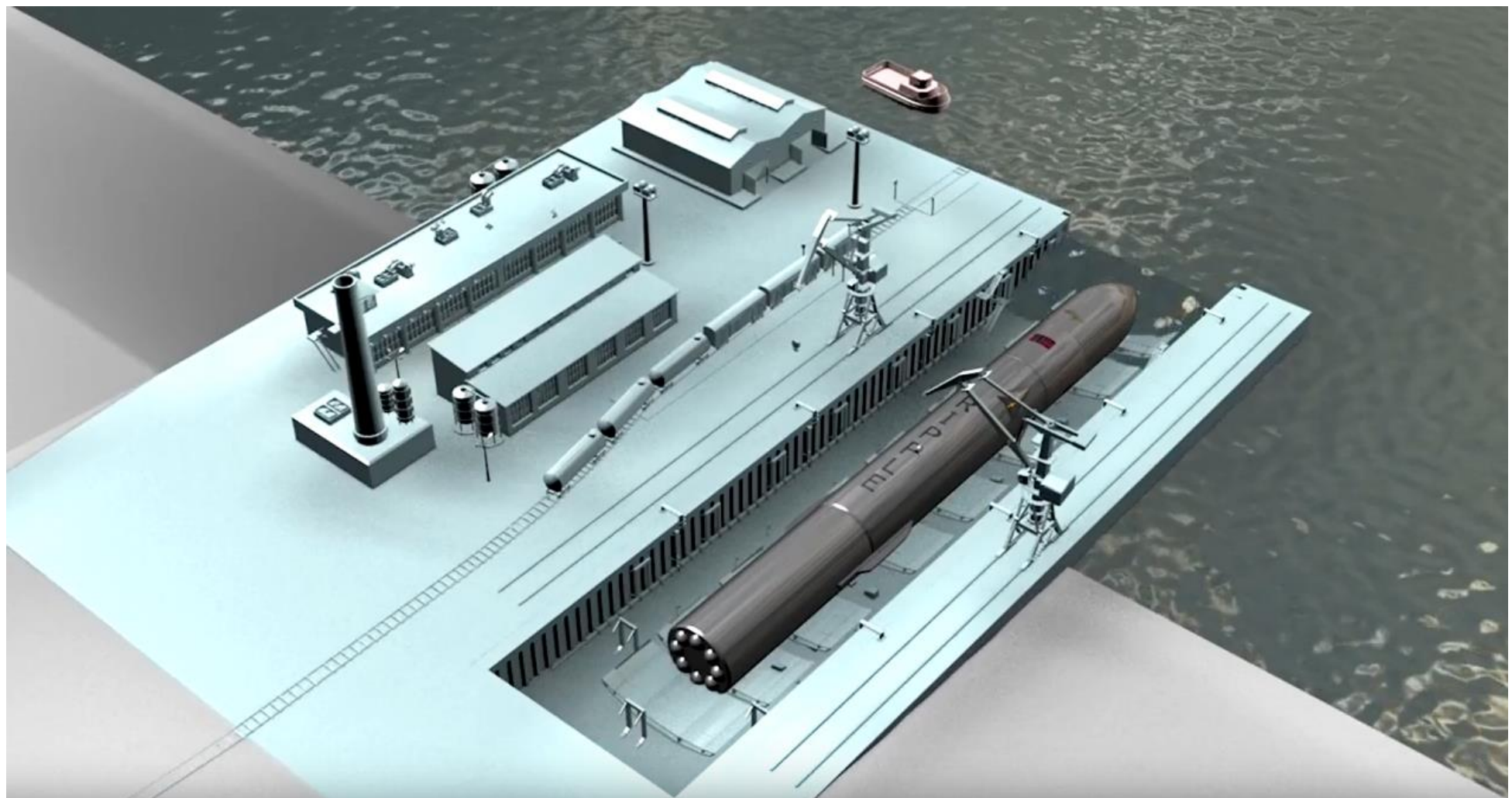


Fig. 41. Assembling a Rocket in a Drydock

9. The Bulldog Demo Flight Demonstrator. The Steps of the Project Implementation.

9.1. Demonstrator

Lin Industrial company has worked on Hydrogen Peroxide oxidizer rocket engine development over several years. At the present moment the company is developing series of engines with 15 to 2,500 kg of force thrust, including a mono-propellant engine with up to 300 kg of force thrust (which uses the Peroxide as the only propellant.)

The structural layout of the Bulldog Demo reproduces the primary project idea, the trifacial pyramid shape. The single-stage demonstrator is intended to solve several problems:

- To determine the aerodynamic characteristics in the subsonic and slightly supersonic velocities;
- To assess controllability and stability of the model;
- To research the dynamic and the acoustic properties during the water surface launch;
- To practically test the nose fairing leaves' opening and closing;
- Rectification of the structural layout.

We propose to outfit the demonstrator with three engines providing a 300 kg of force thrust at sea level. The demonstrator's design parameters estimation is given in the Table 13.

Table 13. Design Parameters of the *Bulldog Demo* rocket

Launching Weight, kg	550.00
Payload, kg	50.00
Payload content	telemetry, sensors, recovery parachute system, etc.
The Initial Mass of the Module, kg	500.00
The Burnout Mass of the Module, kg	100
Isp (atm) (s)	263.6
Isp (vac) (s)	290
Vacuum Thrust, tf	0.99
Fuel Consumption, kg/s	3.41
Burn Time, s	119

The diagram of the *Bulldog Demo* demonstrator is shown at Fig. 42. The spherical tank with 0.84 m diameter can hold about 400 kg of the Peroxide. The pyramid's base is an equilateral triangle with about 1.5 m long side. While flying

straight up, the demonstrator can reach the altitude of about 90 km and accelerate to about 1,050 m/s. If the payload mass is cut to 20 kg, the maximum reached altitude grows to 140 km, and the top speed to 1,350 m/s.

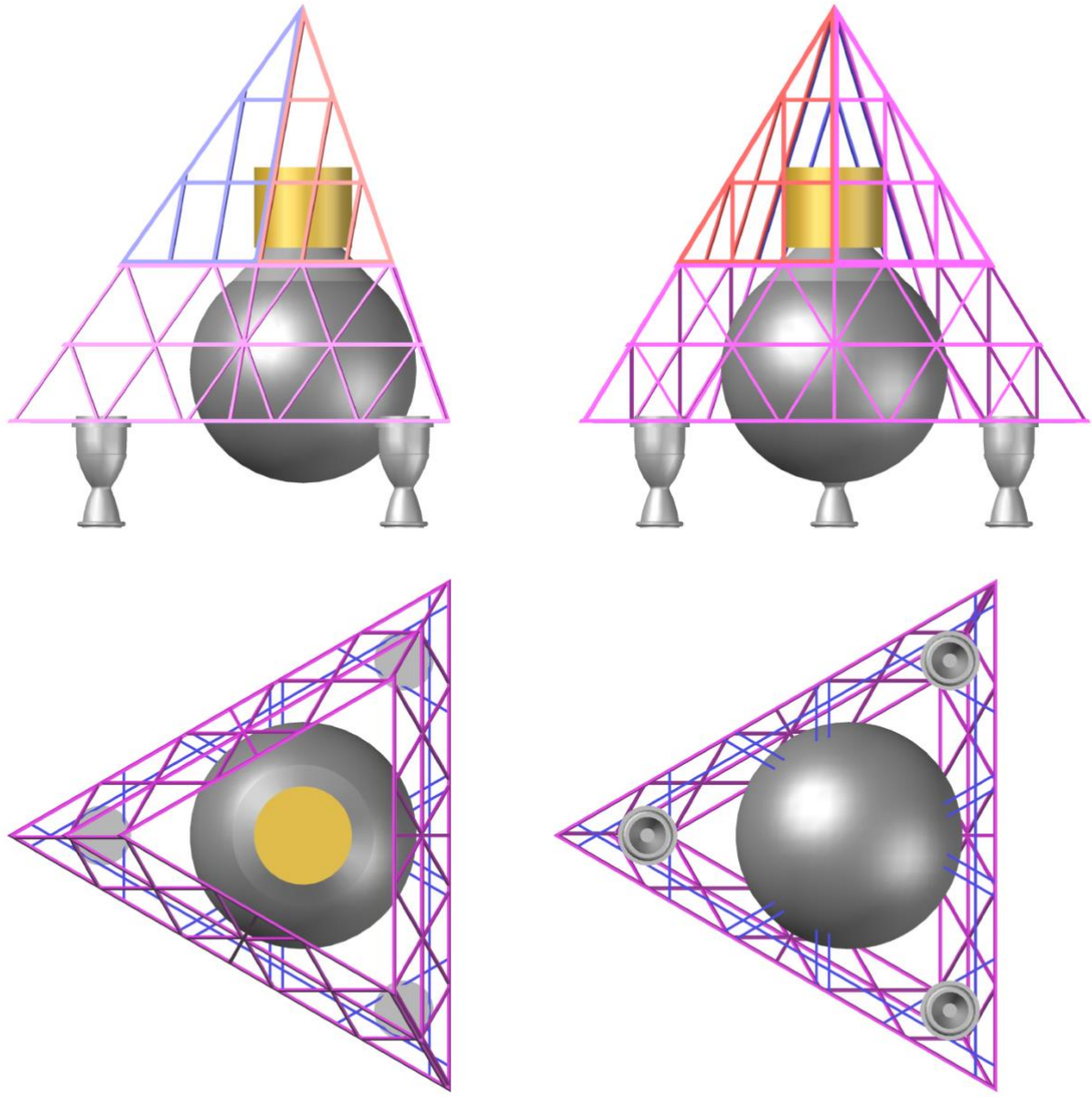


Fig. 42. The *Bulldog Demo* Demonstrator Structure

9.2 The Project Roadmap

The project is implementable in several stages, which we describe in this report at high level.

Stage 1. Development and Testing of the Bulldog Demo demonstrator

This stage is projected to take 18 months. The contractor at this stage may be Lin Industrial company. The work scope includes:

- Developing the projects of the liquid propellant engine and of the Bulldog Demo rocket;
- Building and testing of the engines;
- Building the demonstrator;
- Ground and flight testing of the demonstrator;
- Performing the experimental flight program, water launches, refinement of the aerodynamic and acoustic characteristics.

This stage's cost is about **\$150,000**. In the outcome of this stage we get a concept proof of the “flying pyramid” feasibility and initial data for a real launcher vehicle's designing.

Stage 2. Designing and Building of the Bulldog Puppy

This stage will be 60 months long. It is probably justified to select a USA-based company as the primary contractor at this time. Lin Industrial company will dispose itself to consulting and supplying of various services. The works at this stage include:

- Designing of the rocket, fabricating the test and flight hardware;
- Foundation of the manufacturing space and the seaport infrastructure;
- Ground and flight tests;
- Entering the commercial service;
- Clarification of the commercial prospects on the changing space launch market;
- Deciding on the further development of the larger specimen of the *Bulldog* family.

This stage's cost is estimated from **15 to 100 million** US Dollars. In the end of it, the company will have: a light class rocket available for commercial services, a feasibility study of the larger rockets development, a production ready technology and manufacturing environment, a team of dedicated professionals.

Stage 3. The complete implementation of the project

The exact work scope of this stage, its overall feasibility and required expenses should be determined upon the practical results obtained on the 1st two stages, with consideration of the would-be state of affairs at the commercial launch market.

10. Conclusions and Recommendations

10.1. Conclusions

Upon completion of the performed engineering study, we found the following:

- The computations have shown that the pyramidal rocket concept is feasible;
- We have been able to select commercially available rocket engines with near-optimal thrust levels for almost the entire scoped range of payload masses;
- To ensure recovery and reuse of the 1st stage, it's necessary to utilize additional air-braking devices; otherwise the stage is going to be seriously damaged;
- Any measures reducing the structural heating should be deemed necessary, because the projected heating level is dangerous. The calculated top heating temperatures exceed the steel flowing temperature, which means, the structure is going to disintegrate in the peak heating points;
- It's best to develop a midget-sized demonstrator to test proof the concept and rectify the issues of concern;
- The pyramidal structure helps a simple spatial framework assembling, but results in a sparse packaging density, which increases the dry mass of the rocket and the drag force.

10.2. Recommendations

In this case our recommendations are concerning countering the found issues of the trifacial pyramid structure. In particular, we propose to consider a six-faced pyramid with unequal sides (Fig. 43.) Such a configuration, should, of course, pass an optimization. However, it can decrease the drag and possibly decrease the structure's weight while maintaining the technological simplicity of the original concept.

One more idea is to change the geometric proportion of the pyramid by making it taller (Fig. 44.) In this case we have to reject the multiple modular layout of the 1st stage's propellant compartment. In addition, the pyramid may be four- or six-faced.

These and other configurations should be reviewed on the following stages of design.

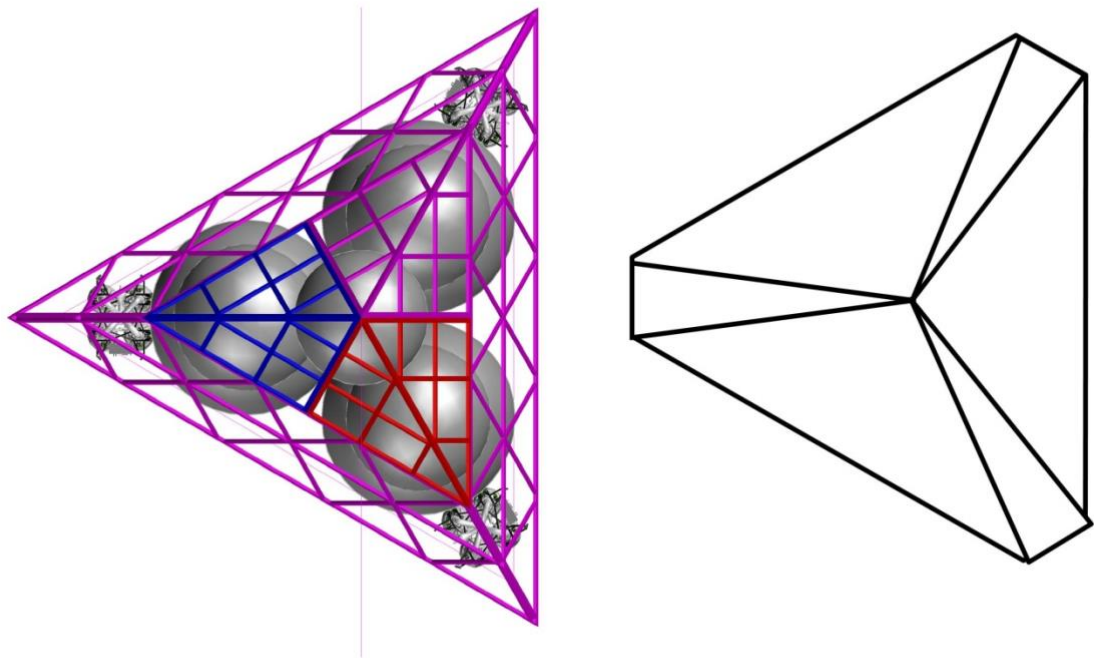


Fig. 43. A Better Shape Proposal: at left side is the initial shape; at right side is a six-faced pyramid

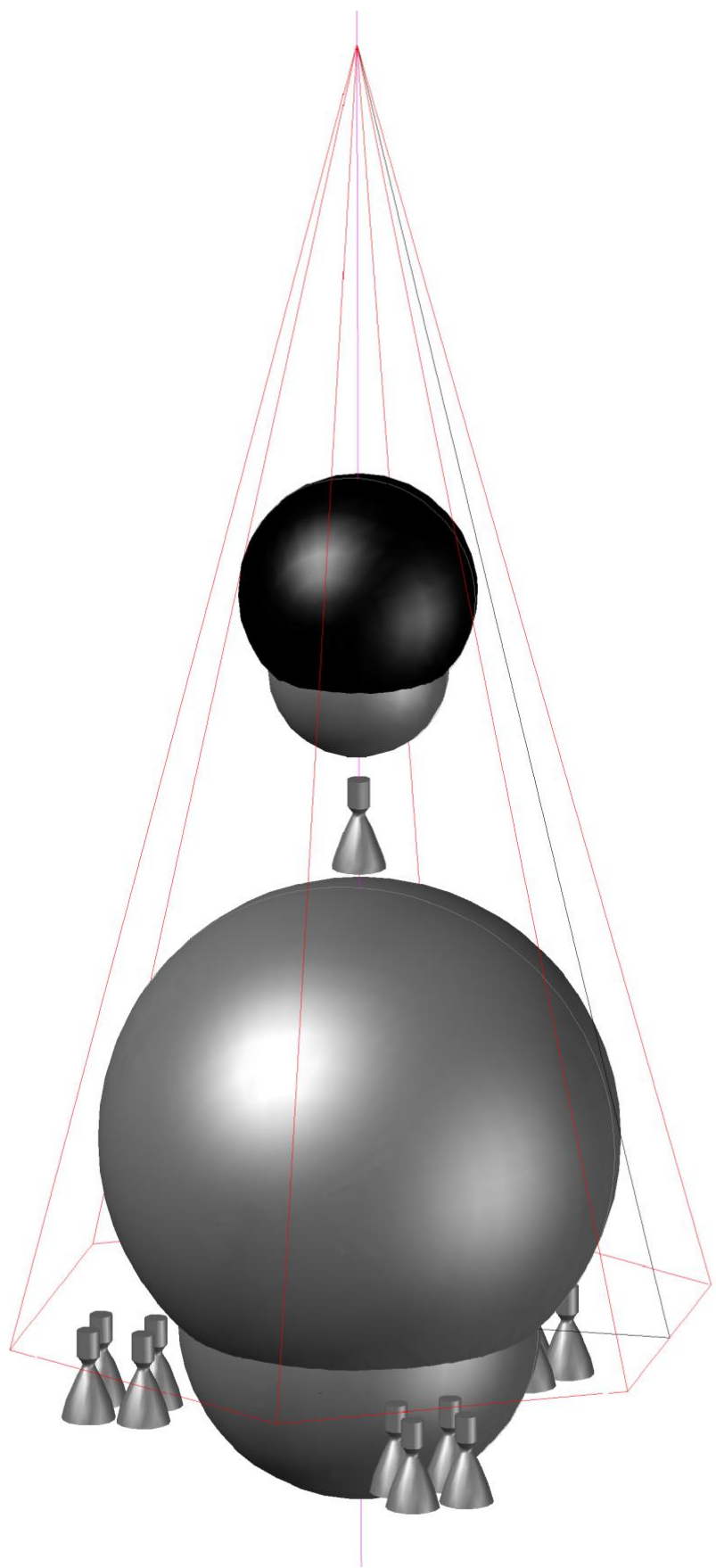


Fig. 44. The 6-faced Pyramid's Layout with the Single-Block Propellant Compartments

Sources

1. <https://trade.glavkosmos.com/ru/catalog/launch-vehicles/engines/liquid-fuel-rocket-engine/rd-120-ms/>
2. <http://www.geocities.ws/levinkirill/SpaceModel/rus/LaunchModel.html>
3. <https://trade.glavkosmos.com/ru/catalog/launch-vehicles/engines/liquid-fuel-rocket-engine/rd-120-ms/>
4. <http://www.geocities.ws/levinkirill/SpaceModel/rus/ReentryModel.html>
5. <https://www.ursamajortechnologies.com/>
6. <https://www.youtube.com/watch?v=g5OdEtsJDpM>

Appendix 1

The Bulldog Rocket Assembling

To assemble a *Bulldog* rocket, the following set of steps should be followed:

1. Propellant tanks are welded at the special manufacturing area near the dock. The workspace is organized like it was done at the Starship fabrication pad in Boca Chica (Fig. 1.) Meanwhile, the assembling of the base truss begins in the drydock. Engines are then installed on the base frame. This assembly becomes the “groundwork” of the rocket.



Fig. 1. Tank Assembling

The welded and put together tank modules are moved to the assembling dock where they are connected inside the building berth with the load frame before the final assembling commences. The Figures 2-27 show the assembling sequence.

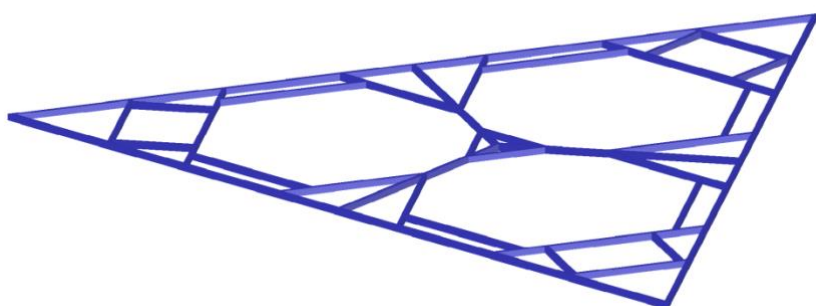


Fig. 2. The 1st Stage's Base Truss

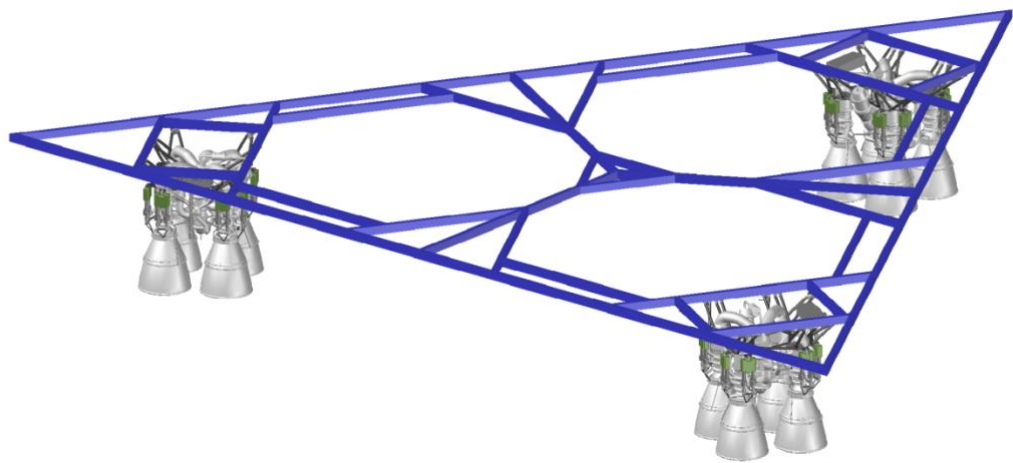


Fig. 3. Mounting the Engines onto the Base

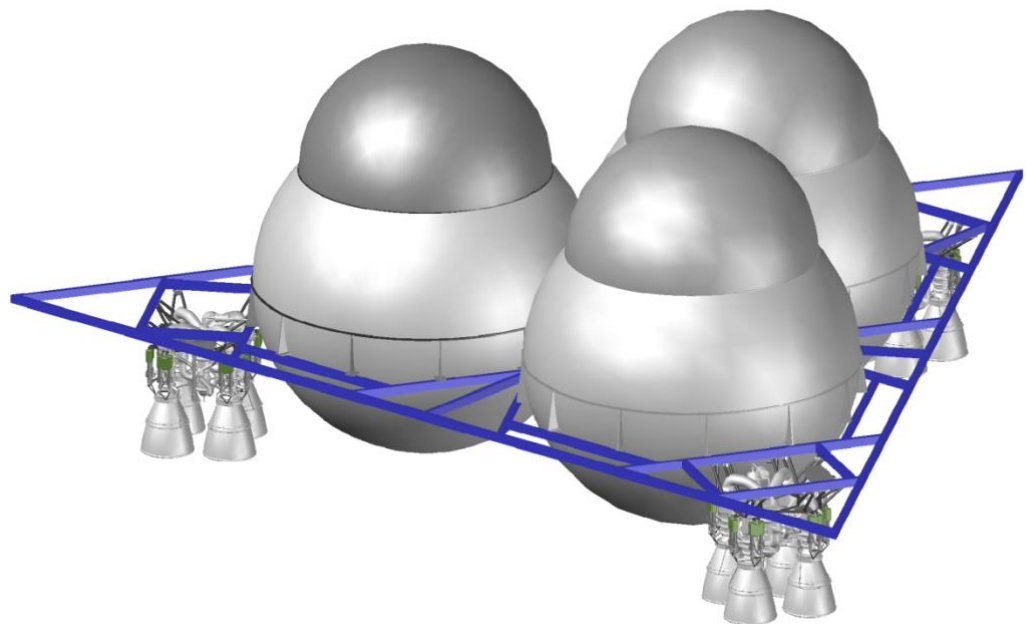


Fig. 4. Mounting the Propellant Tank Modules onto the Base

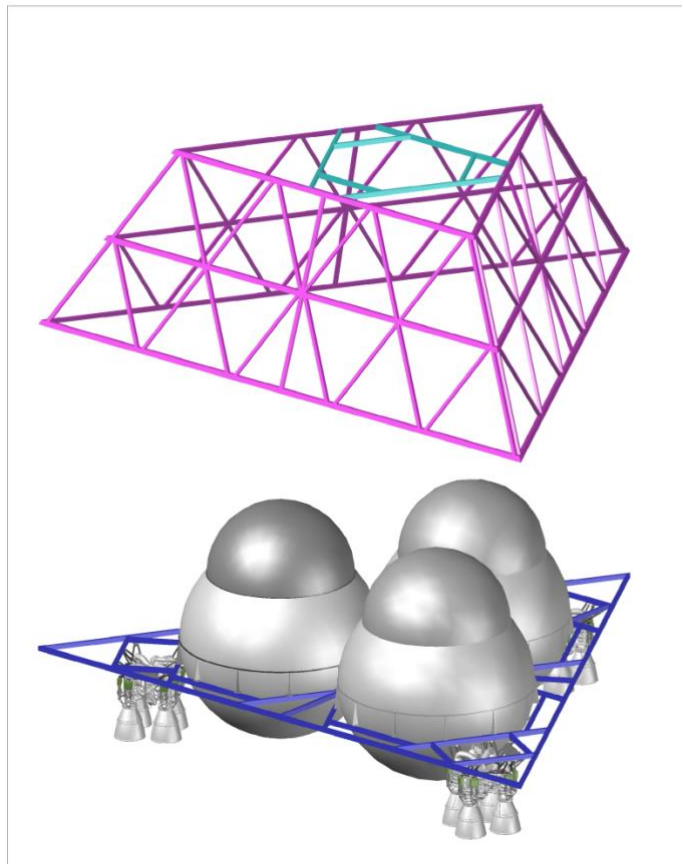


Fig. 5. Assembling the 1st Stage's Spatial Framework

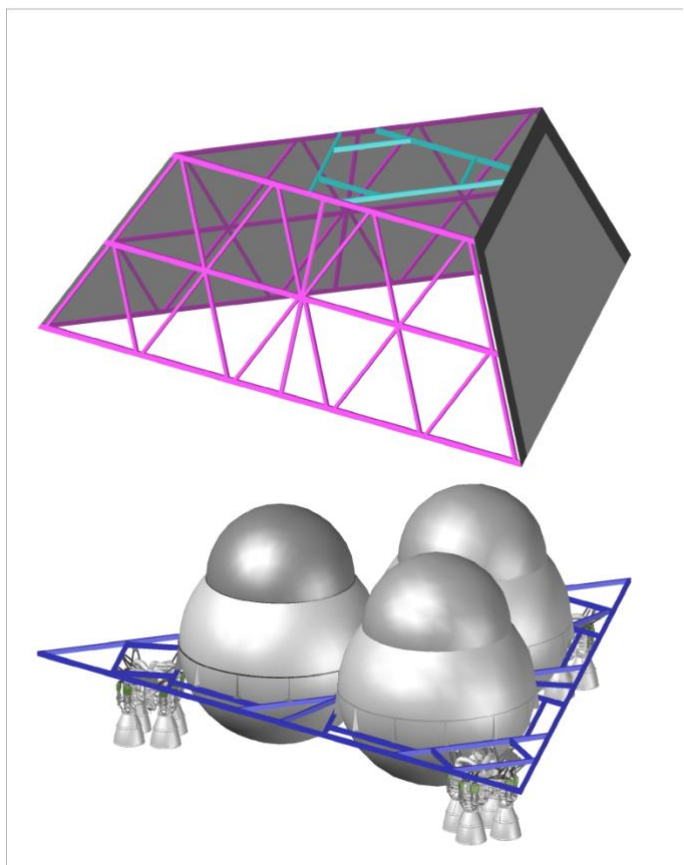


Fig. 6. Installing of the Skin onto the Framework

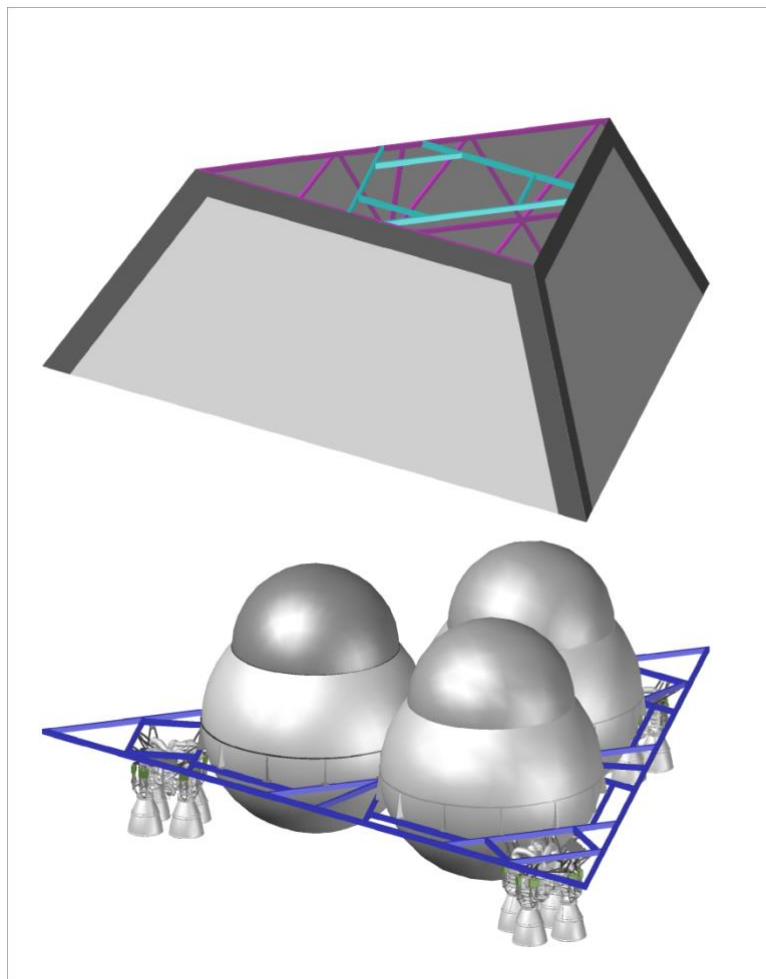


Fig. 7. Assembling the 1st Stage in a Drydock

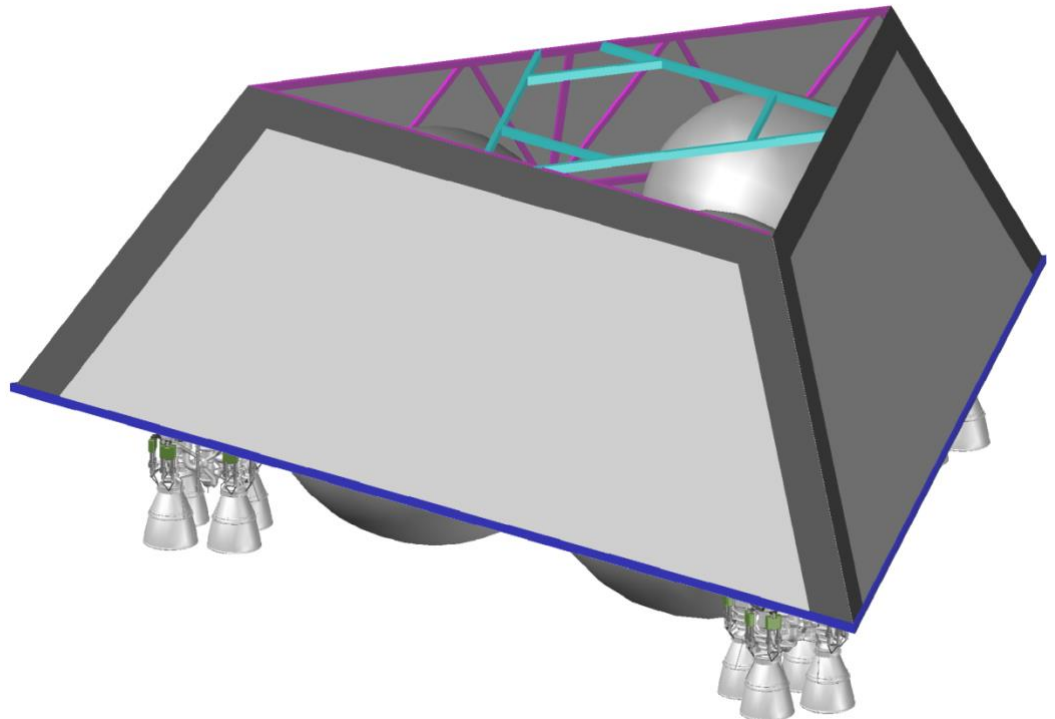


Fig. 8. The Assembled 1st Stage

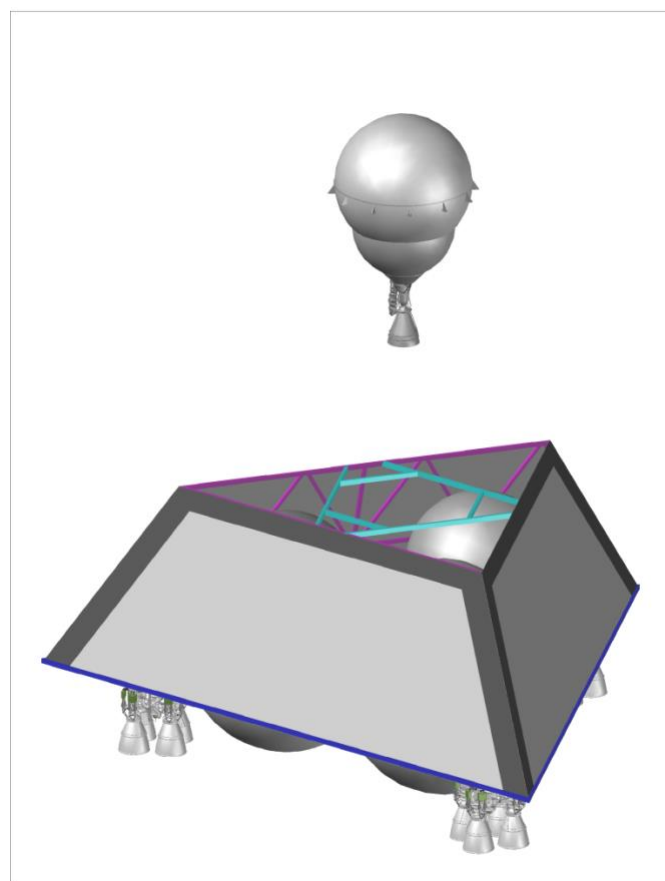


Fig. 9. Installing of the 2nd Stage's Propulsion Module atop the 1st Stage

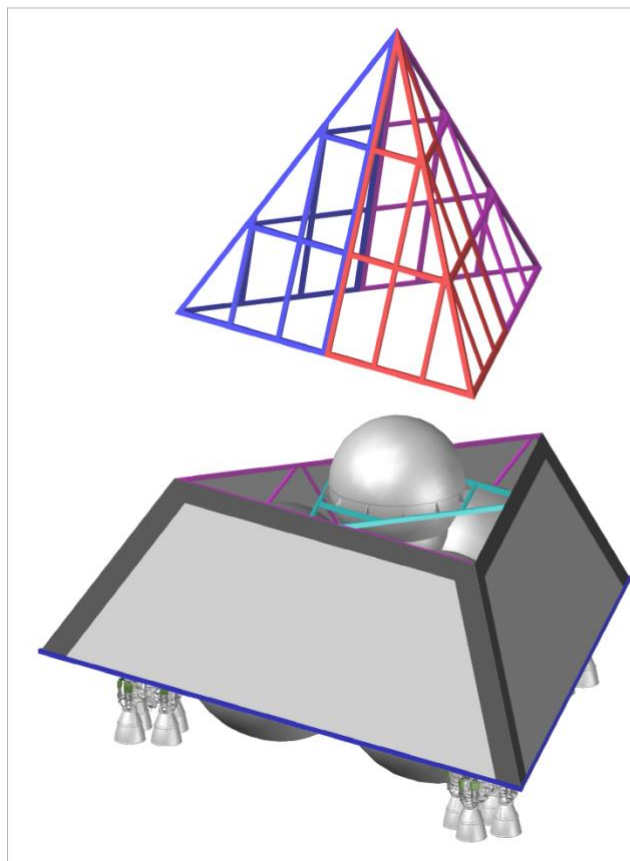


Fig. 10. Assembling of the Nose Fairing's Truss

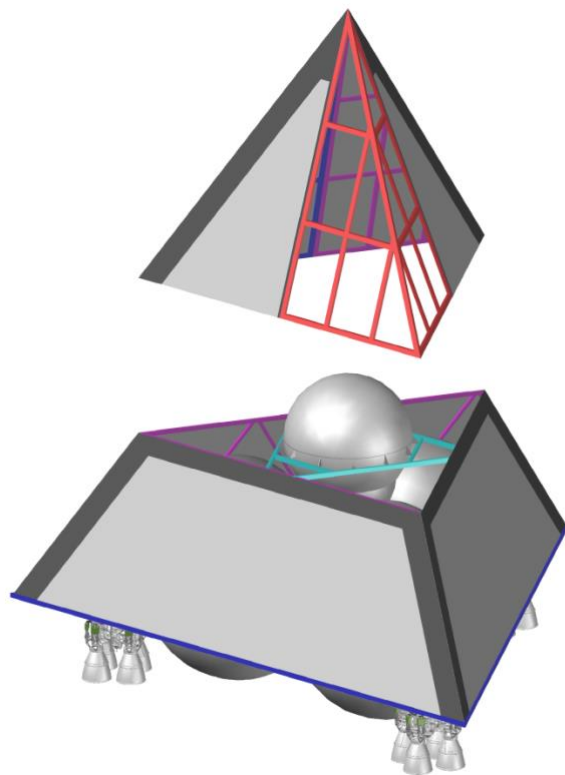


Fig. 11. Installing of the Skin on the Nose Fairing

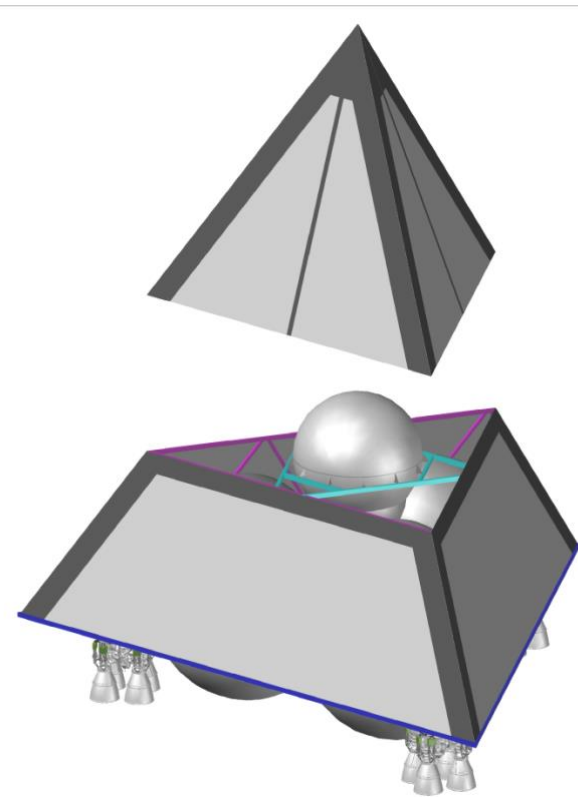


Fig. 12. Mounting of the Nose Fairing on the Rocket in a Drydock

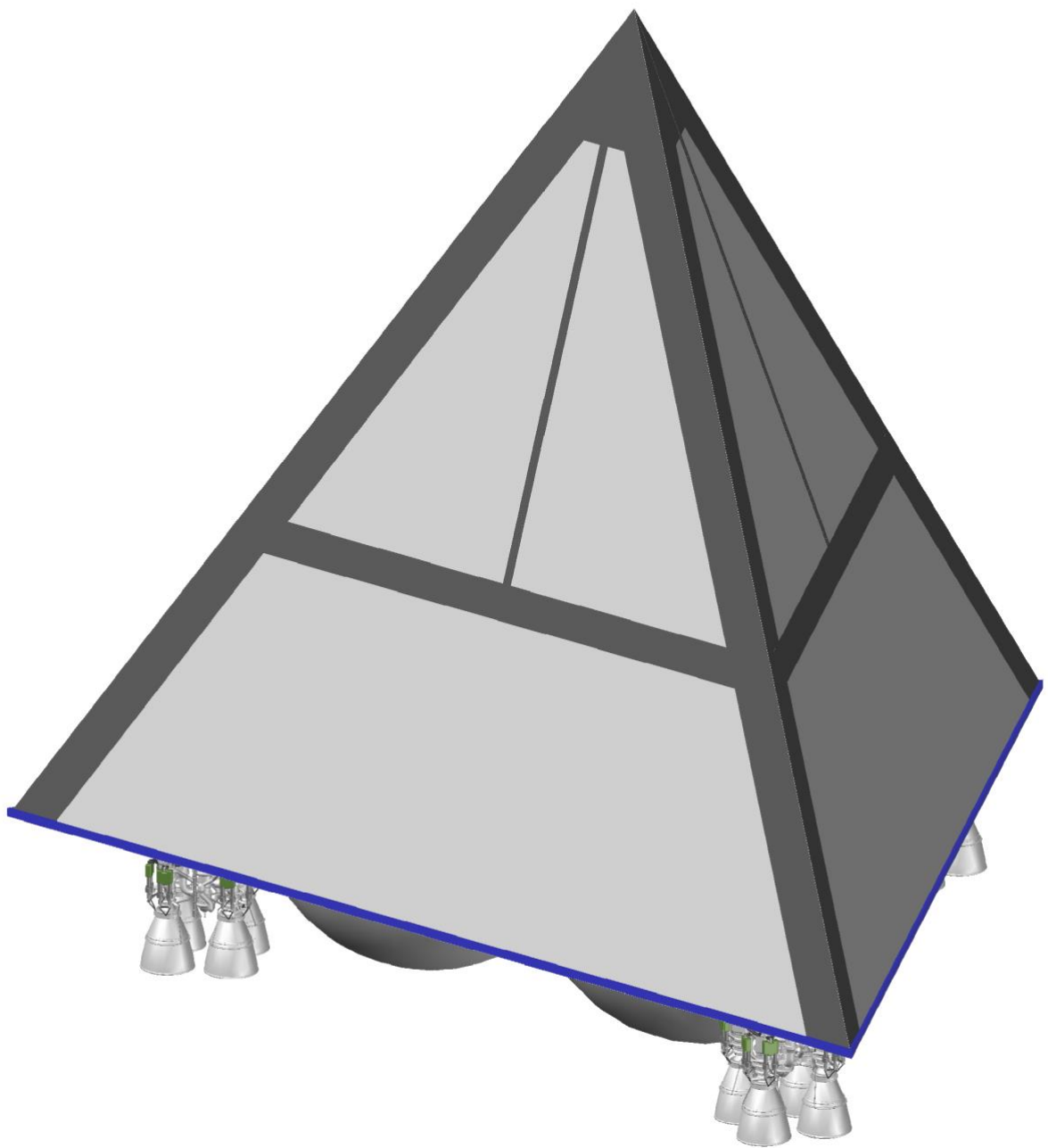


Fig. 13. The Assembled Rocket

The side face truss is assembled from stainless steel pipes with triangular and rectangular cross-section. The pyramid's edges are fabricated from the triangular

sectioned pipes (Fig. 14,) and the rest of the elements are made from the rectangular sectioned pipes. In the beginning the triple flat trusses of the side faces are assembled for the 1st and the 2nd floors of the pyramid. The assembling is performed using bolts and angle brackets (Fig. 15, 16.)

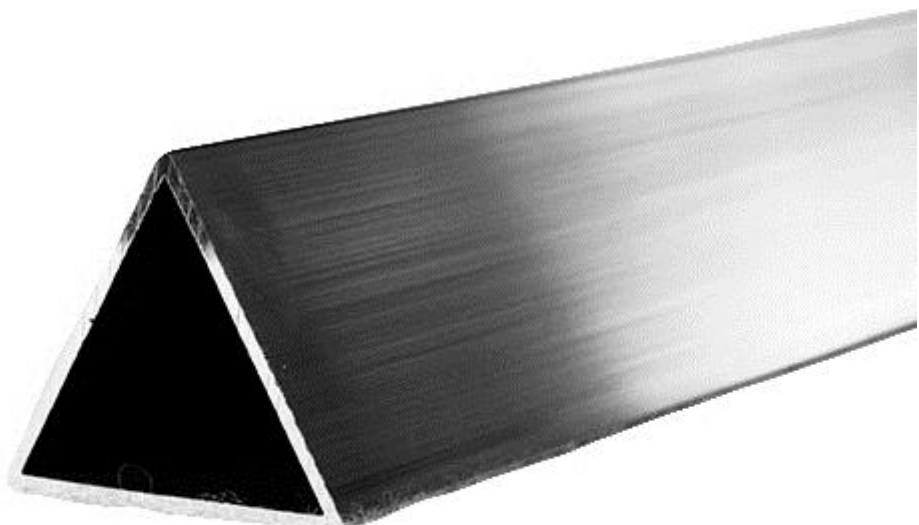


Fig. 14. A Stainless Steel Pipe with a Triangular Cross-Section

After the assembling is done, the drydock is flooded, the assembling berth is removed from under the rocket, and the ready rocket is towed away to the ocean towards the launch point.

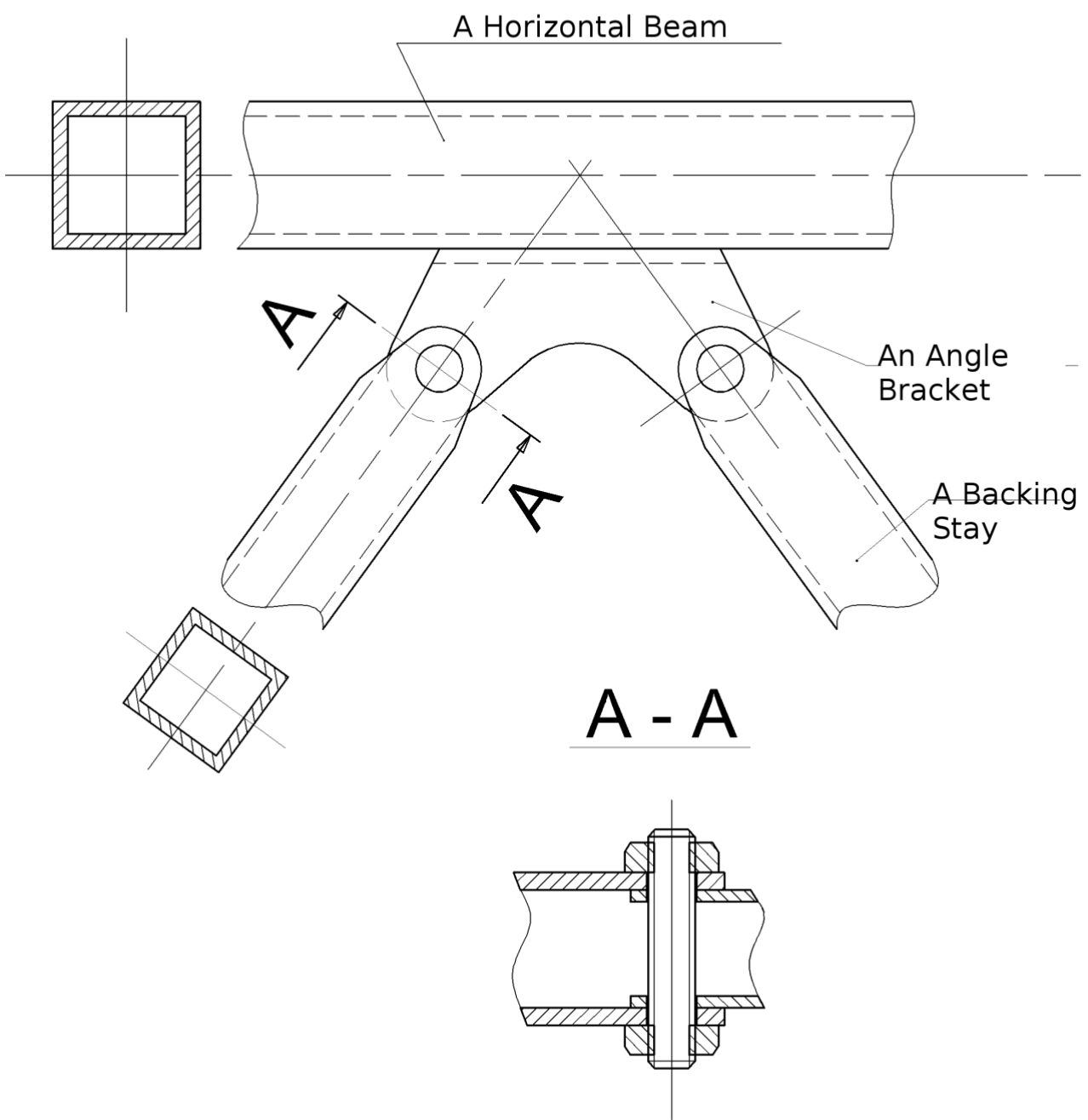


Fig. 15. The Side Truss Assembling

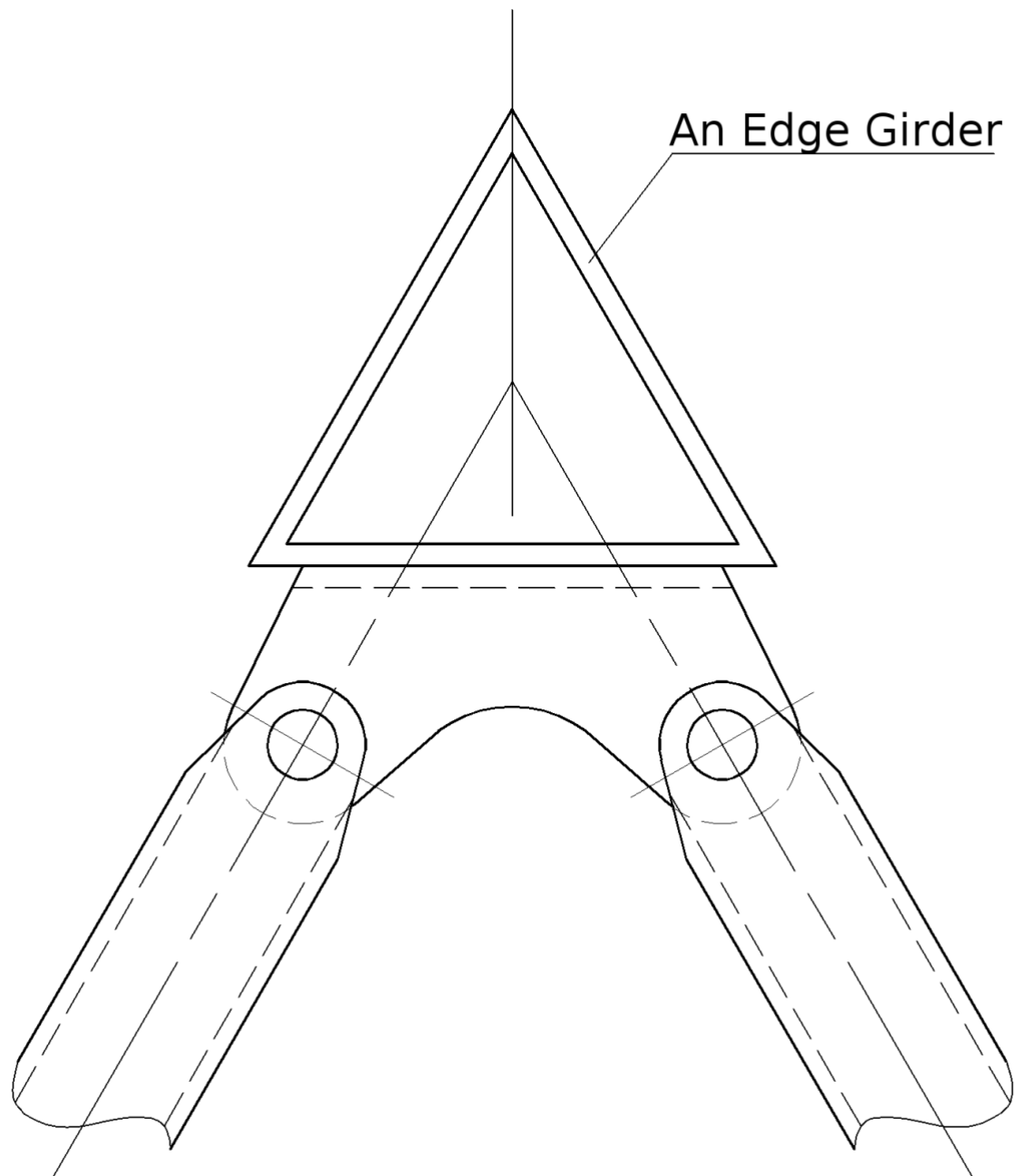


Fig. 16. Attachment of the Horizontal Beams to the Edge

Appendix 2

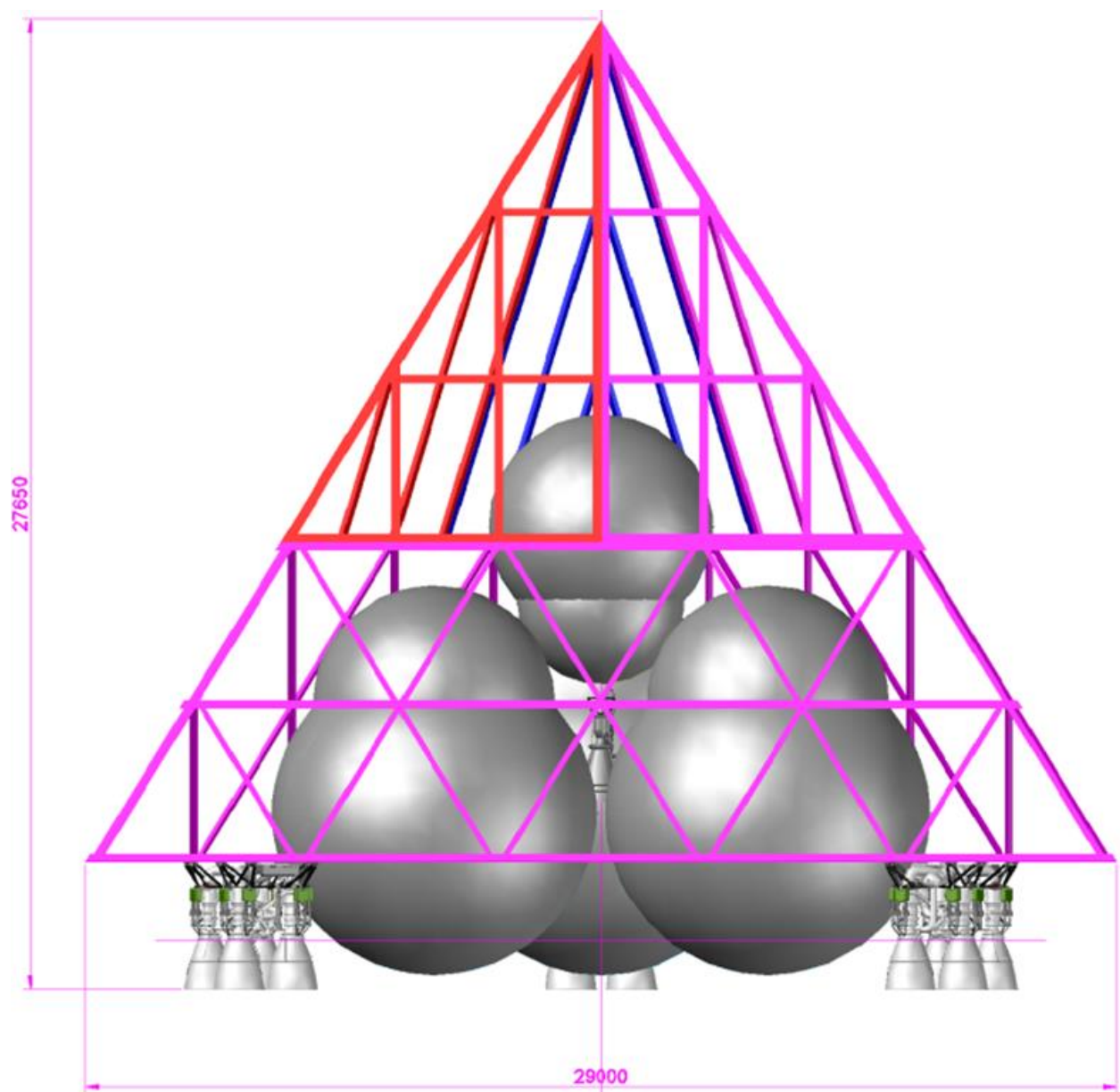
Study of the Primary Aerodynamic and Heat Parameters of a Pyramid Shaped Launch Vehicle

Zhurin, S.V., Cand. Sc. Physics and Mathematics

Aleksandrov, E.N.

Introduction

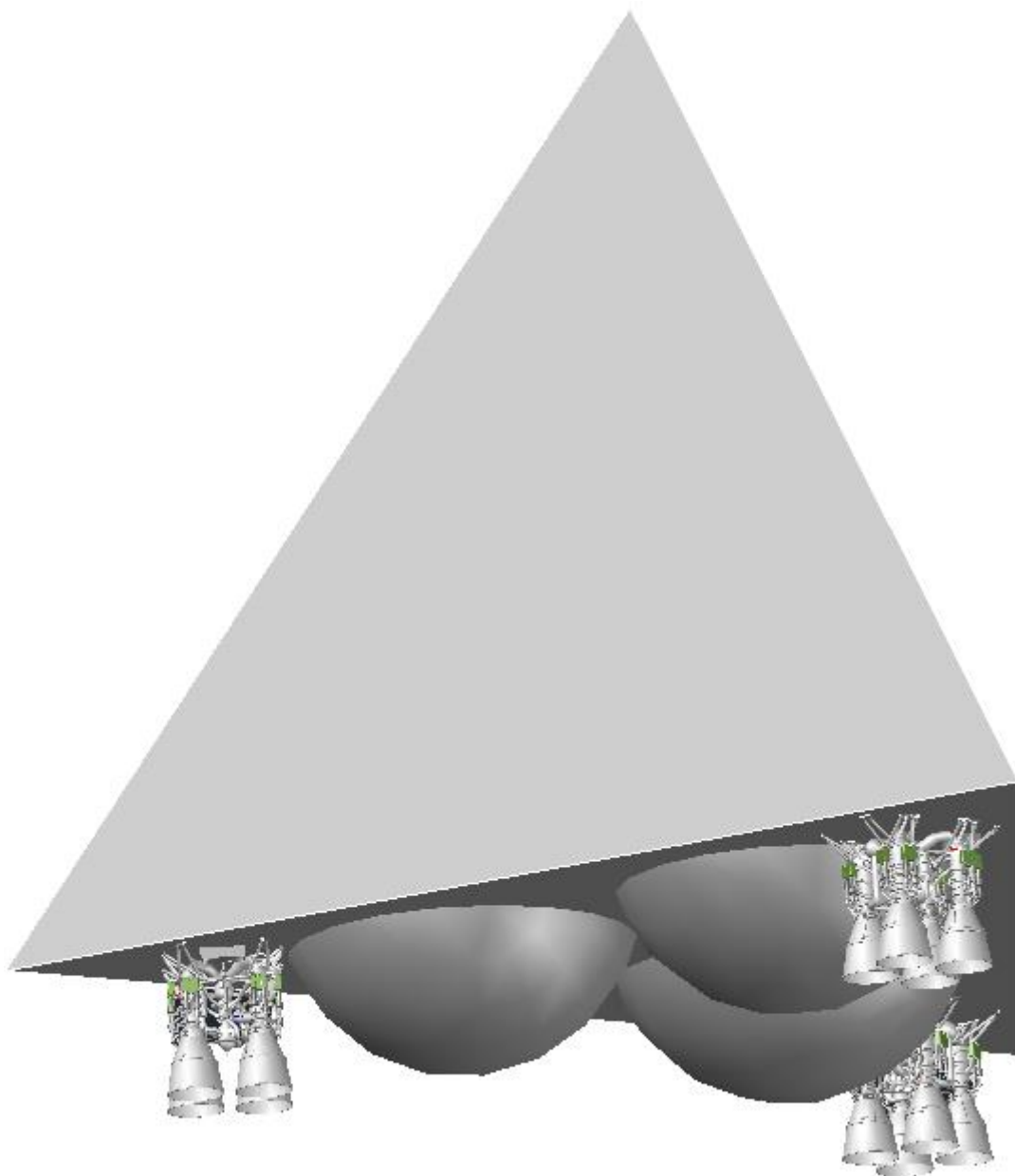
Excalibur Almaz company is considering a launch vehicle's (LV's) shape in the form of a regular tetrahedron with a 29 m long edge. The LV structural diagram with the primary dimensions is shown at Pic. 1. It's necessary to assess the primary aerodynamic parameters and the outer shell aerodynamic heating parameters for the purpose of the Draft Proposal design stage.



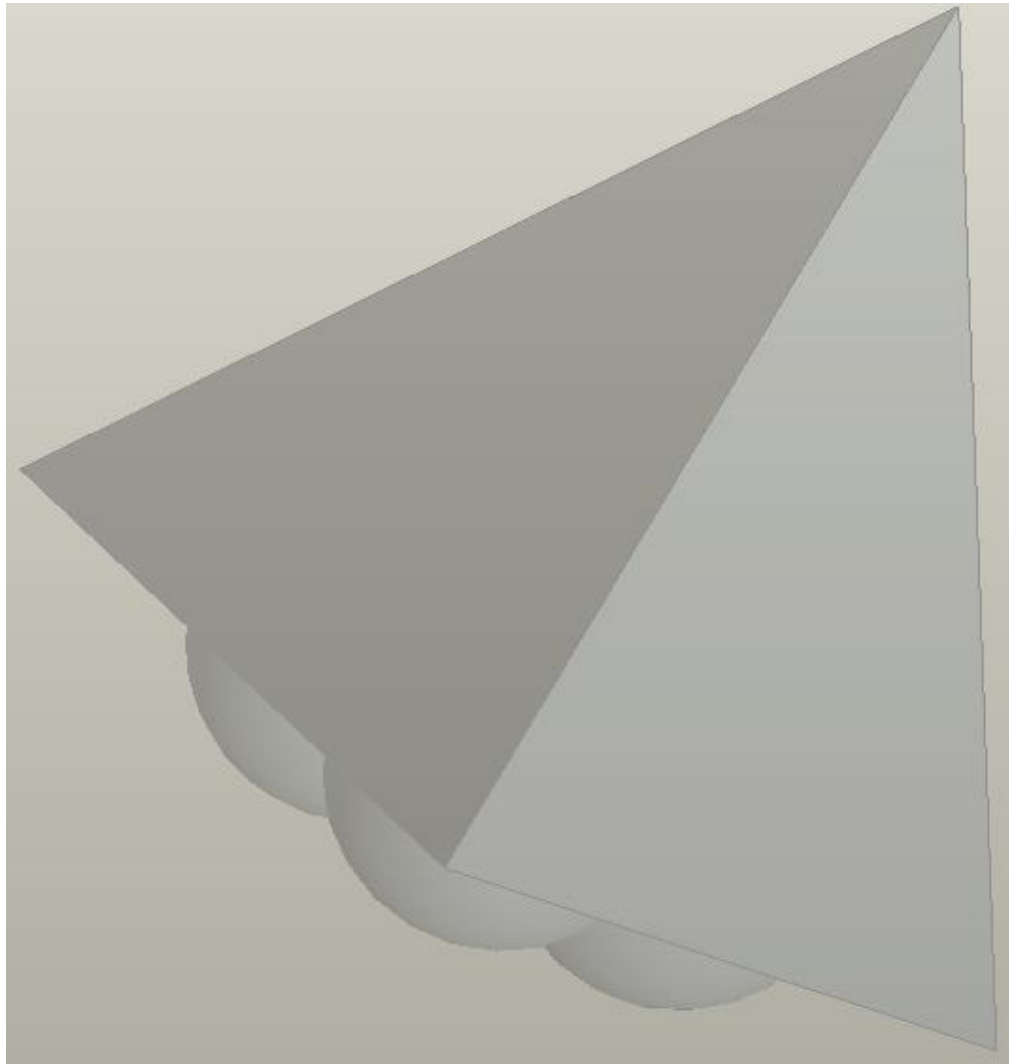
Pic. 1. The LV's Structural Diagram with the Primary Dimensions

The Rocket's Geometry Considered for Aerodynamic Parameters Study

The overall appearance of the LV is shown at Pic. 2. To the bottom part, the remarkably complex shaped rocket engines having multiple details are attached. We ignored them in the study considering their low relative area ratio in the aeroperformance computational model. The computational geometry model is shown at Pic. 3.



Pic. 2. The LV's Overall Appearance.



Pic. 3. Aeroperformance Computation Geometrical Model.

The Study Method: using FloEFD Software

As the study method, we have selected modeling in FloEFD software. It allows to automatically capture the 3D-model with a computational mesh, which allows making the computation considerably effortless.

FloEFD allows to compute fluid (gas or liquid) movement, to study flow fields around models, solve thermal exchange problems in convective and radiation heat transfers, and also to study thermal conductivity in solid bodies.

FloEFD software solves three-dimensional fluid dynamics equations: those for mass, momentum and energy conservation. When computing complex flows coming along with additional physical phenomena, additional equations describing such processes are solved.

The differential equations are approximated on the computational mesh upon an assumption that each cell in the mesh is a finite volume, inside which the variation speed of physical parameters changing is balanced by the transfer of those parameters through the cell's faces.

The Study Cases and Results

The LV aeroperformance study is done in the body-fixed coordinate system, the OX axis is normal to the pyramid's base which holds the rocket engines.

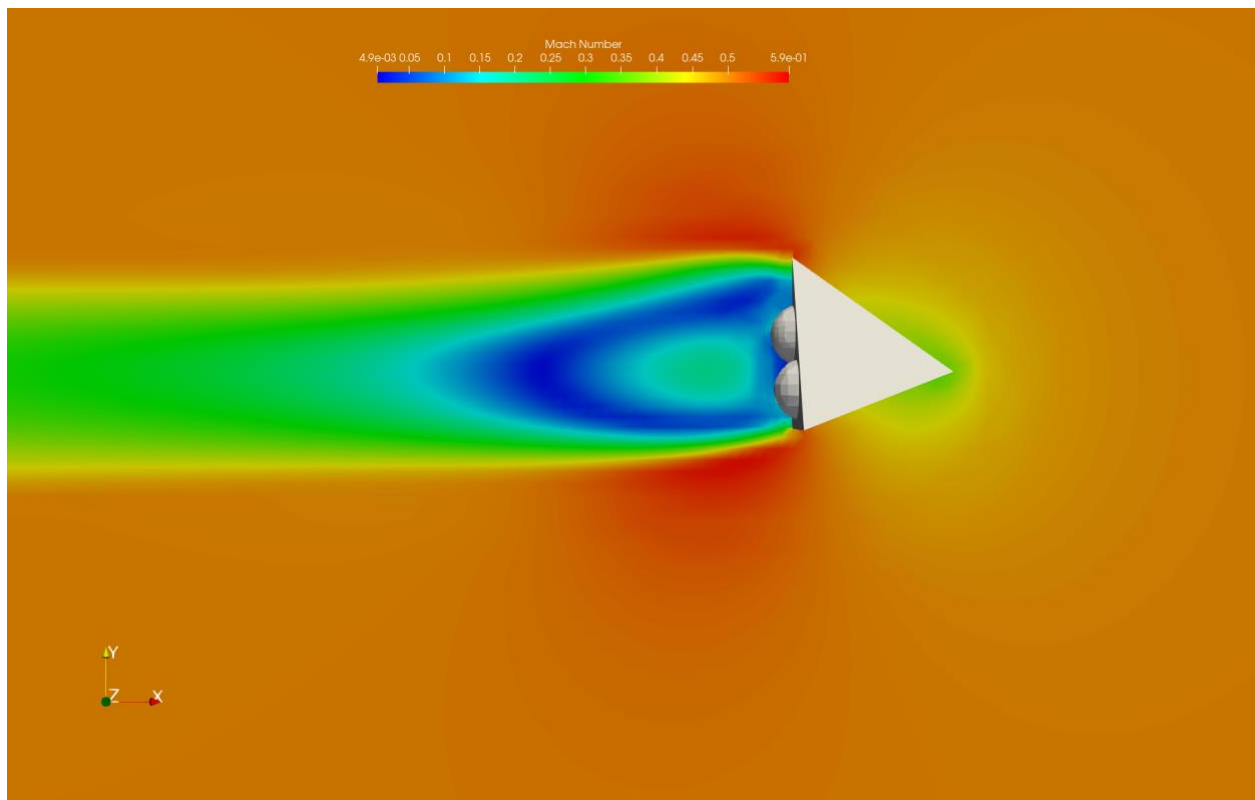
The study cases and results in the form of C_x coefficient values are shown in Table 1.

Table 1. The Study Cases

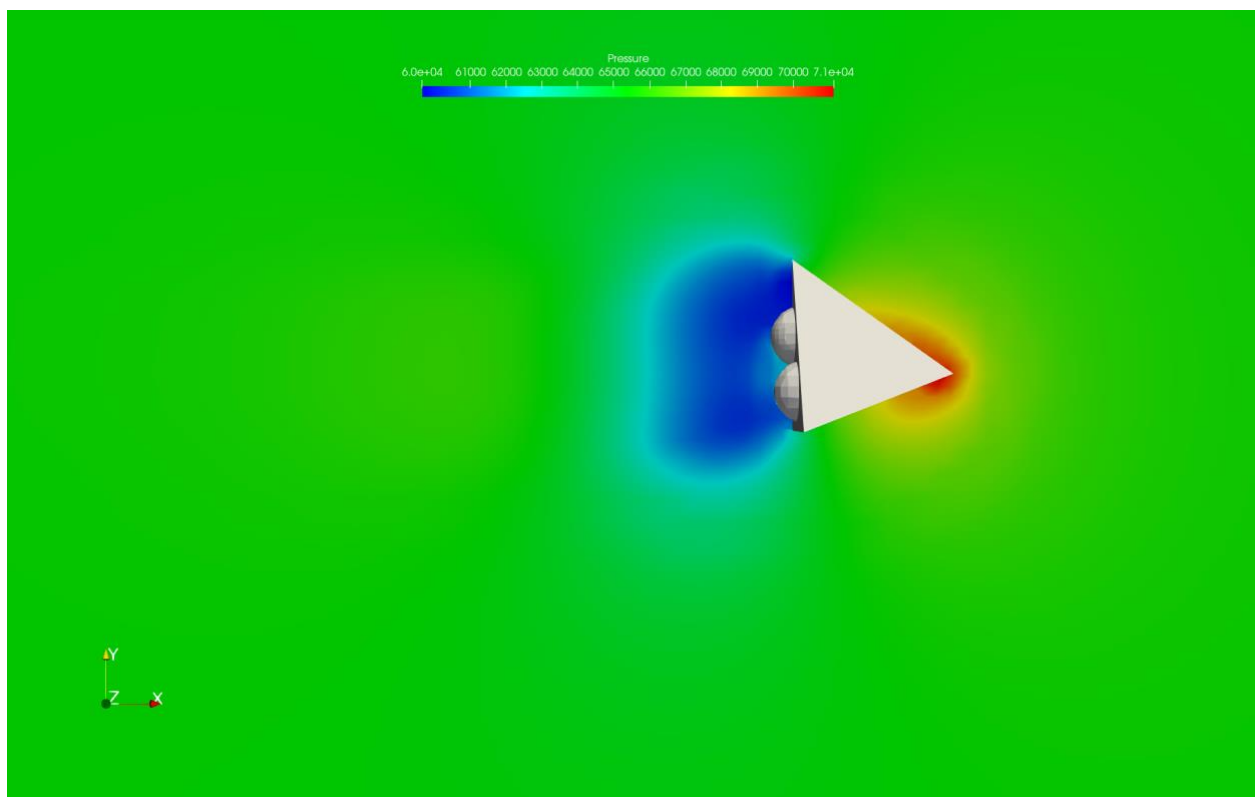
Case #	t, s	H, m	P, Pa	V, m/a	M	$\alpha, {}^\circ$	C_x
1	51	3,547	65,383	164	0.5	0	0.57
2	81	10,848	23,246	359	1.21	0	0.96

$C_x = \frac{F_x}{qS}$ is the axial drag coefficient, where q is the impact air pressure, $S = 374.1 \text{ m}^2$.

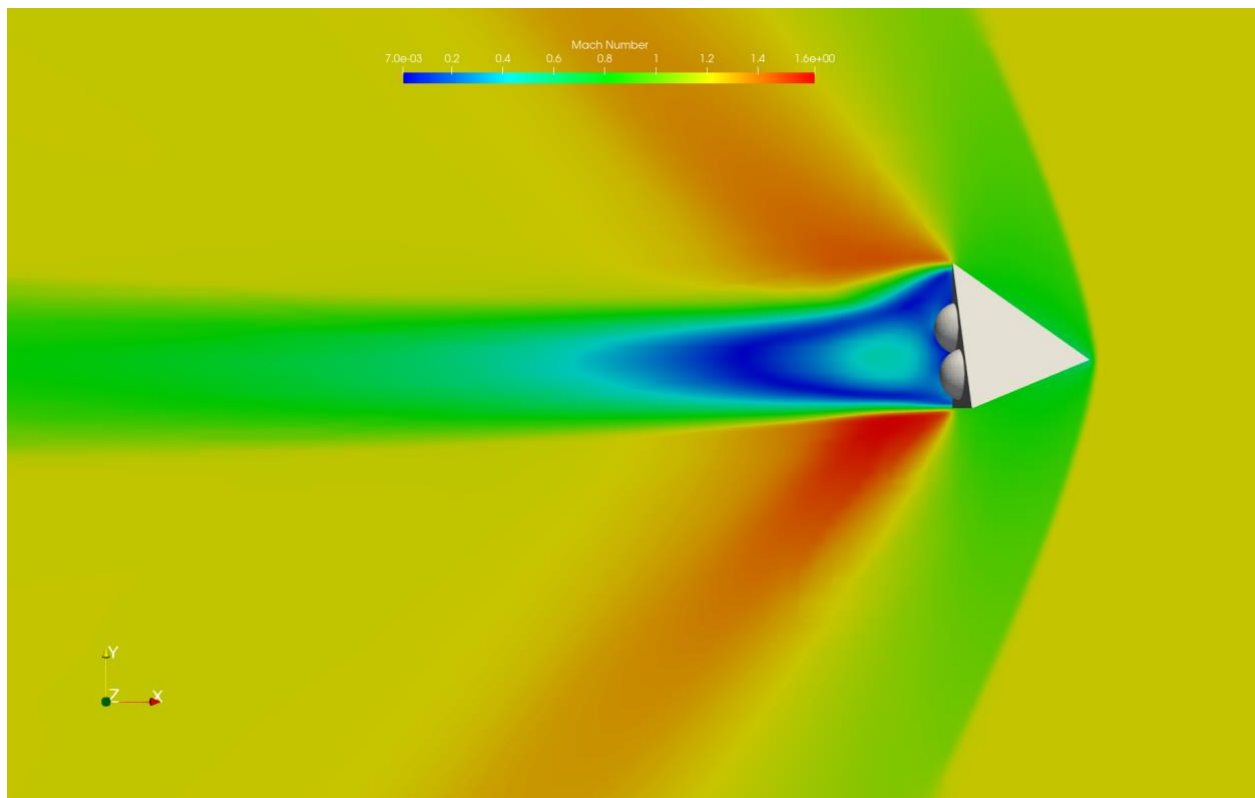
The computation results expressed as gradient fills for the Mach number field and the pressure field in the flow's axial plane for the Table 1's study points, are shown at Pic. 4-7.



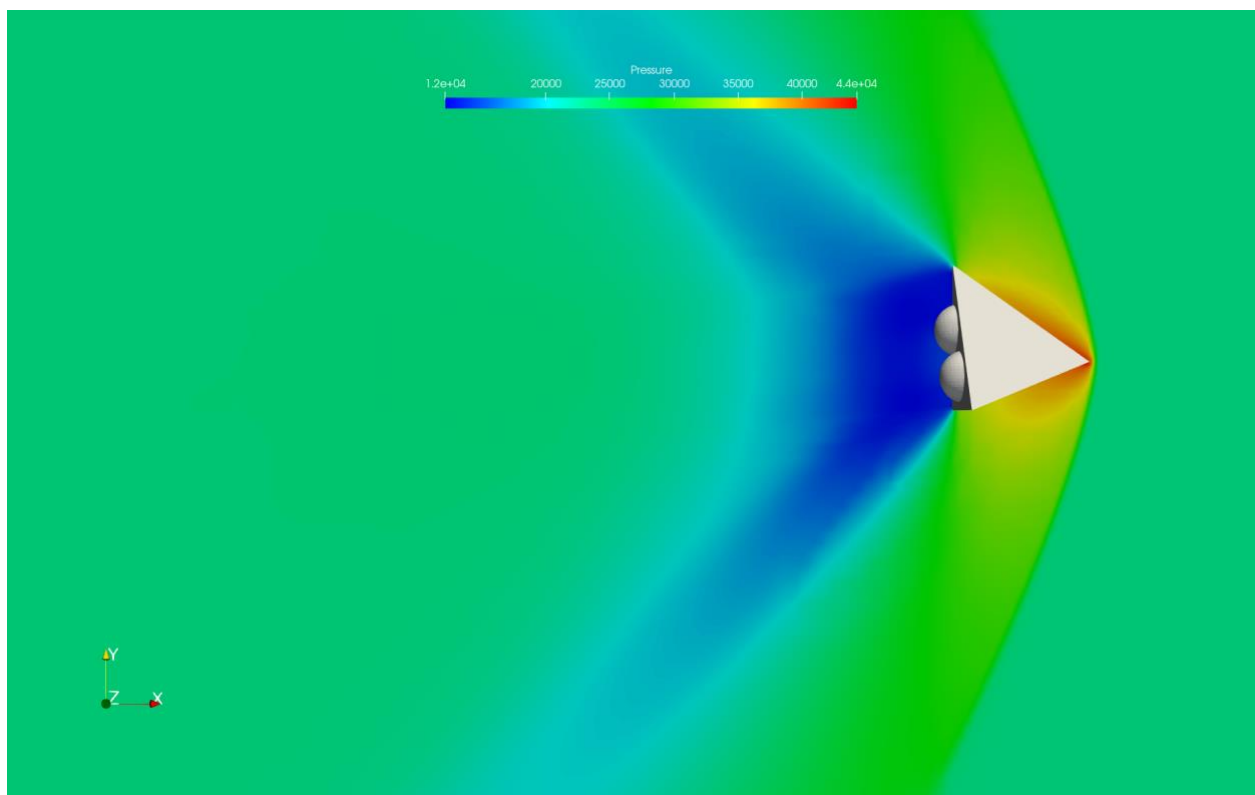
Pic. 4. Mach Number Gradient Fill. Study Case #1. M=0.5



Pic. 5. Pressure Gradient Fill. Study Case #1. M=0.5



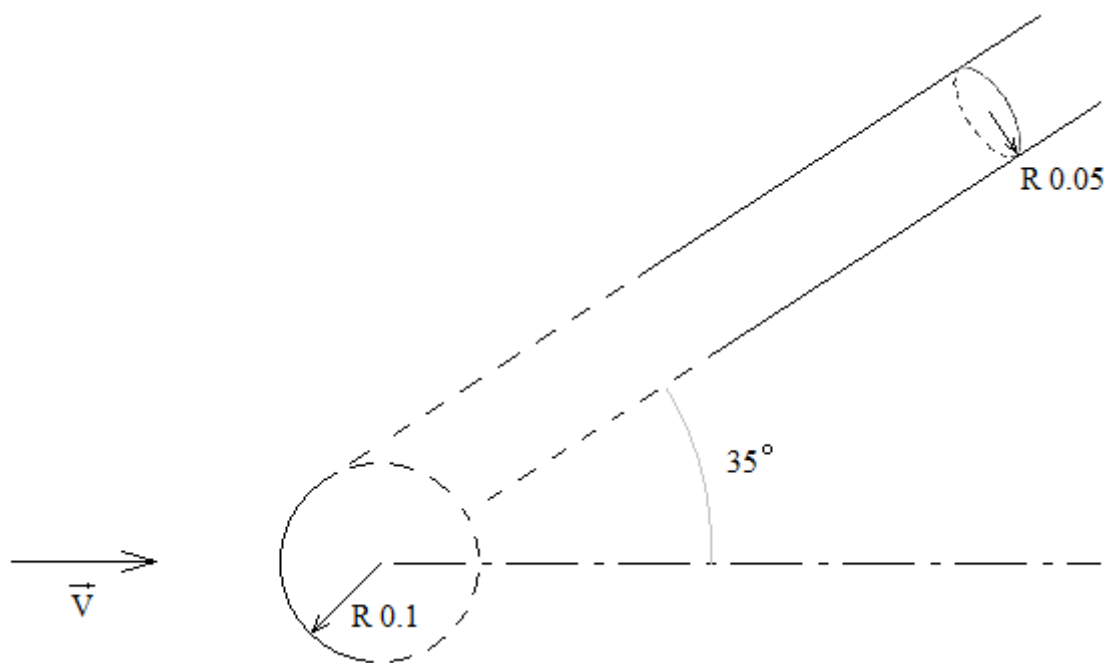
Pic. 6. Mach Number Gradient Fill. Study Case #2. $M=1.21$



Pic. 7. Pressure Gradient Fill. Study Case #2. $M=1.21$

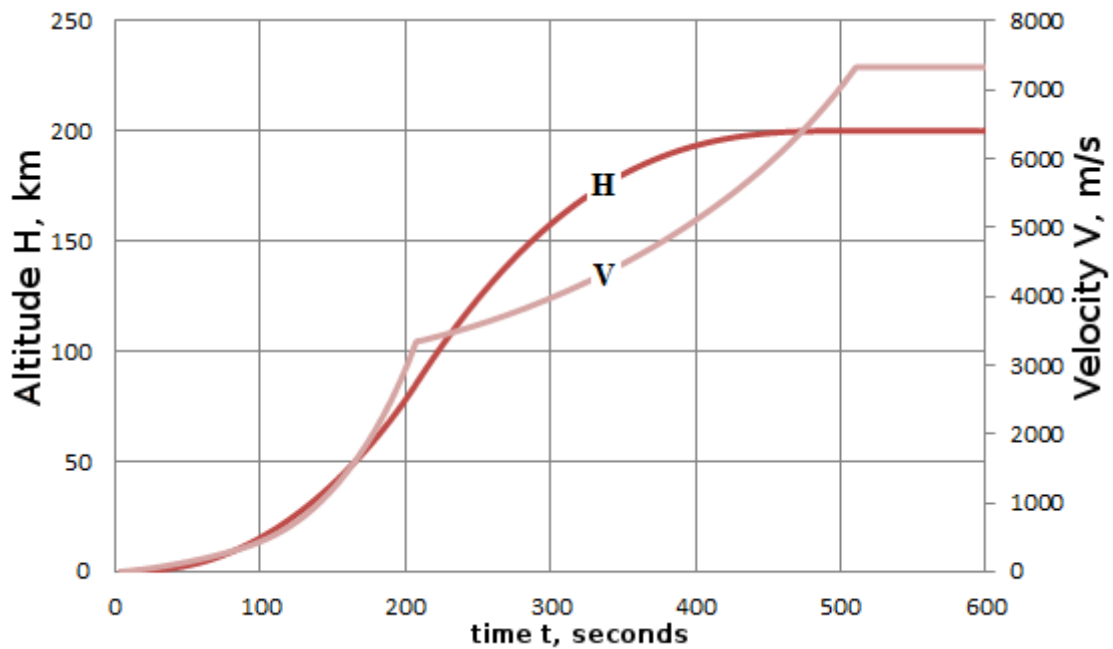
The Aerodynamic Heating Estimation

The worst heating areas of the LV is the blunting at the nose tip and the pyramid's edges. The blunting radius is assumed to be 0.1 m at the nose point, the rounding-off radius on each edge is assumed to me 0.05 m. To estimate the heat flow on the pyramid's edge, we model it as a cylinder with the lateral axis tilted to the flow's vector by 35° . The arrangement of the worst air heated outer shell's details is shown at Pic. 8.

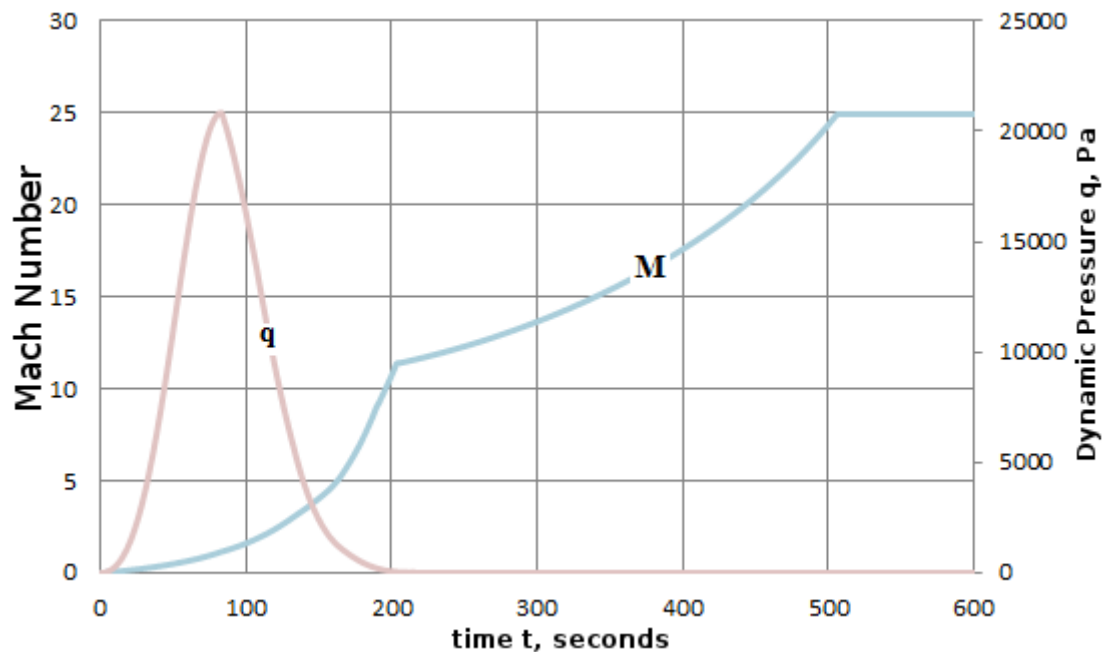


Pic. 8. Arrangement of the worst air heated outer shell's LV details

Pic. 9 shows the graphs of the trajectory parameters for the LV movement as a dependence on time. Pic. 10 displays the dependence of the impact air pressure and Mach number on time.



Pic. 9. Dependence of LV Altitude and Velocity on Time



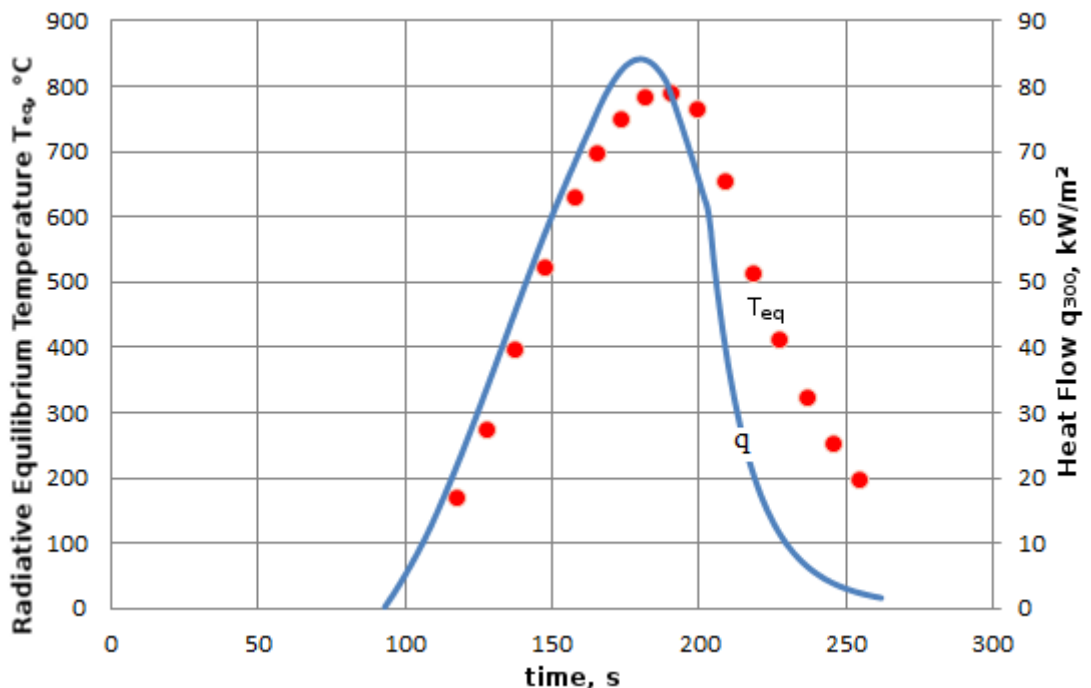
Pic. 10. Dependence of Dynamic Air Pressure and Mach Number on Time

We evaluate the maximum convective heat transfer by the empirical expression for the critical point on the sphere

$$q_{0l} = 1.93 \cdot 10^{-4} V_{\infty}^{1.08} \sqrt{\frac{\rho_{\infty}}{R_{c\phi}}} (H_0 - i_w). \quad (1)$$

The formula (1) is obtained for a equilibrium dissociating air, in the work [1] they claim a 10% error margin inside the velocity range of $V_\infty=0.5\text{-}8$ km/s.

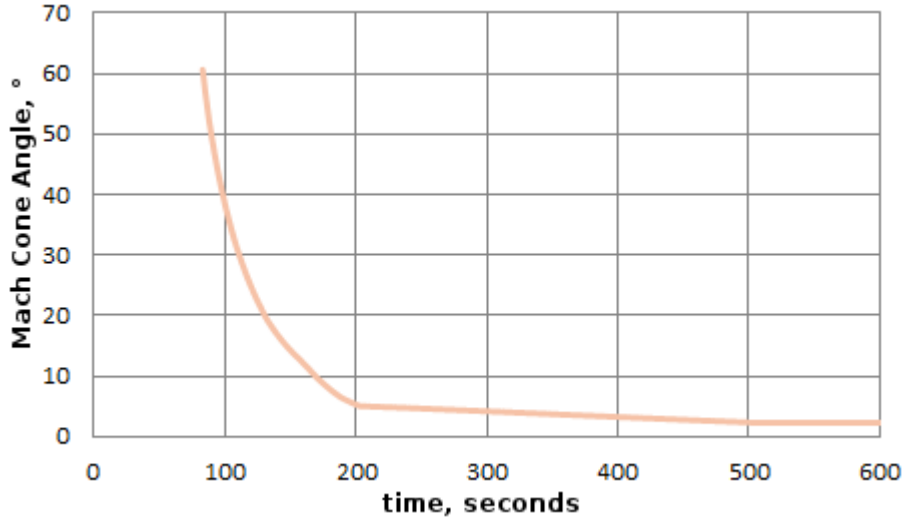
The resulting dependence of the convective heat flow on time into the surface with $T_w = 300$ K temperature in the critical nose blunting point, is shown at Pic. 11. The top heating happens after 180 seconds of flight at $M = 7.3$ and 64 km altitude. Also the Pic. 11 shows the graph of the radiative equilibrium temperature of the LV's nose blunting. The measure of the surface's blackness is $\varepsilon = 0.85$. The top temperature of the heat insulated surface is 800 °C.



Pic. 11. Dependence of the Convective Heat Flow and the Radiative Equilibrium Temperature on Time

We evaluate the aerodynamic heating of the pyramid's edge upon assumption that it's subject to flowing round similar to a cylinder tilted at some angle of attack to the impact flow. This assumption is most correct when the Mach number's cone angle is less than the cylinder's axis AOA. We take the cylinder's angle of attack $\approx 35^\circ$ (which is approximately the angle between the edge and the normal to the base of a regular tetrahedron.) The dependence graph for the Mach number's cone $\varphi =$

$\arcsin\left(\frac{1}{M}\right)$ on time is on Pic. 12. The considerable aerodynamic heating happens at $M \geq 2.5$. The Mach number's cone angle at these flight conditions is $\varphi \leq 25^\circ$, which makes the basic assumption for the pyramid edge's flowing round correct.



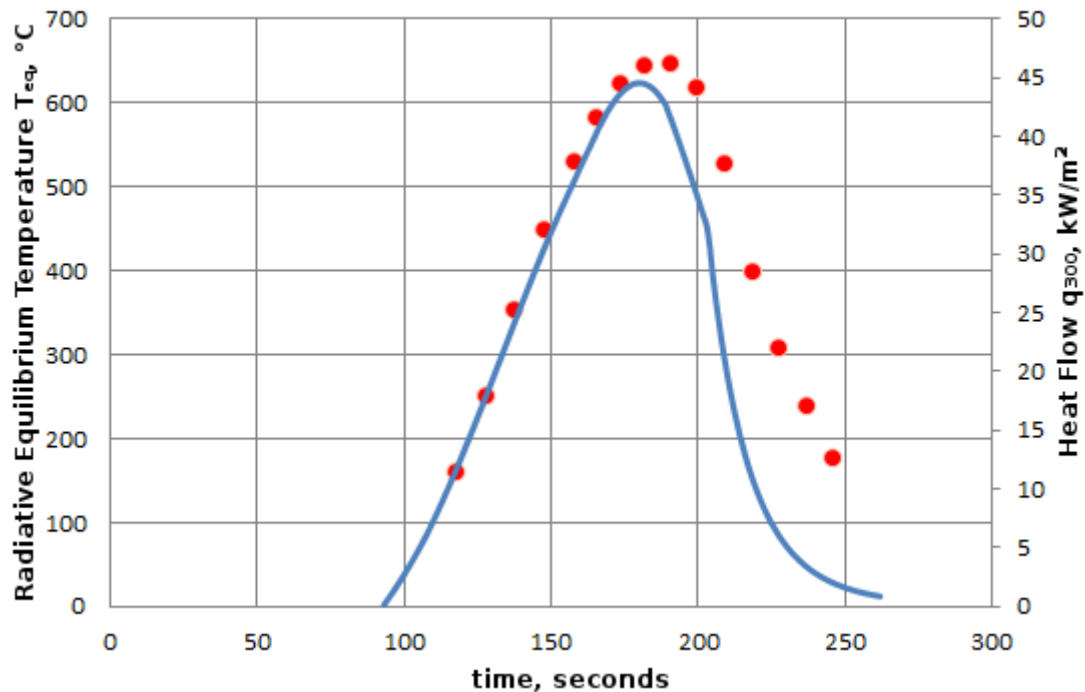
Pic. 12. Dependence of Mach Number's Cone Angle on Time

The edge is represented by a cylinder tilted at $\lambda = 90-35 = 55^\circ$ away from the undisturbed impact flow vector.

We evaluate the thermal flow on a cylinder by the equations for a sphere, having them multiplied by 0.75 coefficient [2]. The dependence of the relative heat flows on the edge's sweep angle is described by the empirical expression [2]:

$$\frac{q_w(\lambda)}{q_w(0)} \approx \cos^{1.25} \lambda. \quad (2)$$

The dependence of the convective heat flow on time into the surface with $T_w = 300$ K temperature at the pyramid's edge is shown at Pic. 13. The top temperature of the heat insulated edge's surface is 650 °C.



Pic. 13. Dependence of the Convective Heat Flow and the Radiative Equilibrium Temperature at the Pyramid's Edge on Time

Conclusions

1. The drag coefficient of the regular tetrahedron shaped LV is $C_x = 0.57$ at $M = 0,5$ and $C_x = 0,96$ at $M = 1,21$.
2. The top radiative equilibrium temperature of the heat insulated surface is:
 - $T_{eq} = 800 \text{ } ^{\circ}\text{C}$ at the nose blunting with 0.1 m radius,
 - $T_{eq} = 650 \text{ } ^{\circ}\text{C}$ at the edge with 0.05 m rounding-off radius.

Sources

1. Lunyov, V.V. *Real gases high velocity flow*. Moscow, PHYSMATLIT, 2007. 760 p. (in Russian.)
2. *Convective heat exchange in aircraft*. sci. ed. Zemlyansky, B.A. Moscow, PHYSMATLIT, 2014. 380 p. (in Russian.)